University of Nevada, Reno

The Complexities of cAMP Signaling in the Heart

A dissertation submitted in partial fulfillment of the
requirements for the degree of Doctor of Philosophy in
Cellular and Molecular Pharmacology and Physiology

by

Michael W. Rudokas

Dr. Robert Harvey/Dissertation Advisor

May, 2021

THE GRADUATE SCHOOL

We recommend that the dissertation
prepared under our supervision by

MICHAEL W. RUDOKAS

entitled

The Complexities of cAMP Signaling in the Heart

be accepted in partial fulfillment of the
requirements for the degree of

DOCTOR OF PHILOSOPHY

Robert D. Harvey, Ph.D.

Advisor

Scott Earley, Ph.D.

Committee Member

Normand Leblanc, Ph.D.

Committee Member

Brian Perrino, Ph.D.

Committee Member

Christine Cremo, Ph.D.

Graduate School Representative

David W. Zeh, Ph.D., Dean
Graduate School

May, 2021

Abstract

The autonomic nervous system regulates heart function to meet the metabolic demands of the body. The sympathetic branch of the autonomic nervous system provides an increase in ventricular force of contraction and rate of relaxation. These changes in contractility occur through the activation of cardiac adrenergic receptors (ARs), which can be divided into two types: β (βARs) or α (αARs). βARs, the more prominent ARs in the heart, utilize the diffusible second messenger molecule 3',5'-cyclic adenosine monophosphate (cAMP) to translate sympathetic stimulation to changes in cardiac functional properties. α_1ARs, which is the only αAR subtype expressed in the heart, also produce small functional changes and cardioprotective effects in the case of heart disease. Traditionally, α_1ARs signal through a different modality from βARs. However, α_1AR stimulation has been previously shown to inhibit βAR cardiac functional changes. The first part of this dissertation presents an investigation into whether α_1ARs can also regulate cAMP through a non-canonical signaling pathway. The second portion of this dissertation delves deeper into the mechanisms of βAR subtype (β_1AR or β_2AR) regulation of cAMP signaling. I hypothesized that intracellularly segregated cAMP microdomains allow for the unique set of functional effects seen from selective stimulation of each βAR subtype. To answer these questions, I utilized cAMP sensitive fluorescence resonance energy transfer (FRET)-based biosensors with live cell imaging techniques. Using the non-targeted cytosolically expressed Epac2-camps FRET

biosensor, I was able to demonstrate that α_1ARs can indeed control basal and

βAR induced cAMP levels through a tyrosine kinase mediated pathway that

works at the level of the βAR. Furthermore, I characterized a novel FRET

biosensor, Epac2-αKAP, which is targeted to the non-junctional sarcoplasmic

reticulum. The application of the two biosensors allowed for the confirmation of a

compartmentalized β_2AR cAMP signal due in part to the activity of

phosphodiesterase types 2 and 3. The findings documented in this dissertation

provide important advancements in the understanding of the regulation of cardiac

cAMP signaling through receptor and compartmentation mechanics. Leveraging

these discoveries could lead to a better understanding of heart disease and the

possible development of therapeutic treatments.

Dedication

For Mom, Dad, and Grandma

Acknowledgements

Innumerable individuals have contributed to my success leading up to and throughout graduate school. While I wish I could thank each one of them individually, I'm just going to have to settle with key acknowledgments for the sake of everyone's time. Whether you are listed below or not, please know that I value everything you have done for me and I hope that I was able to contribute something back.

The first person I have to acknowledge is my mentor, Dr. Robert Harvey. He took a shot on a young man not sure where he was going in life and what an adventure it has been. I cannot express enough the debt of gratitude I owe for all your patience and guidance. Dr. Shailesh Agarwal follows close behind in the amount of gratitude he deserves. On top of being the humblest man I know (even though he'll deny it), he can be directly linked to almost all my knowledge and skills in a laboratory setting. I also must thank my committee members (Dr. Scott Earley, Dr. Norm Leblanc, Dr. Brian Perrino, and Dr. Christine Cremo) who were always available to provide additional mentorship. Next up to acknowledge is the Harvey Lab members, past and present. Working in an environment where you are friends as well as coworkers makes the day-to-day so much better. A shout out must be also given to all the friends I have made while in Reno. There is no way I would have kept sane all these years without all our escapades, happy hours, and lunch time conversations. Haviva, I consider the time we have spent together my favorite part of graduate school if not of life. I look forward to all the places we will go and accomplishments we will achieve together. Lastly, I must

must thank my mom, dad, brother, grandma and the rest of my family members who set the foundation of who I am and continue to be the best support squad I could have ever asked for.

Table of Contents

List of Figures

Chapter 1

Introduction: cAMP Regulation in Ventricular Myocytes

1.1 Heart Physiology

Hearts are muscular pumps responsible for driving oxygenated and deoxygenated blood through the circulatory system. They are comprised of three primary types of cardiac muscle: atrial, ventricular, and excitatory/conductive muscle[1]. The atrial and ventricular muscle are responsible for physically contracting the heart and pushing blood through its various chambers. The excitatory and conductive muscle are responsible for controlling and propagating the rhythmic contraction of the heart. Each of these types of muscle are composed of individual cardiac muscle cells (myocytes), which act as a cohesive unit to allow for organized contraction.

The sinoatrial (SA) node is a bundle of excitatory muscle located near the top of the right atrium and is the primary pacemaker of the heart. The electrical stimuli released from the SA node cause the atrial muscle to contract, forcing blood into the ventricular chambers. Once the electrical impulse reaches the atrioventricular (AV) node, a cluster of conductive/excitatory muscle at the bottom of the right atrium, the signal is briefly delayed before being conducted throughout the ventricles. The ensuing ventricular contraction provides the primary pumping force of the heart, propelling blood to the systemic or pulmonary circulation.

1.2 Excitation-Contraction Coupling

The connection between the electrical stimulus input and contraction output of a cardiac myocyte is known as excitation-contraction (EC) coupling.

The process of EC coupling begins when an action potential, the transient reversal of electrical potential across the myocyte membrane, travels through the cardiac myocytes and cause the cells to depolarize. This triggers a self-amplifying inward flux of Na^+ ions into the cardiac myocyte through voltage-gated sodium channels leading to a further depolarization of the membrane potential. This allows for the activation of L-type Ca^{2+} channels (LTCC) primarily found in transverse (T)-tubules to open and allow calcium ions to flow into the cell. T-tubules are membrane invaginations of the sarcolemma. The spike in intracellular calcium (Ca^{2+}) ions coming through LTCC activate ryanodine receptors (RyR) located on the sarcoplasmic reticulum (SR) in cardiac myocytes. Once activated, the RyR release large stores of Ca^{2+} ions from the SR, which further increase the cytosolic Ca^{2+} concentration. The Ca^{2+} interacts with troponin associated with the contractile fibers of the cardiac myocyte allowing for contraction to occur[2]. To allow for relaxation, Ca^{2+} ions are transported back into the SR through sarco/endoplasmic reticulum Ca^{2+}-ATPases (SERCA). Additional Ca^{2+} is also extruded through sodium-calcium exchangers located in the sarcolemma. This cycle repeats continuously to allow for the continued contraction and cycling of blood through the circulatory system.
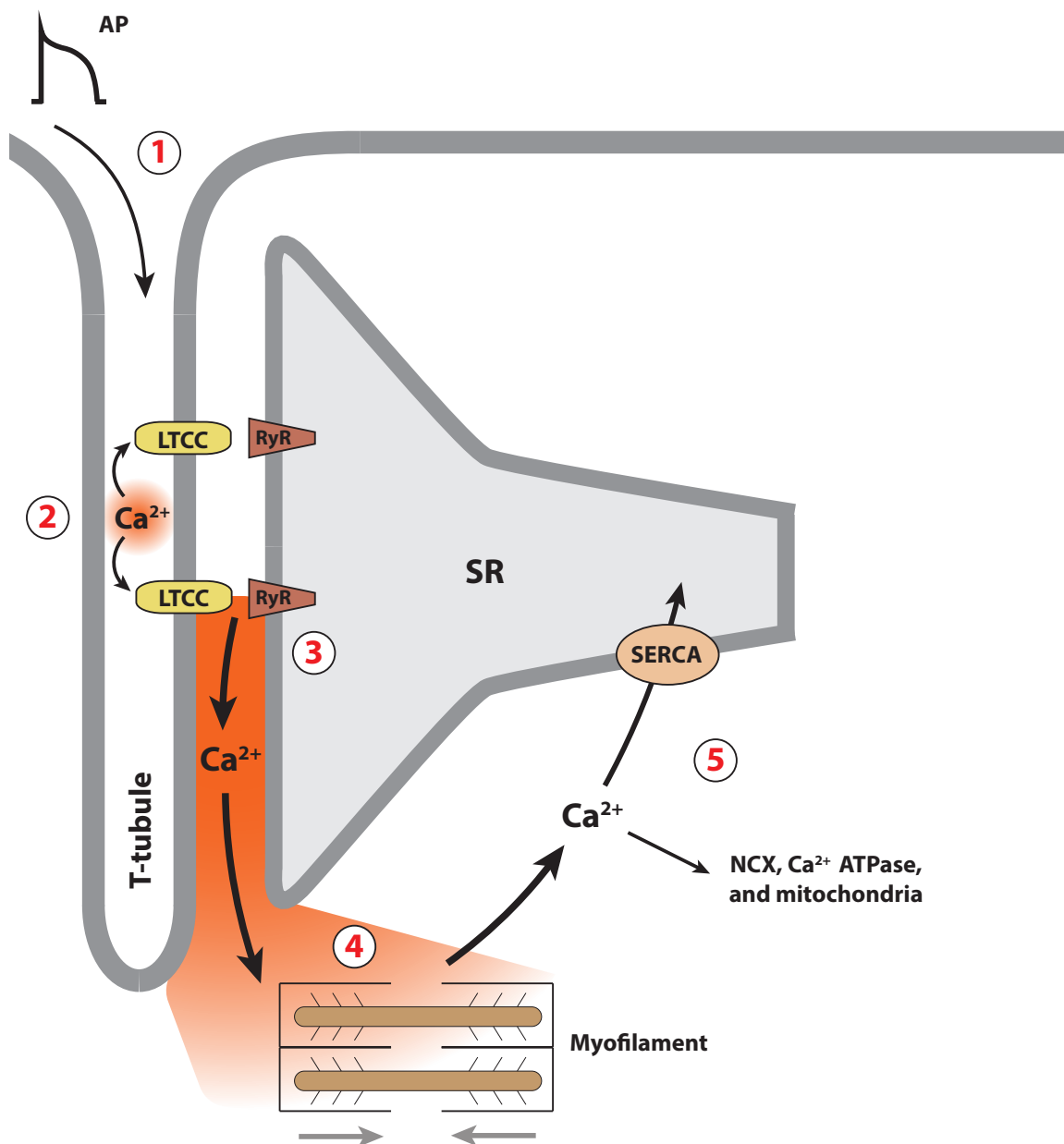
Figure 1: Cardiac excitation-contraction (EC) coupling

(1) An action potential (AP) travels across the sarcolemma and depolarizes the cell membrane in a T-tubule. **(2)** The depolarization permits extracellular Ca^{2+} entry through L-Type Ca^{2+} channel (LTCC). **(3)** The Ca^{2+} influx triggers ryanodine receptors (RyR) to release Ca^{2+} stores housed in the sarcoplasmic reticulum (SR). **(4)** Ca^{2+} binds to troponin associated with myofilament allowing for contraction. **(5)** Cytosolic Ca^{2+} is primarily reduced through the sarco-endoplasmic reticulum Ca^{2+}-ATPase (SERCA) sequestration of Ca^{2+} to the SR. Additional Ca^{2+} removal occurs through the sodium-calcium-exchanger (NCX), sarcolemmal Ca^{2+} ATPase, and mitochondria Ca^{2+} uniporter.

1.3   Autonomic Nervous System Regulation of the Heart

The autonomic nervous system (ANS) is the primary means of regulating cardiac output to meet the metabolic needs of the body. The autonomic nervous system has two branches that affect the heart: the sympathetic nervous system and the parasympathetic nervous system. The sympathetic nervous system is responsible for what is known as the "fight or flight response". This response was first described by Walter Cannon in 1916 and encompasses the set of physiological changes that occur in settings of acute stress[3]. In the heart, the sympathetic nervous system is responsible for increasing the rate of pacing of the sinoatrial node (chronotropy), the speed of conduction of the atrioventricular node (dromotropy), the force of myocyte contraction (inotropy), and the rate of myocyte relaxation (lusitropy). Sympathetic stimulation of the heart occurs through nerves that arise from the sympathetic ganglia and innervate many regions of the heart. The stimulation can be elevated to increase the amount of blood pumped by the heart or inhibited to decrease the cardiac output.

The other branch of the ANS in the heart is the parasympathetic nervous system. It is responsible for a decrease in chronotropy, dromotropy, inotropy, and lusitropy. Parasympathetic stimulation is conducted to the heart mainly through the vagus nerve, which innervates primarily the SA and AV nodes with additional efferent connections to the atria and ventricles. Therefore, vagal stimulation primarily decreases heart rate compared to the strength of contraction. Increases in vagal tone will decrease cardiac output while inhibition of vagal tone increases cardiac output.

1.4   β-Adrenergic Receptor Signaling

The sympathetic nervous system regulates heart activity predominantly through local post-ganglionic neuronal release of norepinephrine (NE) directly onto cardiac tissue. Additionally, chromaffin cells in the adrenal medulla secrete systemic NE and epinephrine (Epi), which play a lesser role in cardiac sympathetic stimulation[4]. These catecholamines bind to G protein-coupled receptors (GPCR) located in the sarcolemma of cardiac myocytes. β-adrenergic receptors (βARs) are a subclass of GPCR and are responsible for the cardiac "fight or flight" sympathetic responses. βARs are traditional GPCR and therefore possess seven transmembrane helices and stimulate an intracellular heterotrimeric G-protein complex when activated[5]. Three isoforms of βARs have been characterized in cardiac myocytes: β_1ARs, β_2ARs, and β_3ARs[6,7]. Although some contractility effects have been associated with β_3AR activity, it has been largely linked to metabolic regulation and therefore will not be discussed in this introduction[7]. A fourth subtype of βAR (β_4ARs) has also been proposed but remains controversial[8].

β_1ARs and β_2ARs comprise the dominant isoforms of βARs expressed in cardiac myocytes at a ratio of approximately 80% β_1ARs to 20% β_2ARs[9]. When a catecholamine binds to these receptors (primarily NE binding to β_1ARs in normal physiologically conditions), they undergo conformational changes which in turn activate and dissociate their G-protein complex (G_α and $G_{\beta\gamma}$ subunits). There are four types of G-protein classified by their α subunit: G_s, G_i, $G_{12/13}$, and G_q[10]. The

resulting downstream of effects of GPCR activation depend on the type of G-protein that was activated[11]. The stimulatory G-protein (G_s) is associated with all βARs and leads to the canonical βAR signaling pathway[5]. Activated G_s α subunits stimulate adenyl cyclase (AC) in the plasma membrane which catalyzes the production of 3',5'-cyclic adenosine monophosphate (cAMP) from adenosine triphosphate (ATP). The cAMP then binds to the regulatory subunit of protein kinase A (PKA) allowing the catalytic domains of PKA to activate. The catalytic domains of PKA then phosphorylate target proteins. Some of the prominent proteins include phospholamban, troponin I, LTCC and RyR.
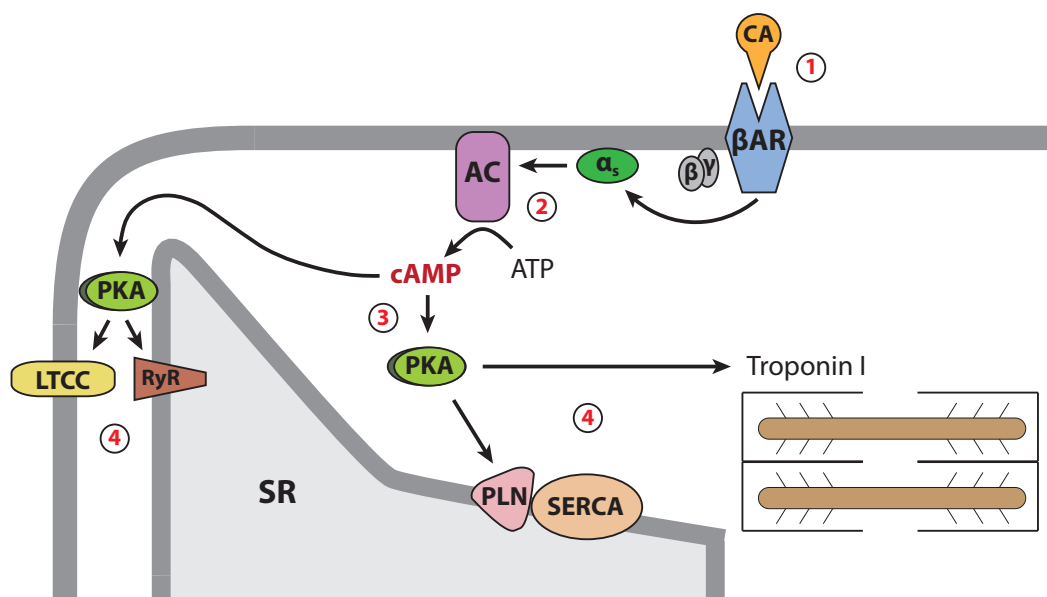
Figure 2: Canonical G_s/β-adrenergic receptor (βAR) signaling pathway

(1) A catecholamine binds to a βAR in the sarcolemma of a cardiac myocyte activating the G_s G-protein complex (α/β/γ). **(2)** The dissociated G_s α subunit stimulates adenylyl cyclase to produce cAMP from ATP. **(3/4)** cAMP activates PKA, which phosphorylates key EC coupling proteins throughout the myocyte including phospholamban (PLN), troponin I, L-Type Ca^{2+} channel (LTCC), and ryanodine receptors (RyR).

The phosphorylation of these proteins alters their functional properties allowing for changes in the overall cellular contractile activity. Phospholamban (PLN) is a SR transmembrane protein, which associates with and regulates SERCA. When unphosphorylated, PLN inhibits SERCA Ca^{2+} reuptake activity[12]. Upon PKA-mediated phosphorylation, PLN reduces it's inhibitory influence on SERCA allowing for an increased rate of SR Ca^{2+} reuptake. The increased rate of SERCA Ca^{2+} reuptake leads to an overall positive cellular lusitropic effect (increase in rate of relaxation). Additionally, PKA phosphorylation of troponin I reduces its affinity for Ca^{2+} which further increases the positive lusitropic effect seen with βAR signaling. Amongst these two proteins, PLN phosphorylation is the primary mechanism for the observed lusitropic effect[13]. The inotropic effect due to βAR activation occurs through increased intracellular and SR Ca^{2+} content from LTCC and PLN phosphorylation. PKA phosphorylated LTCC allow for the entry of more Ca^{2+} ions into the cell, which is represented by an increase in L-type calcium current ($I_{Ca,L}$). A recent study has shown that the LTCC may not be directly phosphorylated but require the phosphorylation of Rad, a monomeric G protein, to allow for the increase in $I_{Ca,L}$[14]. In either case, increased intracellular Ca^{2+} concentration leads to more contractile fiber activation and stronger overall contractions. The functional effects of RyR phosphorylation are disputed with some data showing that phosphorylation increases the RyR open probability[15,16] while other data shows that there is no effect resulting from RyR phosphorylation[17]. In summary, non-specific βAR stimulation activates the G_s-

AC-cAMP pathway leading to positive inotropic and lusitropic responses in cardiac ventricular myocytes.

1.5 α-Adrenergic Receptor Signaling

A second class of catecholamine activated GPCR, known as the α-adrenergic receptors (αARs), have been found to be present at a ratio of 10:1 (β:α) in the human myocardium[18]. αARs can be separated into two primary subtypes, α_1ARs and α_2ARs. Only α_1ARs have been found in cardiac myocytes[19]. α_1ARs can be further subdivided into three isoforms: α_{1a}ARs, α_{1b}ARs, and α_{1d}ARs. Although mRNA for all three subtypes are detected in cardiac myocytes, only the α_{1a}ARs and α_{1b}ARs are expressed. The α_{1b}AR is the dominant isoform and is found at a ratio of 1:2-4 (α_{1b}AR:α_{1a}AR)[20–22]. α_1ARs are primarily coupled to $G_{q/11}$ G proteins, with α_{1b}ARs also coupling to G_i[23,24]. Upon receptor stimulation, the $G_{q/11}$ subunits activate phospholipase Cβ1 (PLCβ1). PLCβ1 hydrolyzes phosphatidylinositol 4,5-bisphosphate (PIP$_2$) to inositol triphosphate (IP$_3$) and diacylglycerol (DAG). IP$_3$ can then bind to intercellular IP$_3$ receptors causing the release of internal Ca^{2+} stores. More importantly, DAG can activate protein kinase C (PKC), which phosphorylates select intracellular targets[25]. From this point, the $G_{q/11}$ signaling diverges into many different branches with a multitude of downstream effectors[26].
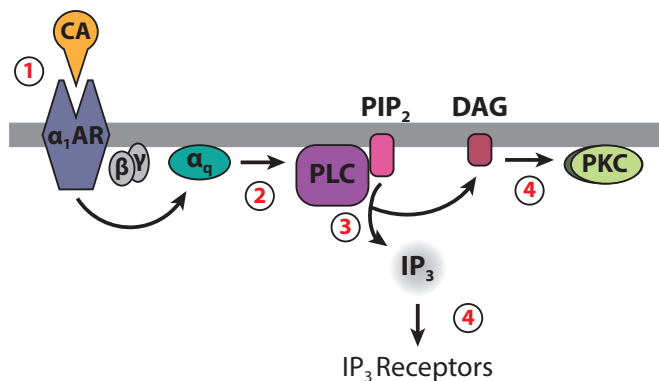
Figure 3: Canonical G_q/α_1-adrenergic receptor (α_1AR) signaling pathway

(1) A catecholamine binds to an α_1AR, which activates the G_q G-protein complex (α/β/γ). **(2/3)** The dissociated G_q α subunit then activates phospholipase C (PLC), which hydrolyzes phosphatidylinositol 4,5-bisphosphate (PIP$_2$) to inositol triphosphate (IP$_3$) and diacyl glycerol (DAG). **(4)** The second messenger IP$_3$ stimulates cardiac IP$_3$ receptors and DAG induces protein kinase C (PKC) to phosphorylate various intracellular targets.

Through this signaling pathway, α_1ARs are capable of creating minor PKC-mediated positive inotropic effects[27]. Interestingly, α_1ARs have also been found to produce negative inotropic effects[28]. The mechanisms for these positive and negative inotropic effects include activation of $I_{Ca,L}$, inhibition of βAR-stimulated $I_{Ca,L}$, inhibition of K^+ current, Na^+/H^+ exchanger activation resulting in cellular acidification and myofilament Ca^{2+} sensitivity regulation[29–33]. Recently, it has been shown that α_1ARs can produce cardioprotective functional effects in cases of prolonged catecholaminergic stimulation. Chronic α_1AR activation results in non-pathological hypertrophy in cardiac myocytes that does not reduce contractile function[34]. α_1AR stimulation also promotes survival signaling through activation of ERK, GATA4, and NFAT[35–37]. Furthermore, α_1AR activation induces

ischemic preconditioning where short periods of ischemia provide protection against later periods of longer ischemia[38].

The location of α_1ARs in cardiac myocytes is controversial. The classic GPCR signaling view is that the α_1ARs are located in the plasma membrane[39–41]. However, evidence has been presented that α_1ARs are actually primarily located in the nuclear membrane[42,43]. Either way, the resulting functional effects of α1AR stimulation in the heart are generally agreed upon.

1.6   Muscarinic Receptor Signaling

While sympathetic nervous system regulation of the heart occurs through the adrenergic receptors, parasympathetic nervous system regulation occurs through muscarinic receptors[44]. Muscarinic receptors are traditional seven transmembrane domain GPCRs activated by acetylcholine[45]. There are 5 subtypes of muscarinic receptors, M_{1-5}, expressed throughout various tissues[46,47]. These muscarinic receptor subtypes exhibit slight pharmacological and structural differences allowing them to be individually classified. The traditional means of signaling for the odd-numbered muscarinic receptor subtypes (M_1, M_3, and M_5) is believed to be due to $G_{q/11}$ coupling, which activates the PLC signaling pathway[48]. However, evidence has been found that M_1 and M_3 can also couple to G_i G-proteins leading to other cellular effects[49]. The even numbered muscarinic receptor subtypes (M_2 and M_4) couple to $G_{i/o}$ resulting in the inhibition of AC cAMP production[48]. Additionally, M_2 receptors can directly

couple to the G-protein-gated inwardly rectifying K$^+$ (GIRK) channel through the $\beta\gamma$ subunits of G$_i$[50].

In the heart, acetylcholine is released from the parasympathetic nerve varicosities, which stimulates cardiac muscarinic receptors[51]. M$_2$ is the primary muscarinic receptor subtype in mammalian cardiac tissue although evidence has been presented that M$_1$, M$_3$, and M$_4$ may also be present[46,52–54]. The presence of these other muscarinic receptor subtypes appears to be species and cardiac location specific leading to uncertain physiological roles. In a similar vein, the functional effects mediated by muscarinic receptors in the heart vary greatly based on the species, location, agonist concentration, and age of the cardiac preparation being studied[55]. In general, ventricular myocyte muscarinic stimulation leads to a decrease in inotropy, but usually only if there has been a preceding increase in cAMP[56]. Rat ventricular myocytes are one of the exceptions where muscarinic stimulation can cause a negative inotropic effect without prior cAMP stimulation due to the presence of ventricular GIRK channels, which hyperpolarizes the myocyte when activated by muscarinic stimulation[57].

For most mammalian species, parasympathetic regulation of ventricular myocytes is mainly through acetylcholine stimulation of M$_2$ G$_i$ signaling. The classical view of this muscarinic signaling pathway is that the M$_2$ G$_i$ α subunit inhibits AC5/6 production of cAMP leading to decreased PKA phosphorylation of EC coupling associated proteins including L-type Ca^{2+} channels[58–60]. More recently, M$_2$ activation of G$_i$ has also been tied to a cAMP stimulatory response due to G$\beta\gamma$ activation of AC4/7 in the presence of G$_s$[61,62]. Even with this

stimulatory component, the net cAMP-dependent response of ventricular M_2 activation is inhibitory leading to a decrease in ventricular inotropy[63].

An alternate explanation for the positive and negative muscarinic control of cAMP has been proposed to be through M_2 induced nitric oxide (NO)/cGMP production. The proposed pathway is acetylcholine activates M_2, which induces Ca^{2+}/calmodulin activation of nitric oxide synthase, which results in the production of NO, which in turn activates soluble guanylyl cyclase[64]. The soluble guanylyl cyclase then produces cGMP, which antagonizes cAMP effects by either stimulating PDE2 activity or activating protein kinase G (PKG)[65,66]. The stimulatory cAMP effect of muscarinic activation could also be explained by the cGMP inhibition of PDE3 activity leading to an increase in cellular cAMP[67]. Despite the observations that NO/cGMP inhibits cAMP and cAMP mediated functional effects, the evidence is inconsistent and contradictory in regards to whether NO/cGMP may be linked to muscarinic activation especially in ventricular myocytes[68–70].

1.7   Other cAMP Regulating Receptors

In addition to adrenergic and muscarinic receptors, a collection of other G-protein coupled receptors located in the ventricular myocardium have been shown to directly regulate cAMP. The stimulation of these receptors usually only occurs under certain physiological conditions or perturbations. Moreover, they are not considered part of the autonomic control of the heart. However, due to their ability to affect cAMP levels, these GPCR will be discussed briefly.

Histamine receptors are seven transmembrane domain GPCRs activated, as the name would suggest, by the autacoid histamine[71]. Of the four histamine receptor subtypes, H_1 and H_2 are the primary subtypes found in ventricular myocytes at varying levels based on cardiac location and species[72]. H_2 are G_s coupled and the predominantly expressed subtype in human ventricular myocardium[73,74]. In humans, histamine application leads to an increase in ventricular inotropy and lusitropy due to H_2/G_s mediated AC stimulation leading to increased cAMP levels and the resulting functional effects including increases in $I_{Ca,L}$[75,76].

Another autacoid, adenosine, has been shown to regulate βAR-stimulated cAMP levels and functional properties in ventricular cardiac myocytes. The adenosine receptor subtype A_1 is a GPCR associated with G_i and is located in ventricular myocardium[77,78]. Activation of this receptor inhibits AC activity and cAMP production, especially in the case of previous βAR G_s stimulation. Functional experiments confirm this signaling pathway as adenosine, in certain species, has no significant effect on basal contractility or baseline action potential parameters, unless they were previously stimulated through βAR signaling[79]. However, similarly to M_2, A_1 can also activate GIRK channels. Therefore, in species where GIRK channels are present in ventricular myocardium, such as rat, A_1 activation causes functional effects even at baseline conditions. Nonetheless, adenosine does not inhibit basal cAMP levels, but does antagonize βAR induced increases in cAMP[80]. Due to its anti-βAR signaling, adenosine has ventricular antiarrhythmic effects[78].

The hormonal peptide glucagon, normally known for its glycogenolysis and gluconeogenesis properties, also causes increases in ventricular inotropy through its interaction with cardiac glucagon receptors[81,82]. Glucagon receptors are GPCR mainly coupled to G_s resulting in AC stimulation and cAMP production experimentally[83]. There is some debate whether the glucagon induced functional effects in the heart are mediated through cAMP *in vivo*[84]. Glucagon receptors have also been shown to have promiscuous G-protein binding leading to coupling with G_i and G_q[85]. The variety of G-protein coupling options could explain the species-dependent differences in glucagon induced functional effects and increases in $I_{Ca,L}$[86,87].

Serotonin (5-HT) has been shown to produce inotropic and lusitropic increases in human atrial myocardium through a cAMP-dependent pathway[88]. A variety of 5-HT GPCR have been found in the heart, but it appears the G_s coupled 5-HT$_4$ receptor is responsible for mediating these functional changes[89]. Despite its effects on the atrium, 5-HT failed to illicit any functional effect in human ventricular tissue[90]. 5-HT$_4$ mRNA has been found in human ventricular myocardium, indicating possible expression. However, only under the special circumstances of combined congenital heart failure and non-selective PDE inhibition were 5-HT induced ventricular inotropic and lusitropic changes observed[91].

Prostaglandin receptors are also known to regulate cAMP in the heart. The prostaglandin, PGE$_2$, has been associated with a variety of cardiovascular diseases[92]. The PGE$_2$ receptors, EP receptors, are GPCR and are located in

cardiac myocytes[93]. The cAMP stimulating subtypes are EP_2 and EP_4, which couple to G_s[94]. The EP_3 subtype mainly couples to G_i and inhibits cAMP production[95].

1.7   cAMP Compartmentation

In 1979, it was observed that βAR and EP receptor stimulation both produced cAMP in perfused rat hearts. Notably, βAR activation also caused an increase in the rate of rise of left ventricular pressure among other functional changes, whereas prostaglandin E_1 (PGE1) activation of EP receptors, did not cause any functional changes even though it was producing cAMP[96]. Similar observations were seen again when the receptors were stimulated and contractile proteins were analyzed[97]. The results from these experiments indicated that simply increasing intracellular cAMP levels was not responsible for the functional effects associated with βAR activation. βAR activation had to be producing a more complex/regulated cAMP signal.

Furthermore, when β_1ARs or β_2ARs are selectively activated in rat cardiac myocytes different functional responses are observed. The stimulation of either receptor leads to a positive inotropic effect through increased I_{Ca} and intracellular Ca^{2+} transient[98]. However, β_1AR selective stimulation also leads to a positive lusitropic effect that does not occur from β_2AR selective stimulation[99]. These different sets of responses from the same type of receptor indicate that another level of physiological cAMP regulation must exist.

The theory of compartmentation was proposed to explain these divergent responses[100]. This theory stated that different receptor types are associated with distinct microdomains of cAMP that control specific cellular functions. Although further research over the years has confirmed this theory, the cellular mechanisms leading to compartmentation are still not well understood and many have been proposed over the years. Some of the prominent ones include: location of cAMP signaling complexes, localized cAMP degradation, intracellular physical barriers and cell shape, cAMP buffering, and alternative GPCR G-protein isoform coupling to name a few[101].

One of the primary mechanisms of cAMP compartmentation that has been investigated is the cellular localization of cAMP signaling proteins. GPCR activation is known for its rapid signaling kinetics that would be very difficult to achieve if the sarcolemma bound signaling proteins involved in the cAMP pathway (GPCR and AC) were uniformly distributed throughout the cellular membrane and interacting in a stochastic manner. This has led to the conclusion that the signaling proteins are located in complexes within plasma membrane microdomains. Regions of high concentration of glycosphingolipids and cholesterol within the plasma membrane, known as lipid rafts, have been proposed as one of these microdomains[102,103]. AC isoforms have been shown to be lipid raft or non-lipid raft specific[104]. In cardiac myocytes, β_1ARs and β_2ARs are localized to lipid rafts in the T-tubules, while β_1ARs are also found in non-raft domains of the sarcolemma[105]. The βARs in the T-tubules specifically couple to AC5, while the β_1ARs in the peripheral sarcolemma couple to AC6[106]. By creating

distinct subsets of coupled GPCRs and ACs with unique signaling properties, an initial framework for compartmentation is created through localized cAMP production.

Similarly to the initial cAMP signaling proteins, PKA has been shown to be specifically localized as well. PKA is a heterotetramer holoenzyme comprised of a regulatory subunit dimer (R) and two catalytic subunits (C)[107]. Upon cAMP binding to the regulatory subunit, the catalytic subunits are activated and proceed to phosphorylate target proteins. Similarly to AC and βARs, there are a variety of PKA isoforms, which are defined by their catalytic and regulatory subunits[108]. The catalytic domains possess relatively similar kinetics and target specificity[109]. Therefore, the regulatory subunits (RI and RII) have been of primary interest. The biochemical properties of PKAI (RI containing PKA) and PKAII (RII containing PKA) were found to be different with PKAI being more sensitive to cAMP activation[110,111]. Furthermore, PKAI and PKAII were found to be differentially expressed and targeted in cells through binding to specific A kinase anchoring proteins (AKAPs) [112,113]. AKAPs also bind other crucial signaling proteins including phosphatases, regulatory proteins, and phosphodiesterases (PDEs)[114]. For example, AKAP18δ targets PKAII into a complex with SERCA2 and PLN allowing for the targeted phosphorylation of PLN and the resulting increase in SERCA activity in response to βAR stimulation[115]. By regionalizing the signaling components, AKAPs allow for the preferential PKA-dependent phosphorylation of key functional proteins creating distinct cAMP signaling compartments.

Beyond localization of signaling proteins, one of the most logical mechanisms for cAMP compartmentation are intracellular barriers (chemical and physical). Phosphodiesterases (PDEs) are a class of enzymes that hydrolyze the cyclic nucleotides cAMP and cGMP[116]. By degrading cAMP, PDEs can act as chemical barriers assisting in the compartmentation of cAMP[117]. The properties of these barriers can be modulated through the expression of different PDE isoforms with unique enzymatic regulatory mechanisms, substrate specificity, kinetics, and intracellular localization[118,119]. In cardiac myocytes, the expressed cAMP-hydrolyzing PDE families are: PDE1, PDE2, PDE3, PDE4, and PDE8[120]. PDE1 is Ca^{2+}/calmodulin activated, PDE2 is cGMP activated, PDE3 is cGMP inhibited, and PDE4 is cGMP independent[121]. PDE4 and 8 preferentially hydrolyze cAMP, while PDE1, 2, and 3 hydrolyze both cAMP and cGMP at varying efficiencies[122]. The kinetics of each PDE are also slightly different[123]. Care must be taken, as each family of PDE has further isoforms with distinctive properties and expression. For example, PDE1A is the dominant isoform in rat and mouse heart and is cGMP selective. In contrast, PDE1C, the prominent isoform in human, dog, and rabbit, has a balanced specificity for cAMP and cGMP[124].

Furthermore, PDEs have been found to be differentially localized to distinct intracellular compartments. PDE3 and PDE4 were shown to have different expression patterns as seen through confocal imaging of immunolabeled neonatal rat ventricular myocytes with PDE3 having a non-homogenous trabecular pattern, while PDE4 displayed a granular and striated

pattern[125]. The localization of PDEs to unique intracellular regions occurs through

protein-protein interactions and direct binding to membrane lipids[119,126]. Of note is

the previously mentioned binding of PDEs to AKAPs. By targeting PDEs to cAMP

signaling complexes through AKAPs, the cAMP signal produced can be

restricted to the region of the signaling complex. As an example, mAKAP binds

PDE4 and PKA to a signaling complex in cardiac myocytes to allow for a

negative feedback loop to maintain cAMP compartmentation[127].

While chemical barriers established through PDE activity present an

important mechanism for cAMP compartmentation, computational models have

shown that PDE activity alone is not enough to prevent the intracellular free

diffusion of cAMP[128,129]. Researchers therefore hypothesized that physical

barriers of some sort had to also be playing a role in compartmentalizing the

cAMP signals. The distinct shapes of neuronal cell architecture were shown to be

creating physical barriers leading to higher cAMP gradients in dendrites

compared to the neuronal cell body[130]. Cardiac myocytes, on the other hand,

have a much more uniform overall cell shape, so another means of physical

cAMP separation had to be at play. Models with intracellular physical barriers

were able to recapitulate a compartmentalized cAMP signal while maintaining

physiological AC and PDE properties[131]. Experimental testing to determine

intracellular tortuosity demonstrated significant intracellular barriers in cardiac

myocytes supporting the conclusion for some form of physical

compartmentation[132]. Which intracellular structures are acting as physical

barriers are still unknown with many structures including the SR membranes, T-

tubules, and mitochondria being suspected. An anatomical computational model of the dyadic cleft (space between t-tubule membrane and junctional SR membrane) in cardiac myocytes was able to demonstrate cAMP compartmentation but only at reduced cAMP diffusion coefficients[129]. The reduced diffusion coefficients could occur through the anatomical barriers but also through the aid of molecular crowding and PKA buffering.

PKA binds cAMP with a high affinity and is present in large quantities in cardiac myocytes[133,134]. Additionally, it has been shown that a significant portion of the available cAMP pool is bound to PKA even when cAMP production is not being stimulated[135]. By binding a large portion of the available cAMP, cAMP diffusion can therefore be restricted to PKA containing regions. This phenomenon is known as PKA buffering and has been described as another mechanism of cAMP compartmentation.

The classical βAR signaling paradigm relies on the coupling of β_1ARs and β_2ARs to G_s proteins to stimulate cAMP production. However, β_2ARs have also been found to couple to G_i proteins[136–138]. G_i proteins act in opposition to G_s proteins and inhibit AC production of cAMP[139]. Interestingly, it was found that inhibiting G_i proteins with pertussis toxin (PTX), caused an enhanced β_2AR contractile response and allowed β_2AR stimulation to produce a lusitropic effect and phosphorylation of PLN in rat cardiac myocytes[136,140]. This indicates that β_2AR-G_i coupling is also possibly a mechanism for cAMP compartmentation. However, FRET-based experiments do not support the loss of β_2AR cAMP

compartmentation to PTX exposure and the physiological mechanism that would be responsible for β_2AR-G$_i$ cAMP compartmentation is unknown[105,140].

1.8   Cellular cAMP Measurement and Visualization Methods

Various techniques have been employed and developed to render a more complete picture of cAMP levels and localization in cells. The initial techniques were rather rudimentary and involved biochemical assays including cellular fractionation studies and radioimmunoassays. Although these assays are rather one dimensional in their measurements, crucial data was recovered and started investigation into the field of cAMP compartmentation. Using fractionation studies, Corbin et al. was able to demonstrate several important early findings including that approximately 50% of cellular cAMP was bound to PKA, mainly PKAII, in the low speed particulate fraction[135]. Furthermore, they showed that the application of epinephrine and 1-methyl-3-isobutylxanthine (IBMX), a non-selective PDE inhibitor, increased cAMP levels in the particulate and supernatant fractions. Around the same time as these initial observations, the previously described studies involving the differences between cAMP production of βAR and EP receptors were performed[96,97].

To further investigate cAMP dynamics and the idea of cAMP compartmentation, electrophysiological and fluorescent biosensor techniques were conceived to address the need to perform spatial and temporal cAMP measurements in intact live cells. A preliminary electrophysiological approach involved measuring $I_{Ca,L}$ functional responses to cAMP stimulating agonists,

which provided an indirect measurement of cAMP activity[117]. A technique to directly measure cAMP activity involved expressing cyclic nucleotide-gated (CNG) channels, which activate upon cyclic nucleotide binding, and recording their current responses to changes in cAMP. Rich et al. used genetically modified variants of these channels expressed in cell lines to demonstrate that AC stimulation with forskolin produced a high concentration of cAMP near the channels in the membrane while the global cAMP concentration remained low[131]. Using CNG channels to directly measure cAMP was an important advancement in the study of cAMP compartmentation. However, this technique possessed several critical limitations. One limitation was that CNG channels are targeted to the plasma membrane and cannot be used to measure cAMP dynamics in other specific regions of the cell. Additionally, CNG channels are also regulated by other intracellular signals including PIP3 and Ca^{2+} [141].

The other general approach to measure spatiotemporal cAMP dynamics in live cells is through the use of fluorescent biosensors. These biosensors were primarily designed around the principle of Fluorescence Resonance Energy Transfer (FRET). FRET is a non-radiative transfer of energy from an excited donor to acceptor fluorophore. This process is distance dependent and occurs through intermolecular dipole-dipole coupling[142]. The efficiency of FRET energy transfer (E) is defined by equation 1:

$$E = \frac{1}{1 + (R/R_0)^6} \tag{1}$$

where R is the distance between the donor and acceptor fluorophore and R_0 is a distance parameter called the Forster radius which is the distance where energy transfer is 50% efficient between the donor and acceptor[143]. As can be seen in Equation 1, the distance between donor and acceptor fluorophores is associated to the inverse sixth power of efficiency. Therefore, the efficiency of the FRET energy transfer is very sensitive to the separation of the donor and acceptor fluorophores (usually < 10 nm for transfer to occur) making FRET an ideal physical principle to employ in creating nanoscopic fluorescent biosensors[144].

The initial cAMP detecting FRET fluorescent biosensor was PKA-based[145]. A fluorescein donor fluorophore was attached to the catalytic domain of PKA I and a rhodamine acceptor fluorophore was attached to the regulatory domain of PKA I. When fluorescein stimulating light was shown on the cells, FRET would occur between the fluorescein and the rhodamine on the complexed subunits. As cAMP levels in the cell increased, it was believed that the catalytic domains of the labelled PKA dissociated from the regulatory subunits decreasing the FRET energy transfer. These changes in FRET could be detected using fluorescent microscopy allowing for non-destructive spatiotemporal measurements of cAMP in cells.

One limitation of this initial FRET biosensors was that it had to be microinjected into cells. Since then, a multitude of genetically encoded cAMP FRET biosensors have been created to investigate the different aspects of cAMP signaling in live cells. By varying different components of the biosensor such as using different fluorophores or cAMP binding domains, the FRET biosensors

could be adapted to address specific questions and avoid pitfalls associated with certain biosensor designs. Of note are the Epac-based cAMP FRET biosensors. Epac, exchange protein directly activated by cAMP, is a guanine-nucleotide-exchange factor with a cAMP binding site[146]. The Epac-based FRET biosensors were created by taking the cAMP binding site of Epac and attaching the donor fluorophore cyan fluorescent protein (CFP) and the acceptor fluorophore yellow fluorescent protein (YFP)[147]. When cAMP is not present, the fusion protein exhibits high FRET energy transfer between the two fluorophores. The binding of cAMP to the biosensor causes a conformational change which separates the CFP and YFP fluorophores reducing FRET energy transfer. By recording the FRET ratio of the fluorescence between the two fluorophores, cAMP levels can be measured.
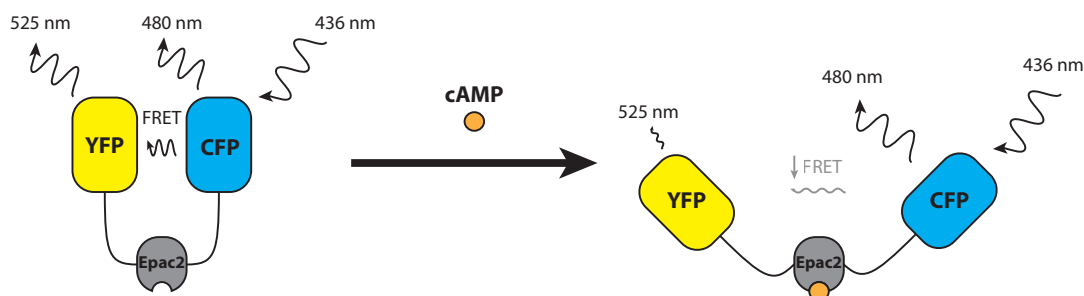
Figure 4: Epac2-camps FRET cAMP biosensor structure and function

Epac2-camps is composed of a yellow fluorescent protein (YFP) attached to the type 2 exchange protein directly activated by cAMP (Epac2) cAMP binding domain, which is in turn attached to a cyan fluorescent protein (CFP). Excitation of CFP with 436 nm light causes the emission of ~480 nm light from the CFP. Additionally, ~525 nm emission occurs from YFP due to the close proximity of the fluorophores, which allows for FRET energy transfer. A conformational change occurs in the biosensor upon cAMP binding to the Epac2 domain, which separates the fluorophores reducing FRET and therefore YFP emission light. Therefore, analyzing the ratio of CFP and YFP emission fluorescence allows for the detection of cAMP activity.

Many variations of the Epac-camps probe have been created including intracellular targeted and transgenically encoded versions[148,149]. Further classes of cAMP detecting FRET biosensors have also been developed. For example, the CUTie biosensor employs the cyclic nucleotide binding domain of the PKA regulatory subunit IIβ and an alternate configuration of CFP and YFP as the FRET fluorophores[150]. Due to the incredible flexibility of FRET-based cAMP biosensors, they have become the standard for intracellular cAMP compartmentation research.

1.9   Adrenergic Signaling in Heart Failure

Pathological changes to autonomic function occur in many life-threatening cardiac diseases, such as heart failure. Heart failure (HF) occurs when the hemodynamic demands of the body cannot be met by the heart. As the US population continues to age, the prevalence of HF continues to increase in the US with approximately 6.2 million adults in the US having heart failure between 2013-2016[151]. Out of the health conditions that are widely spread among the population, HF is one of the most common, disabling, costly, and deadly[152].

Upon changes in the bodies demand for oxygenated blood and/or myocardial injury, the sympathetic nervous system (SNS) is activated. As has been previously reviewed, this acute sympathetic stimulation helps increase cardiac output and causes favorable changes in other organ systems to maintain homeostasis. Problems arise, however, when this acute SNS stimulation becomes chronic. A large body of evidence has shown that chronic catecholamine exposure is deleterious to cardiac myocytes[153,154]. Chronic SNS stimulation causes pathological myocardial remodeling including hypertrophy and genetic expression changes[155]. In addition, βAR signaling is heavily disrupted and altered. β_1AR expression decreases and β_1AR are desensitized. β_2AR and α_1AR expression remains stable and, while still significantly less than β_1ARs, represent a greater proportion of the total adrenergic receptors in the heart during HF[9,156]. Furthermore, β_2ARs are redistributed and demonstrate changes in their cAMP compartmentation[105]. Due to the dysregulation and chronic stimulation of βAR signaling in HF, βAR antagonists, also known as β-blockers,

have been utilized in several clinical trials. These trials demonstrated a decrease in mortality in HF patients taking β-blockers and thus these βAR antagonists have become the standard of care in the treatment of HF[157–160].

Unfortunately, β-blockers are not effective as a treatment for all cases of HF. Approximately 50% of HF patients have a preserved left ventricular ejection fraction (LVEF)[151]. This type of HF is known as heart failure with preserved ejection fraction (HFpEF). While having a preserved LVEF during HF would suggest a better prognosis, this is not the case. HFpEF patients have similar odds for survival, which did not improve over time unlike HF cases with decreased LVEF[161]. HFpEF patients are generally older and the mechanism of heart failure is due to a decrease in left ventricular relaxation and increase in left ventricular stiffness[162]. As of now, there are no effective treatment strategies[163]. This is frightening as the proportion of HFpEF cases is increasing with the increase in age of the American population. Determining the exact mechanism and treatments for this form of HF should therefore be a high priority.

As previously discussed, α_1AR stimulation provides cardioprotective effects that prevent pathological remodeling of the heart. The ALLHAT clinical study was focused on developing better means for treating hypertension but inadvertently demonstrated that blocking α_1ARs increased the risk for heart failure in these patients[164,165]. Although this trial did not directly investigate the cardiac α_1AR blockade, it demonstrated that α_1ARs could be playing an important protective role in the heart.

Further evidence supporting the positive role of α_1ARs was seen in clinical trials where sympathetic stimulation and catecholamine levels were reduced with sympatholytics in HF patients. Based on the logic that sympathetic activity and catecholamine release is increased during heart failure, it would make sense that inhibiting sympathetic activity would improve cardiac function and HF progression. While these trials found that heart rate did in fact decrease and EF increased slightly, a troubling increase in mortality and adverse clinical events was also found. Combining the knowledge that βAR antagonism decreases mortality events in HF, it can be inferred that the resulting blockade of α_1ARs from sympatholytics is harmful to HF patients. Therefore, α_1AR stimulation stands as a potential avenue for HF treatment research.

1.10   Summary

cAMP signaling in ventricular myocytes is a complex process that involves a multitude of receptors and mechanisms to induce changes in cardiac functional properties necessary for maintaining homeostasis in higher order organisms. While a solid foundation of research has been established in this field, many important questions still remain unanswered, especially in regards to receptor function and cAMP compartmentation. Chapter 2 of this dissertation will address non-canonical α_1AR signaling as it relates to cAMP. The research contained in this chapter clarifies the connection between α_1AR and βAR cAMP signaling. Chapter 3 of this dissertation focuses on the characterization of a novel FRET

biosensor, which confirmed that β_2AR cAMP signaling is compartmentalized and that the compartmentalization is through the involvement of certain PDE isoforms. A final concluding chapter will summarize these discoveries and tie in important clinical significance and possible future directions.

Chapter 2

α_1-Adrenergic Receptor Regulation of cAMP Production in Adult Cardiac Ventricular Myocytes

2.1   Abstract

Sympathetic regulation of the heart is largely mediated through the activation of β-adrenergic receptors (βARs) and subsequent stimulation of cAMP production in cardiac myocytes. However, norepinephrine, the main endogenous neurotransmitter that triggers these βAR responses, also activates α_1-adrenergic receptors (α_1ARs). Although canonically not associated with cAMP signaling, α_1AR stimulation has been previously shown to inhibit βAR mediated functional responses in the heart. The purpose of this study was to demonstrate that α_1AR activation does indeed inhibit cAMP production in cardiac ventricular myocytes, and determine the mechanism responsible for this effect. Live-cell imaging of fluorescence resonance energy transfer (FRET) based biosensor responses was used to measure changes in cAMP activity in adult rat ventricular myocytes. Using this approach, α_1AR activation was found to inhibit cAMP activity under baseline conditions as well as in the presence of βAR stimulation. These effects could be explained by a tyrosine kinase-dependent mechanism acting at the level of the βAR. Furthermore, α_1AR stimulation was found to limit βAR production of cAMP by norepinephrine, demonstrating the physiological significance of this signaling mechanism.

2.2   Introduction

Activation of the sympathetic nervous system results in the release of catecholamines that trigger a variety of cardiovascular responses[166]. In the heart, many of these effects are mediated by the β-adrenergic receptor (βAR) signaling pathway, which involves stimulatory G protein (G_s)-dependent activation of adenylyl cyclase (AC) and subsequent production of the diffusible second messenger 3',5'-cyclic adenosine monophosphate (cAMP)[8]. Increased levels of cAMP activate protein kinase A (PKA), which phosphorylates several key targets involved in regulating the electrical and mechanical properties of cardiac myocytes[167]. Despite the fact that most acute functional responses to sympathetic stimulation can be explained by βAR activation, the primary neurotransmitter mediating these actions, norepinephrine, is also a potent α-adrenergic receptor agonist. The α_1-adrenergic receptor (α_1AR) is the predominant subtype found in cardiac myocytes[168], and activation of this receptor has been reported to increase contractility, in addition to producing cardioprotective adaptations such as physiologic hypertrophy, cardiac myocyte survival, and cardiac preconditioning[34]. These α_1AR responses can be attributed to activation of G_q signaling pathways, which are not typically associated with changes in cAMP production[169]. However, α_1AR activation has also been reported to antagonize various βAR responses by a mechanism that is not well characterized[33,170–176]. The goal of the present study was to examine the effects that α_1AR stimulation have on cAMP production in adult ventricular myocytes using fluorescence resonance energy transfer (FRET) based biosensor

technology. The results demonstrate that α_1ARs actually inhibit cAMP production through a tyrosine kinase-dependent mechanism that acts at the level of the βAR. Furthermore, α_1AR stimulation was found to limit βAR production of cAMP by norepinephrine. These results highlight the importance of the interactions between α_1ARs and βARs when evaluating cardiac responses to sympathetic stimulation by endogenous neurotransmitters under physiological and pathological conditions.

2.3   Materials and Methods

Cell Isolation and Culture

Ventricular cardiac myocytes were isolated from 250-300 g male adult Sprague-Dawley rats (Charles River, MA) as previously described[177]. All protocols were performed in accordance with the Guide for the Care and Use of Laboratory Animals as adopted by the U.S. National Institutes of Health and approved by the Institutional Animal Care and Use Committee at the University of Nevada, Reno. In brief, rats were anesthetized by intraperitoneal injection of pentobarbital (150 mg/kg). The hearts were then excised, attached to a Langendorff apparatus, and perfused with a collagenase and protease containing solution in order to obtain isolated myocytes. These cells were then plated in M-199 media (Life Technologies, CA) supplemented with creatine (5 mM), taurine (5 mM), penicillin-streptomycin (1x), and bovine serum albumin (0.1%), and then transduced with an adenovirus encoding the Epac2-camps FRET biosensor. These cells were kept in culture (37°C and 5% CO_2) for no more than 24 hours.

Fluorescence Resonance Energy Transfer (FRET)

Live cell imaging was used to measure changes in cAMP activity detected by the Epac2-camps biosensor as previously described[177,178]. Briefly, cardiac myocytes expressing the biosensor were placed in a bath chamber on the stage of an Olympus IX81 inverted microscope and perfused with extracellular solution at room temperature. The donor fluorophore (eCFP) of the FRET based biosensor was excited using a Lambda DG-4 light source (Sutter Instruments, CA) and a D436/20 bandpass filter. Donor and acceptor (eYFP) fluorescence was measured simultaneously using an OrcaD2 dual chip CCD camera (Hamamatsu, Inc., Japan) fitted with 483/32 and 542/27 bandpass filters. Whole cell cAMP was defined as the change in background and bleed-through corrected eCFP/eYFP fluorescence intensity ratio (ΔR) divided by the baseline ratio (R_0). The FRET responses were then normalized to a maximally stimulated FRET response from the same cell generated by the application of 1 μM of the non-specific βAR agonist Isoproterenol (Iso) and 100 μM of the non-specific phosphodiesterase (PDE) inhibitor 3-isobutyl-1-methylxanthine (IBMX).

Chemicals and Materials

Phenylephrine, forskolin (FSK), Erythro-9-(2-hydroxy-3-nonyl) adenine (EHNA), cilostamide, rolipram, and norepinephrine (NE) were purchased from Tocris Bioscience (Bristol, UK). Lavendustin A was purchased from Cayman Chemical (Ann Arbor, MI). M-199 and penicillin-streptomycin were purchased

from Life Technologies (Carlsbad, CA). All other chemicals were acquired from

Sigma-Aldrich (St. Louis, MO). Fresh stocks of Iso and IBMX were made daily.

Statistical Analysis

Data values are represented as mean ± SEM of *n* cells from the hearts of

N animals (*n/N*) in the text and mean ± SD in the figure scatterplots. Cardiac

myocytes from different isolations were randomly allocated to various

experiments to reach an appropriate number of cells (n = 10-15) based on power

calculations. The cutoff for statistical significance was set at p < 0.05. These p-

values were calculated through unpaired two-tailed Student's t-test for

comparison between two unrelated groups using Prism (version 8.4.3,

GraphPad, CA).

2.4   Results

α_1-AR inhibition of cAMP activity in the presence of βAR activation

Previous studies have demonstrated that α_1AR activation can antagonize

functional responses produced by βAR stimulation[33,171–176]. To test the

hypothesis that these effects are due to inhibition of cAMP production, we

measured cAMP responses in isolated adult rat ventricular myocytes (ARVMs)

expressing the cAMP biosensor, Epac2-camps[147]. These cells were first exposed

to the non-selective βAR agonist isoproterenol (Iso, 10 nM), which produced an

increase in cAMP activity that was 45.3 ± 5.0% (n/N = 13/3) of the maximal

response (%Max) elicited by subsequent exposure to 1 µM Iso + 100 µM IBMX in

the same cells. As predicted, exposure to the α_1AR agonist methoxamine in the continued presence of Iso produced a large inhibitory effect. The decrease in cAMP activity produced by exposure to 3 µM methoxamine was -30.6 ± 5.0 %Max (n/N = 13/3) (Figure 1A). A similar effect was observed in cells exposed to phenylephrine, another selective α_1AR agonist. Exposure to 30 µM phenylephrine in the presence of 10 nM Iso inhibited the cAMP response by -30.7 ± 5.0 %Max (n/N = 11/3) (Supplemental Figure 1). Furthermore, the inhibitory effect of methoxamine was attenuated (-10.9 ± 4.8 %Max, n/N = 11/3) in cells pretreated with the selective α_1AR antagonist prazosin (1 µM, Figure 1B and C). Altogether, these findings support the idea that α_1AR activation inhibits βAR production of cAMP in ARVMs.
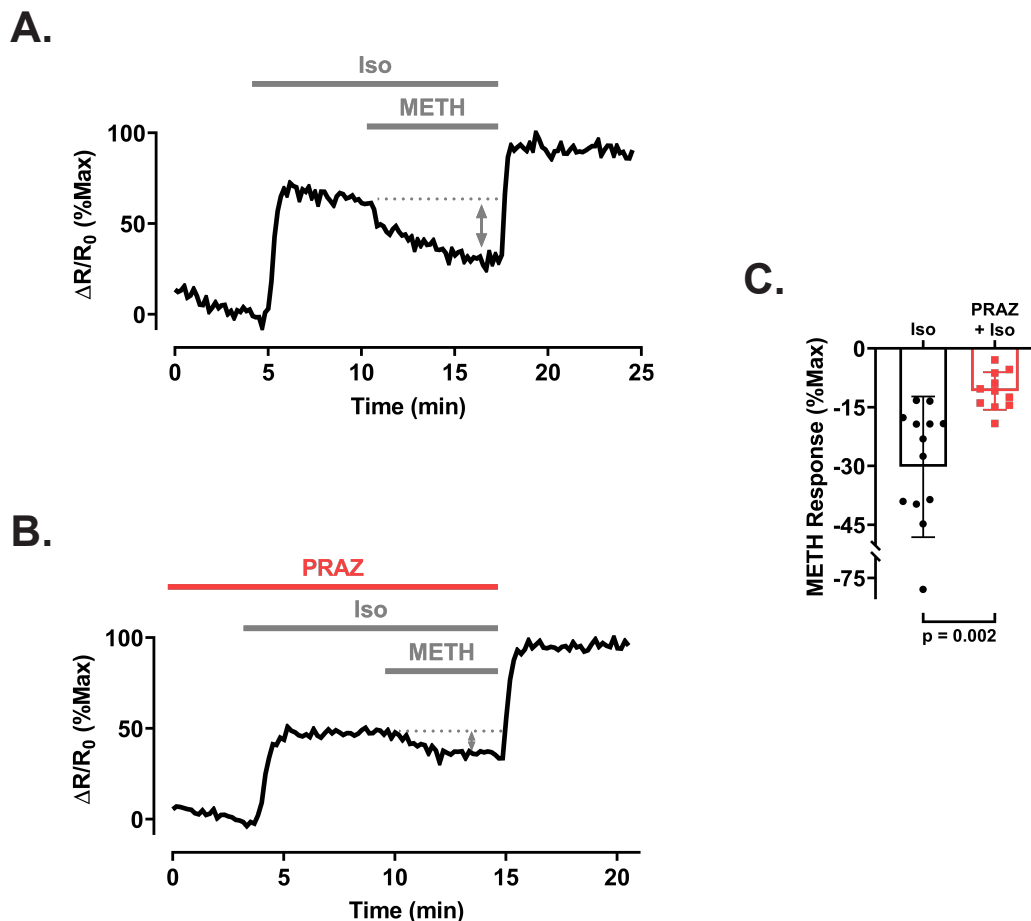
Figure 1: Effect of α₁AR activation on βAR stimulated cAMP

(A) Time course of changes in cAMP activity detected by the Epac2-camps biosensor produced by exposure to the non-specific βAR agonist isoproterenol (Iso, 10 nM) followed by Iso plus the α₁AR agonist methoxamine (METH, 3 μM) in the absence **(A)** and presence **(B)** of the α₁AR antagonist prazosin (PRAZ, 1 μM). FRET responses (ΔR/R₀) were normalized to the magnitude of the maximal cAMP response observed upon exposure to 1 μM Iso + 100 μM IBMX in the same cell. **(C)** Average response (± SD) to METH in the absence (n/N = 13/3) and presence (n/N = 11/3) of prazosin (red) (p = 0.002 as determined by two-tailed Student's t-test).

α_1-AR inhibition of cAMP activity in the absence of βAR activation

To determine whether the inhibitory effect of α_1AR stimulation is specific for βAR production of cAMP, we examined the effect of methoxamine in the absence of isoproterenol. In these experiments, exposure to 3 µM methoxamine alone caused cAMP activity to drop below baseline by -13.5 ± 2.4 %Max, N/n =11/4 (Figure 2A). We also examined the effect of methoxamine in cells where cAMP activity was first stimulated by an agonist acting independent of the βAR; in this case, we used forskolin a direct activator of adenylyl cyclase. For these experiments, myocytes were first exposed to 50 nM forskolin alone, which increased cAMP activity by 34.1 ± 3.7 %Max (n/N = 11/3) (Figure 2B). Subsequent addition of 3 uM methoxamine in the continued presence of forskolin resulted in inhibition of the cAMP response by -14.0 ± 5.9 %Max (Figure 2C).
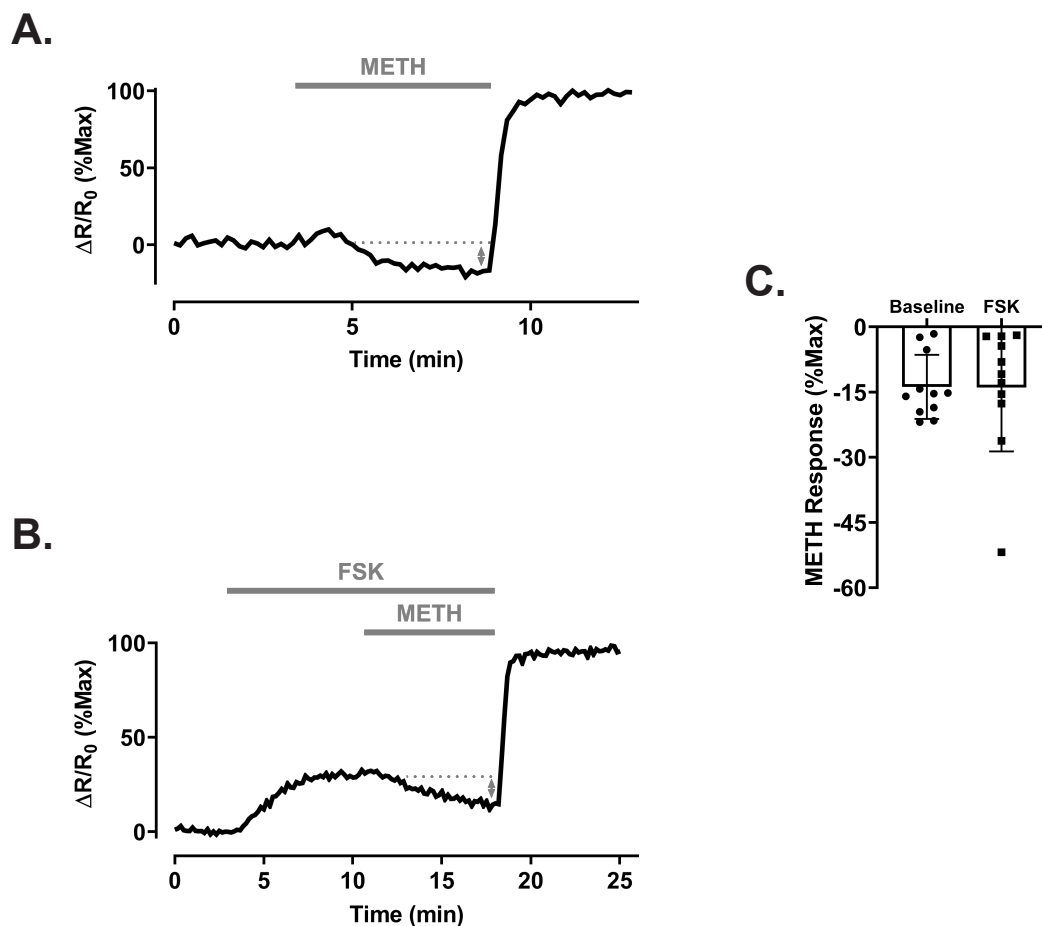
Figure 2: Effect of α₁AR activation on cAMP activity in the absence of βAR stimulation

Time course of changes in cAMP activity detected by Epac2-camps biosensor produced by exposure to the α₁AR agonist methoxamine (METH, 3 μM) alone **(A)** or METH following direct activation of adenylyl cyclase with forskolin (FSK, 50 nM) **(B)**. FRET responses ($\Delta R/R_0$) were normalized to the magnitude of the maximal cAMP response observed upon exposure to 1 μM Iso + 100 μM IBMX in the same cell. **(C)** Average response (± SD) to METH in the absence (n/N = 11/4) and presence of FSK (n/N = 11/3).

The ability of methoxamine to inhibit cAMP activity in the absence of a

βAR agonist might be explained if α₁AR stimulation works by directly inhibiting

AC activity. However, another possibility is that cAMP production is facilitated by

βARs acting on AC, even in the absence of a receptor agonist[179], and that

methoxamine is able to inhibit this effect. To distinguish between these

possibilities, we conducted experiments using the drug nadolol. While

traditionally viewed as a βAR antagonist, nadolol actually exhibits inverse agonist

properties, stabilizing the βAR in an inactive state and reversing agonist-

independent activity[180]. Consistent with this idea, exposure to 10 μM nadolol

alone resulted in a large decrease in baseline cAMP (-124.0 ± 30.0 %Max, n/N =

10/4). Furthermore, subsequent addition of 3 μM methoxamine in the continued

presence of nadolol caused only a small, but insignificant change in cAMP levels

(-3.1 ± 1.4 %Max) (Figure 3A). We also examined nadolol's effect on

methoxamine inhibition of the forskolin response. In myocytes pre-exposed to

nadolol, addition of 50 nM forskolin caused an increase in cAMP activity by 6.6 ±

1.6 %Max (n/N = 10/3) (Figure 3B). This is much smaller than the response to

forskolin in the absence of nadolol, consistent with the idea that βARs facilitate

forskolin responses even in the absence of a receptor agonist. Furthermore,

subsequent addition of methoxamine in the continued presence of nadolol +

forskolin did not affect cAMP activity (-0.6 ± 0.8 %Max) (Figure 3C). These

results support the conclusion that α_1AR inhibition of cAMP activity in the

absence of βAR agonist can still be explained by actions at the level of the βAR.
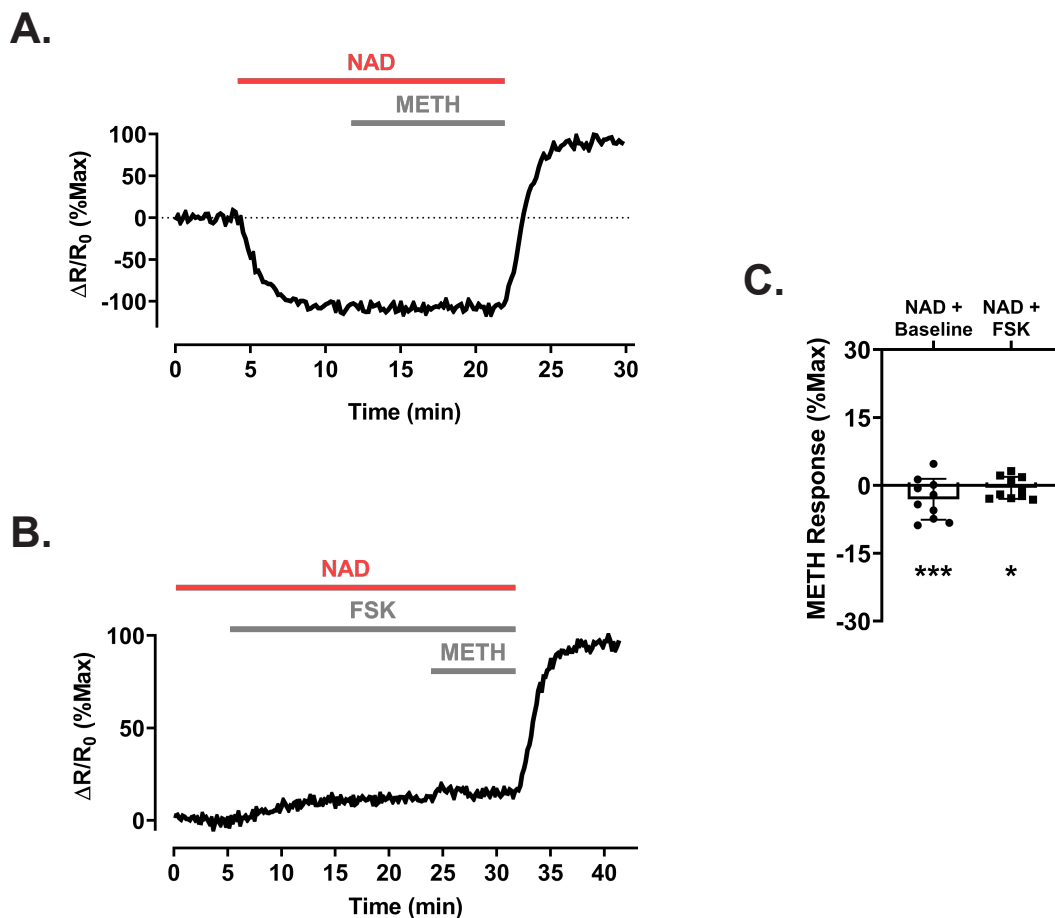
Figure 3: Effect α₁AR stimulation on cAMP activity in the presence of a βAR inverse agonist

(A) Time course of changes in cAMP activity detected by the Epac2-camps biosensor produced by exposure to βAR inverse agonist nadolol (NAD 10 μM) followed by NAD plus the α₁AR agonist methoxamine (METH, 3 μM). **(B)** Time course of changes in cAMP activity following exposure to forskolin (FSK, 50 nM) followed by FSK plus METH in a cell pre-exposed to NAD. FRET responses ($\Delta R/R_0$) were normalized to the magnitude of the maximal cAMP response observed upon subsequent exposure to 1 μM Iso + 100 μM IBMX in the same cell. **(C)** Average response (± SD) to METH in the presence of nadolol (n/N = 10/4) or NAD + FSK (n/N = 10/3). Asterisks indicate the results of two-tailed Student's t-tests of METH response in the absence (Figure 2A) vs. the presence of NAD (A) and METH response in the presence of FSK (Figure 2B) vs. the presence of NAD + FSK (B); ***: $p = 0.0008$, *: $p = 0.01$.

α_1AR inhibition of cAMP activity does not involve changes in PDE activity

An earlier study suggested that α_1AR stimulation inhibits βAR responses by a mechanism involving an increase in phosphodiesterase (PDE) activity. This conclusion was based on the ability of the non-selective PDE inhibitor IBMX to block the effect of α_1AR stimulation[170]. Therefore, we examined the possibility that changes in PDE activity contributed to α_1AR inhibition of cAMP activity in our experiments. The three main PDE isoforms responsible for metabolizing cAMP in ARVMs are PDE2, PDE3, and PDE4[181]. Because of the high basal AC activity in cardiac myocytes, exposure to the non-selective PDE inhibitor IBMX results in cAMP responses that saturate the Epac2-camps biosensor[177]. Therefore, we tested the ability of methoxamine to inhibit cAMP activity in the presence of PDE isoform selective inhibitors. Exposure to the PDE2 inhibitor EHNA (10 µM) resulted in a small increase in steady cAMP activity (3.4 ± 1.4 %Max, n/N = 12/3). However, subsequent exposure to methoxamine still produced a substantial inhibitory effect (-19.4 ± 2.6 %Max) (Figure 4A). Similarly, exposure to the PDE3 inhibitor cilostamide (10 µM) resulted in a slightly larger increase in steady-state cAMP activity (12.5 ± 2.0 %Max, n/N = 10/4) followed by subsequent inhibition upon addition of methoxamine (-18.4 ± 3.3 %Max) (Figure 4B). Exposure to the PDE4 inhibitor rolipram (10 µM) led to a much larger increase in steady state cAMP activity (47.7 ± 11.5 %Max, n/N = 10/3), yet methoxamine still produced a large decrease of cAMP activity (-51.8 ± 10.6 %Max) (Figure 4C). The size of the inhibitory effect of methoxamine observed in the presence of either EHNA or cilostamide was similar in magnitude to that

produced by methoxamine alone (see Figure 2). However, the inhibitory effect

observed in the presence of rolipram was considerably larger (Figure 4D). The

fact that inhibition of PDE activity did not block the response to methoxamine

suggests that that the inhibitory effect of α1AR stimulation on cAMP activity does

not involve upregulation of PDE activity.
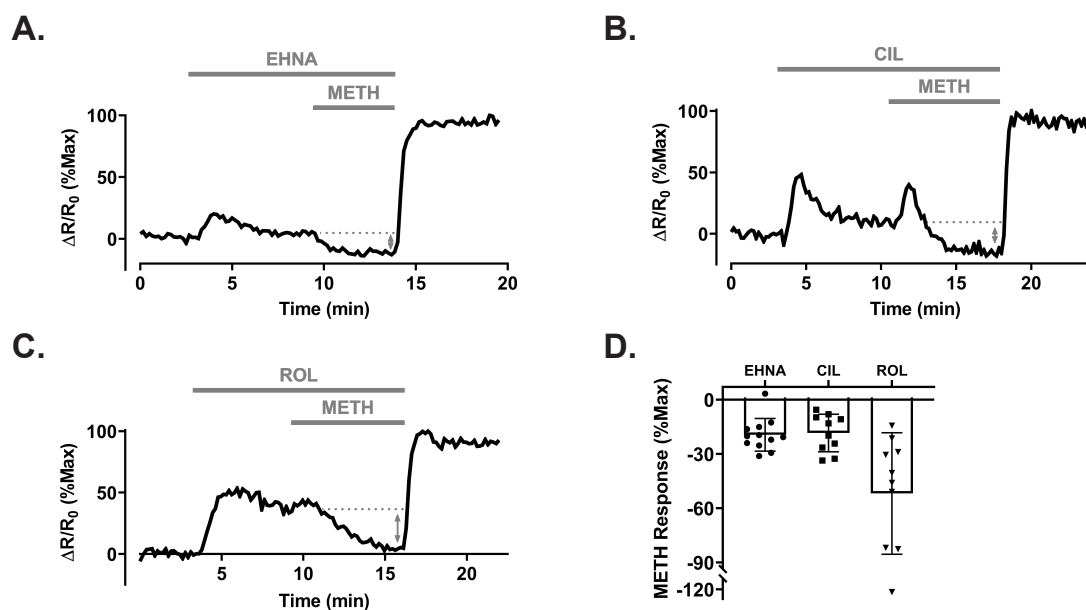
Figure 4: Effect of α1AR stimulation on cAMP activity in the presence of selective PDE isoform inhibition

Time course of changes in cAMP activity detected by Epac2-camps in response to the α1AR agonist methoxamine (METH, 3 µM) following exposure to the PDE2 inhibitor EHNA (10 µM) **(A)**, the PDE3 inhibitor cilostamide (CIL, 10 µM) **(B)**, and the PDE4 inhibitor rolipram (ROL, 10 µM) **(C)**. FRET responses ($\Delta R/R_0$) were normalized to the magnitude of the maximal cAMP response observed upon subsequent exposure to 1 µM Iso + 100 µM IBMX in the same cell. **(D)** Average response (± SD) to METH in the presence of EHNA (n/N = 12/3), CIL (n/N = 10/4), and ROL (n/N = 10/3).

α_1AR inhibition of cAMP operates through a tyrosine kinase pathway

It has been proposed that α_1AR inhibition of βAR induced functional responses involves a tyrosine kinase dependent mechanism acting directly at the level of the βAR[176,182]. To determine whether α_1AR inhibition of cAMP activity involves a tyrosine kinase dependent mechanism, we examined the effects of methoxamine in the presence of tyrosine kinase inhibition. In the first set of experiments, we used cells pre-exposed to the tyrosine kinase inhibitor genistein (50 μM). In these cells, exposure to 10 nM Iso produced an increase in cAMP activity (67.5 ± 2.5 %Max, n/N = 11/3). However, subsequent exposure to 3 µM methoxamine revealed that the inhibitory effect had been mostly attenuated (-6.2 ± 1.6 %Max) (Figure 5A). To confirm this result, we conducted a second set of experiments using cells pre-exposed to another tyrosine kinase inhibitor, lavendustin A (5 µM). Again, exposure to 10 nM Iso produced an increase in cAMP activity (38.9 ± 4.0 %Max, n/N = 12/3). However, addition of methoxamine resulted in an a slight increase, rather than a decrease, in cAMP production (16.3 ± 5.4 %Max) (Figure 5B). These results support the conclusion that α_1AR inhibition of cAMP production involves a tyrosine kinase dependent mechanism.
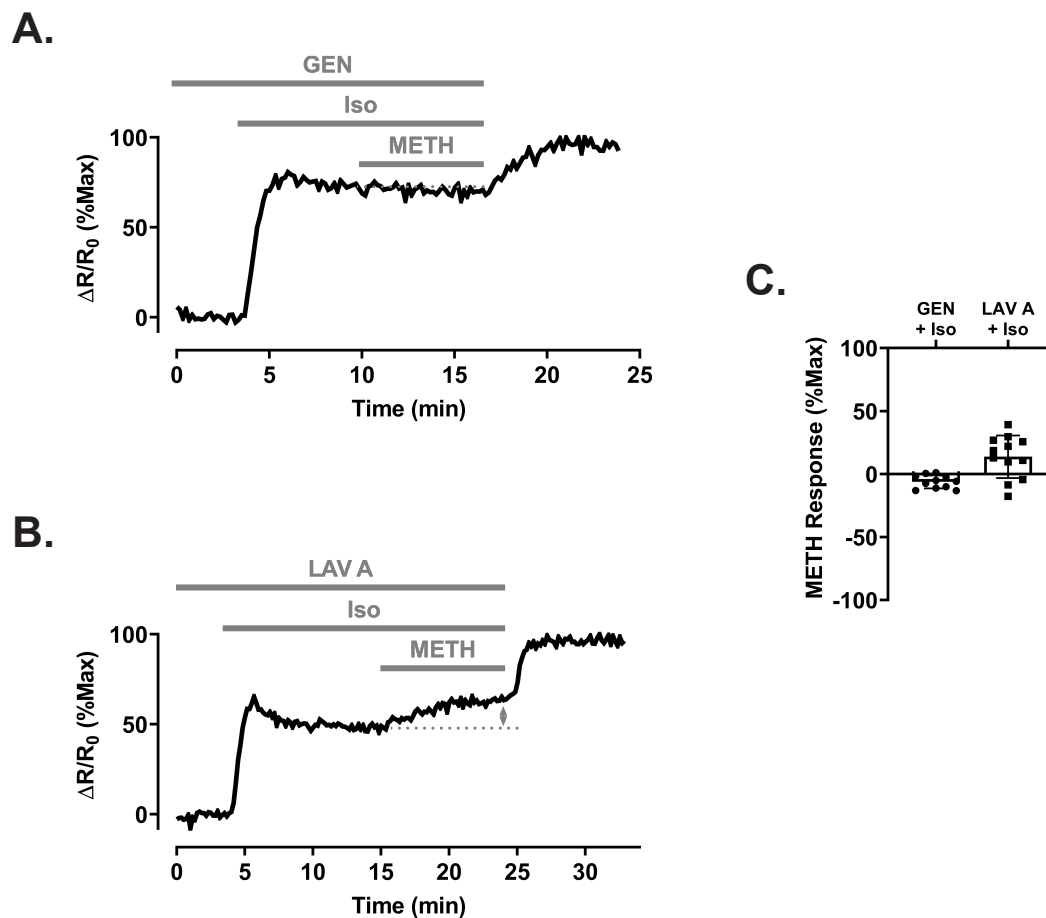
Figure 5: Effect of tyrosine kinase inhibition on the cAMP response to α₁AR stimulation

Time course of changes in cAMP activity detected by the Epac2-camps biosensor produced by exposure to isoproterenol (Iso, 10 nM) and Iso plus the α₁AR agonist methoxamine (METH, 3 µM) in ARVMs treated with the tyrosine kinase inhibitors genistein (GEN, 50 μM) **(A)** or Lavendustin A (LAV A, 5 μM) **(B)**. FRET responses (ΔR/R$_0$) were normalized to the magnitude of the maximal cAMP response observed upon subsequent exposure to 1 μM Iso + 100 μM IBMX in the same cell. **(C)** Average response (± SD) to METH in cells treated with GEN (n/N = 11/3) or LAV A (n/N = 12/3).

α₁AR regulate endogenous stimulation of βAR cAMP

The primary neurotransmitter responsible for mediating sympathetic

effects on the heart is norepinephrine (NE). The acute functional responses

produced by this endogenous catecholamine are most often associated with the activation of β_1ARs[183]. However, NE is also a potent α_1AR agonist[184]. Furthermore, we have previously demonstrated that blocking α_1AR activation significantly enhances the sensitivity of functional responses produced by NE[173]. To directly test the hypothesis that this behavior can be explained by the effects of α_1ARs on cAMP production, we measured the change in cAMP activity produced by NE in the presence and absence of prazosin (Figure 6A). In untreated cells, exposure to 30 nM NE resulted in an increase in cAMP activity of 15.0 ± 2.0 %Max (n/N = 11/3). However, the magnitude of the response to NE more than doubled (33.2 ± 3.3 %Max) in cells pretreated with the α_1AR antagonist prazosin (1 μM) (Figure 6B). These results indicate that α_1AR attenuation of the cAMP response produced by β_1AR activation contributes to the net effect of the endogenous neurotransmitter NE.
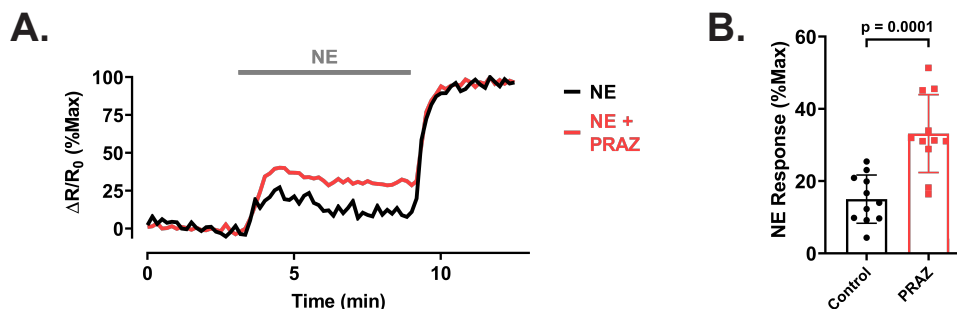
Figure 6: Contribution of α_1AR stimulation to the cAMP response produced by the endogenous neurotransmitter norepinephrine.

(A) Time course of changes in cAMP activity detected by the Epac2-camps biosensor produced by exposure to norepinephrine (NE, 30 nM) in the absence (black) or presence (red) of the α_1AR antagonist prazosin (PRAZ, 1 μM). FRET responses ($\Delta R/R_0$) were normalized to the magnitude of the maximal cAMP response observed upon subsequent exposure to 1 μM Iso + 100 μM IBMX in the same cell. **(B)** Average response (± SD) to NE in the absence (n/N = 11/3) or presence (n/N = 11/3) of PRAZ (p = 0.0001 as determined by Student's t-test).

2.5   Discussion

Previous studies have demonstrated that α_1AR activation antagonizes

βAR induced functional responses in the intact heart as well as isolated

ventricular myocytes. This includes inhibition of βAR regulation of ventricular

contraction and various ion channel responses[33,171–176]. One possible explanation

for this behavior is that α_1AR stimulation, acting through one of its canonical

signaling pathways, exerts its influence at the level of the functional effector

involved. Along these lines, it has been suggested that α_1AR antagonism of

cAMP-dependent L-type Ca^{2+} channel activity can be explained by a protein

kinase C (PKC) dependent mechanism acting directly at the level of the ion

channel[174]. However, this cannot explain the ability of α_1AR stimulation to inhibit

most cAMP-dependent responses[173,176]. A simpler mechanism would be if α_1ARs

somehow affect the production or degradation of cAMP, which mediates these βAR responses. Several studies have examined the effect of α_1AR activation on cAMP activity in various cardiac preparations using conventional biochemical assays, and the reported results have ranged from inhibition to stimulation of cAMP[40,170,185–188]. The goal of the present study was to evaluate the effects of α_1AR stimulation on cAMP activity using a newer, more sensitive approach. To that end, we measured changes in cAMP activity in adult ventricular myocytes expressing the FRET-based biosensor Epac2-camps, using a live cell imaging technique.

Consistent with prior studies investigating functional effects, we found that the increase in cAMP activity produced by the βAR agonist isoproterenol could be inhibited by the selective α_1AR agonist methoxamine, and this effect could be mimicked by phenylephrine and attenuated by prazosin. Such responses can be explained by either α_1AR inhibition of cAMP production or stimulation of cAMP degradation. Our previous work suggested that α_1AR stimulation actually inhibits cAMP production by acting directly at the level of the βAR[173,176]. This conclusion was supported by evidence that α_1ARs inhibit cAMP-dependent ion channel responses to β-adrenergic, but not histamine (H_2) receptor activation in guinea pig ventricular myocytes[173,176]. We could not replicate this approach in the present study, because histamine does not produce a sustained cAMP response in ARVMs (unpublished observation). However, we were able to examine the effects of α_1AR stimulation on cAMP responses under baseline conditions and in response to direct activation of AC with forskolin. In both cases, we found that

methoxamine produced an inhibitory effect, which could be taken as evidence that the decrease in cAMP activity was mediated by a mechanism that is independent of the βAR. However, this response was eliminated in the presence of nadolol, a direct βAR inverse agonist. Nadolol itself produced a large decrease in basal cAMP activity. This suggests that βARs affect AC activity, even in the absence of agonist stimulation. Furthermore, the absence of a response to methoxamine under these conditions supports the conclusion that α_1ARs act through a mechanism that involves the βAR.

Although the results of our current and previous work support the idea that α_1AR stimulation decreases cAMP levels by inhibiting βAR stimulation of AC activity, it has also been suggested that this α-adrenergic effect may be explained by an increase in PDE activity[170]. This conclusion was based on the observation that the α_1AR-dependent decrease in cAMP activity was not observed in the presence of IBMX, a non-selective PDE inhibitor. However, this approach is problematic as it cannot discern between stimulation of PDE activity or inhibition of βAR stimulated cAMP production as the α_1AR-dependent mechanism for decreasing cAMP. In the present study, we used a more precise approach by selectively inhibiting the different PDE isoforms one at a time. The fact that methoxamine continued to elicit an inhibitory effect in all cases, suggests that PDE activity is not being stimulated and that α_1AR inhibition of cAMP production may be explained solely on the basis of an effect occurring at the level of the βAR.

The question is then: through what signaling pathway do α_1ARs exert their effect on βARs? We found that the α_1AR-induced decrease in cAMP production is blocked by inhibiting tyrosine kinase activity. This is consistent with our previous work, demonstrating that inhibition of tyrosine kinase activity also blocks α_1AR antagonism of βAR functional responses[176]. Direct phosphorylation of the βARs by a tyrosine kinase could be involved as phosphorylation of tyrosine residues on the β_2AR has been found to uncouple it from downstream signaling in non-cardiac preparations[189]. Although the effect of α_1AR inhibition of cAMP production in the heart most likely involves β_1ARs, it has been demonstrated that β_1ARs are also a substrate for tyrosine phosphorylation[182]. Furthermore, a key tyrosine residue located in the second cytosolic loop of the β_1AR is believed to be associated with G-protein coupling[190]. Therefore, phosphorylation of this site could possibly impede receptor activation of AC.

The specific tyrosine kinase responsible for phosphorylating βARs in the heart is unknown. However, there are many examples of signaling crosstalk between G-protein coupled receptors (GPCRs) and tyrosine kinases in other systems[191]. Several studies have demonstrated that insulin and insulin-like growth factor 1 (IGF-1) are able to antagonize βAR responses in non-cardiac preparations[192,193]. This effect occurs through direct tyrosine phosphorylation of βARs by the insulin and IGF-1 receptors, both of which have intrinsic tyrosine kinase activity[194]. Moreover, the AT1 receptor, another GPCR, has been shown to be phosphorylated by the non-receptor Src tyrosine kinases[195]. Therefore, a

wide array of receptor and non-receptor tyrosine kinases are potential candidates for mediating α_1AR inhibition of βAR responses in the heart.

Cardiac myocytes express at least two isoforms of α_1AR, α_{1A}AR and α_{1B}AR, both of which have been reported to elicit acute functional responses. For example, in the absence of βAR stimulation, phenylephrine has been previously shown to produce both positive and negative inotropic effects in different cardiac preparations[28,196]. These opposing actions are believed to involve different α_1AR subtypes[197,198]. It has been suggested that the α_{1A}AR mediates positive inotropic responses through the traditional G_q/PKC pathway[199], whereas the α_{1B}AR produces negative inotropic effect through a $G_{i/o}$ pathway[40]. While $G_{i/o}$-dependent signaling typically includes direct inhibition of AC, our previous work demonstrates that α_1AR inhibition of βAR responses is PTX insensitive[175], suggesting that a G_q signaling mechanism is most likely involved. Consistent with this idea, O-Uchi et al. demonstrated that phenylephrine inhibition of βAR responses in ARVMs specifically involves the α_{1A}AR[182]. Interestingly, overexpression of α_{1B}ARs has also been reported to decrease βAR stimulation of cAMP production in the hearts of transgenic mice. However, that effect was attributed to a mechanism that involves heterologous desensitization of the βAR by PKC, and it required overexpression of exogenous α_{1B}ARs[200].

The physiologic significance of the α_1AR-dependent effect described in the present study is most clearly illustrated in the experiments demonstrating that it contributes significantly to the net effect that norepinephrine has on cAMP production (see Figure 6). This contradicts earlier work suggesting that α_1ARs do

not contribute to NE responses[170]. The apparent discrepancy may be explained by the greater sensitivity of the FRET-based biosensor approach used in the present study, which makes it possible to detect cAMP responses in intact, live cardiac myocytes. This self-limiting effect of α_1AR stimulation on the cAMP response to NE could be part of an intrinsic mechanism for fine-tuning sympathetic signaling. Furthermore, in heart failure, β_1AR expression decreases with little or no change in the number of α_1ARs[201,202]. It would be interesting to speculate whether the increase in α_1AR:β_1AR ratio contributes to reduced β_1AR responsiveness that occurs under these conditions. Likewise, it is conceivable that α_1AR inhibition of cAMP production contributes to the cardioprotective effect associated with these receptors[34]. Future studies assessing the effects of α_1AR stimulation using targeted FRET-based biosensors in normal or cardiac disease models could help uncover possible novel mechanisms contributing to pathophysiological changes in compartmentalized cAMP signaling.

2.6   Supplemental Information

A.

B.
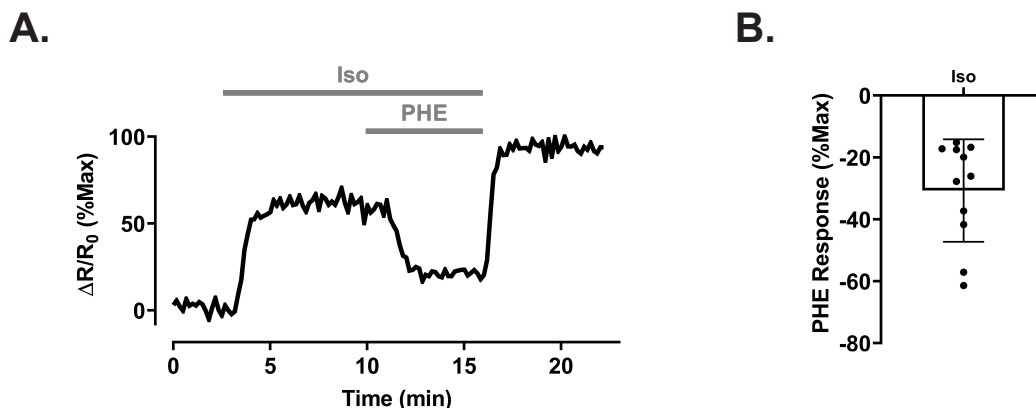
Supplemental Figure 1: Effect of α₁AR activation on cAMP response to βAR stimulation

(A) Time course of changes in cAMP activity detected by the Epac2-camps biosensor produced by exposure to the non-specific βAR agonist isoproterenol (Iso, 10 nM) followed by Iso plus the α₁AR agonist phenylephrine (PHE, 30 μM). FRET responses ($\Delta R/R_0$) were normalized to the magnitude of the maximal cAMP response observed upon subsequent exposure to 1 μM Iso + 100 μM IBMX in the same cell. **(B)** Average response (± SD) to PHE in the presence of Iso (n/N = 11/3).

Chapter 3

Compartmentation of β2-Adrenergic Receptor Stimulated cAMP Responses by Phosphodiesterases Type 2 and 3 in Cardiac Ventricular Myocytes

(Permission to reprint in Appendix 2)

3.1   Abstract

Background and Purpose:

In cardiac myocytes, cAMP produced by both β_1 and β_2-adrenergic receptors (ARs) results in an increase in L-type Ca^{2+} channel activity and myocyte contraction. However, only cAMP produced by β_1ARs is able to enhance myocyte relaxation through phospholamban-dependent regulation of the sarco/endoplasmic reticulum Ca^{2+}-ATPase 2 (SERCA2). The purpose of this study was to test the hypothesis that β_2AR stimulation produces a cAMP signal that is unable to reach SERCA2, and determine what role, if any, phosphodiesterase (PDE) activity plays in this compartmentation.

Experimental Approach:

The cAMP responses produced by β_1 and β_2AR stimulation were studied in adult rat ventricular myocytes using two different fluorescence resonance energy transfer (FRET)-based biosensors: Epac2-camps, which is expressed uniformly throughout the cytoplasm of the entire cell, and Epac2-αKAP, which is targeted to the SERCA2 signaling complex.

Key Results:

Selective activation of β_1 or β_2ARs produces cAMP responses detected by Epac2-camps. However, only β_1AR stimulation produces a cAMP response detected by Epac2-αKAP. Yet, β_2AR stimulation was able to produce a cAMP

signal detected by Epac2-αKAP in the presence of selective inhibition of PDE2 or PDE3, but not PDE4.

<u>Conclusion and Implications:</u>

These results support the conclusion that cAMP produced by β_2AR stimulation is not able to reach subcellular locations where the SERCA2 pump is located. Furthermore, this compartmentalized response is due at least in part to PDE2 and PDE3 activity. Leveraging this discovery could lead to novel PDE-based therapeutic treatments aimed at correcting cardiac relaxation defects associated with certain forms of heart failure.

3.2   Introduction

The sympathetic nervous system plays an essential role in modulating cardiac function in order to meet the metabolic demands of the body during stress and exercise[203]. Many of the resulting effects are mediated through β-adrenergic receptor (βAR) stimulation and subsequent production of 3',5'-cyclic adenosine monophosphate (cAMP)[204]. This second messenger produces many of its effects by activating protein kinase A (PKA), which phosphorylates key proteins involved in excitation and contraction of cardiac myocytes, including L-type Ca2+ channels (LTCCs) and phospholamban (PLN)[205,206].

Although cAMP is a small molecule, which theoretically can diffuse throughout the entire cytoplasmic compartment, responses to βAR signaling are not homogenous. Cardiac myocytes express both β_1 and β_2ARs, and although both are capable of stimulating cAMP production, each receptor subtype produces distinct functional responses[98]. Selective β_1AR activation produces an increase in the rate and magnitude of force generation (positive inotropic effect) as well as an increase in the rate of relaxation (positive lusitropic effect). However, in many species, β_2AR activation enhances cardiac myocyte contraction, without affecting relaxation.

Contraction of cardiac myocytes is mediated by the release of Ca^{2+} from the sarcoplasmic reticulum (SR) via ryanodine receptors (RyRs), a process triggered by extracellular Ca^{2+} entering through LTCCs found in the plasma membrane of transverse (T)-tubules. This Ca^{2+}-induced Ca^{2+} release is critically dependent upon the tight coupling between LTCCs and RyRs in dyadic clefts,

which are junctional membrane complexes created by the close proximity of the T-tubules and the terminal cisternae of the junctional SR. Relaxation occurs when cytosolic Ca^{2+} is pumped back into the SR by the sarco/endoplasmic reticulum Ca2+ ATPase 2 (SERCA2), which is found outside dyadic clefts, in the non-junctional SR.

β_1AR stimulation enhances contraction through PKA-dependent phosphorylation of LTCCs, which causes an increase in the influx of extracellular Ca^{2+}, triggering a greater release of intracellular Ca^{2+} from the SR. β_1AR stimulation also leads to phosphorylation of PLN, which is associated with SERCA2. PKA-dependent phosphorylation of PLN diminishes the inhibitory effect that PLN has on SERCA2, resulting in an increase in the amount of Ca^{2+} taken up into the SR and available for subsequent release. This increase in SERCA2 activity not only contributes to an increase in contractility, it also enhances the rate of Ca^{2+} reuptake and hastens myocyte relaxation. The rate of myocyte relaxation is also affected by PKA-dependent phosphorylation of troponin I[207]. β_2AR stimulation results in PKA-dependent phosphorylation of LTCCs, contributing to an increase in contraction. However, there is little or no phosphorylation of PLN, which helps explain the lack of a lusitropic effect[208].

The differences between β_1 and β_2AR mediated effects in cardiac myocytes are believed to be due, at least in part, to differences in the distribution of the cAMP signal produced by each subtype of receptor. This is supported by evidence that β_1ARs generate a cAMP response that is able to propagate throughout the entire cell, while β_2ARs produce a cAMP signal that is locally

confined[209]. The global cAMP signal generated following the activation of β_1ARs suggests that these receptors are distributed across the entire cell surface. β_2ARs, on the other hand, produce a cAMP response that is restricted to the T-tubules of cardiac myocytes[105], where these receptors are known to form a signaling complex with LTCCs[210]. This is consistent with the hypothesis that β_2ARs concentrated in dyadic clefts are unable to produce a cAMP response that can propagate to the non-junctional SR, where PLN and SERCA2 are found. In addition, there is evidence that cAMP catabolism by different phosphodiesterase (PDE) subtypes can selectively regulate β_1 and β_2AR inotropic and lusitropic responses[211–213].

In the present study, we compared the cAMP responses to β_1 and β_2AR stimulation in adult rat ventricular myocytes (ARVMs) using a novel FRET-based biosensor targeted to the non-junctional SR, Epac2-αKAP. Our results demonstrate that β_1ARs are more effective than β_2ARs at stimulating a cAMP response that can be detected in the microdomain near SERCA2. Furthermore, while phosphodiesterase (PDE) types 2, 3, and 4 were all found to regulate basal cAMP activity near SERCA2, only PDE2 and PDE3 affected the ability of β_2ARs to produce a response that reaches that location. These results identify potential therapeutic targets for enhancing relaxation of cardiac myocytes, which may be useful in treating diastolic dysfunction associated with certain types of heart failure.

3.3 Materials and Methods

Biosensor Plasmid Construction

The 23 amino acid sequence (MLLFLTLWALVPCLVLLTLYFLS) from the N-terminal transmembrane domain of the α-kinase anchoring protein (αKAP)[214] was added to the N-terminus of the Epac2-camps biosensor[147] by site directed mutagenesis using a pcDNA3.1 mammalian expression vector (Life Technologies, CA). DNA encoding fragments for this new probe, Epac2-αKAP, were then amplified using Platinum PCR Supermix High Fidelity (Agilent Technologies, CA), and cloned into the pShuttle-CMV vector. This construct was then used to generate an adenovirus expressing Epac2-αKAP with the AdEasy XL adenoviral vector system (Agilent Technologies, CA).

Cardiac Myocyte Preparation

Cardiac ventricular myocytes were isolated from male and female Sprague Dawley rats (250-300 g) as described previously[178,215]. The methods used were in accordance with the *Guide for the Care and use of Laboratory Animals* as adopted by the National Institutes of Health and approved by the Institutional Animal Care and Use Committee of the University of Nevada, Reno. The rats were housed in same sex pairs in solid bottom polysulfone cages with corncob bedding under a 12 hour light and dark cycle with food and water provided *ad libitum*. Only rats deemed healthy and unstressed were utilized for experimental procedures. These studies are in compliance with the ARRIVE

guidelines and the recommendations made by the *British Journal of Pharmacology*[216].

In brief, rats were anesthetized with an intraperitoneal pentobarbital injection (150 mg/kg). Upon lack of response to bilateral toe pinches, the hearts were then excised and attached via the aorta to a Langendorff apparatus. After perfusion with a Ca^{2+}-free solution containing collagenase and protease, the ventricles were removed, minced, and isolated myocytes were collected by filtering through nylon mesh. These cells were then plated in minimum essential media (MEM) (Life Technologies, CA) supplemented with penicillin-streptomycin (100 U/ml and 100 μg/mL), bovine serum albumin (BSA) (1 mg/ml), 2,3-butanedione monoxime (10mM), and insulin-transferrin-selenium (1x). After 1 hour of incubation at 37° C and 5% CO_2, the cells were treated with adenovirus encoding either Epac2-αKAP or Epac2-camps. Transduced cells were kept in culture for no more than 72 hrs.

Immunocytochemistry and Confocal Imaging

Freshly isolated myocytes were plated on 35 mm glass-bottom fluorodishes (World Precision Instruments, Inc, FL) coated with 0.01% poly-L-lysine (Sigma Aldrich, MO). After transduction with Epac2-αKAP, cells were fixed with 4% paraformaldehyde for 15 min at room temperature, permeabilized with 0.3% Triton X-100 for 30 min, and blocked with 1% BSA for 30 min. These cells were then incubated with mouse anti-SERCA2 monoclonal antibody (1:100) [Thermo Fisher Scientific, Cat# MA3-919, RRID: AB_325502] overnight at 4° C,

followed by goat anti-mouse IgG (H+L) Alexa Fluor 647 (1:500) [Thermo Fisher

Scientific, Cat# A-21235, RRID: AB_2535804] for 1 hour at room temperature.

Samples were then counterstained with 0.3 μg/mL 4′,6-diamidino-2-phenylindole

(DAPI) for 10 min. Cells were washed twice with phosphate buffered saline

(PBS) between each step. Confocal microscopy was performed using an

Olympus Fluoview 1000 microscope with a 60x oil objective (PlanApo N, NA

1.42, WD 0.15 mm). Epac2-αKAP fluorescence was excited using a 488 nM

argon laser and Alexa Fluor 647 fluorescence was excited using a 635 nM diode

laser. Image and line intensity analysis was performed using ImageJ software.

GSDIM Super-resolution Microscopy

Isolated ARVMs were plated on coverslips (1.5#, Marienfeld Superior,

Germany) cleaned by sonicating with 5 N NaOH for 2 hrs, rinsed with water, and

then coated with collagen (20 µg/mL) for 30 min. After transduction with either

Epac2-αKAP or Epac2-camps, cells were fixed with 3% PFA/0.1%

glutaraldehyde for 15 min at 37° C, treated with 10 mM sodium borohydride for

10 min, permeabilized with 0.1% Triton-X for 20 min, and blocked with 50% SEA

Block (Thermo Fisher Scientific, MA) in PBS solution for 2 hrs. SERCA2 was

labeled with a monoclonal antibody [Thermo Fisher Scientific, Cat# MA3-919,

RRID: AB_325502] overnight at 4°C at a 1:100 dilution in 20% SEA Block, 0.05%

Triton-X and 1% BSA in PBS. After washing with 20% SEA Block in PBS

solution, anti-mouse Alexa Fluor 568 secondary antibody (1:1000 in PBS)

[Thermo Fisher Scientific, Cat# A-11004, RRID: AB_2534072] was added for 2

hrs. Epac2-αKAP and Epac2-camps were labeled with GFP booster nanobody conjugated to Alexa Fluor 647 [ChromoTek, Cat# gb2AF647-50, RRID: AB_2827575] at a 1:500 dilution. Cells were washed with PBS between steps.

The coverslips were then mounted on a depression slide with Glox-MEA imaging buffer (50 mM Tris/10 mM NaCl (pH 8), 10 mM mercaptoethylamine (pH 8), 10% glucose, 0.50 mg/mL glucose oxidase, and 58 µg/mL catalase)[217]. Cells were imaged using a Leica DMI6000B microscope with a 160x HCX PL-APO/1.47 NA objective capable of super-resolution imaging using ground-state depletion with individual molecule return (GSDIM) microscopy. The system is equipped with a 523 nm laser used to image the Alexa Fluor 568 secondary antibody and a 647 nm laser used to image the GFP booster antibody. An electron multiplying charge-coupled device (EMCCD) camera (iXon3 897, Andor Technology, UK) was used to acquire images.

Typical acquisition parameters were 10 ms exposure per frame, EM gain of 300 and 8000-10000 frames at a rate of 100 Hz. 100% laser intensity was used to transfer the fluorophores to dark-state and was reduced to 40-50% to maintain blinking of single emitters. Localization maps were constructed in the Leica LAX software and exported after background correction. Post-acquisition images were merged in NIH ImageJ software after correcting for lateral chromatic aberrations using 100 nm fluorescent TetraSpeck microspheres (T7279, Invitrogen, CA) with the Detection of Molecules (DoM) plugin for ImageJ. PSFj was used to evaluate the point spread function and determine a full width at half-maximum (FWHM) of 29 ± 2.1 nm[218]. Non-transduced ARVMs were

incubated with secondary antibodies (A-11004 and gb2AF647-50) to measure non-specific labeling (Supplemental Figure 1).

Calibration of Biosensor

Human Embryonic Kidney 293 (HEK293) [ATCC Cat# CRL-1573, RRID:CVCL_0045] cells kept in DMEM supplemented with 10% fetal bovine serum were transduced with Epac2-αKAP 48 hours before being lysed for *in vitro* FRET measurements, as described previously[149,219]. Briefly, HEK293 cells expressing Epac2-αKAP were washed twice with ice-cold PBS, scraped from the culture dishes, and then centrifuged for 5 min at 200 g. The resulting cell pellet was resuspended in 5 mM Tris-HCl, 2 mM EDTA (pH 7.3) and lysed by passing through a 21-gauge needle. The lysates were then centrifuged at 200,000 g for 20 min at 4° C. The resulting supernatant was collected and plated in a 96 well plate with varying concentrations of cAMP. A Chameleon V multitechnology plate reader (Hidex, Finland) was used to excite eCFP with a 440/20 band pass filter, and measure eCFP and eYFP (FRET) fluorescence with 480/30 and 535/24 band-pass filters, respectively. The eCFP/eYFP fluorescence ratio was then plotted as a function of the cAMP concentration and fit to a three parameter logistic equation using SigmaPlot (Systat Software, Inc. CA) to determine the EC_{50} and Hill coefficient.

Fluorescence Resonance Energy Transfer (FRET)

Isolated myocytes transduced with adenovirus encoding either Epac2-αKAP or Epac2-camps were imaged as previously described[178,215,220,221]. Cells were perfused with an extracellular solution containing (in mM): 137 NaCl, 5.4 KCl, 0.5 $MgCl_2$, 1 $CaCl_2$, 0.33 NaH_2PO_4, 5.5 glucose, and 5 HEPES (pH 7.4) at room temperature. Fluorescence images were collected simultaneously through 440/20 (eCFP) and 535/24 (eYFP) band-pass filters using an OrcaD2 dual chip CCD camera attached to an Olympus IX71 inverted microscope. HCImage software (Hamamatsu, Inc., Japan) was used for acquisition and analysis. Changes in cAMP activity were defined as the change in eCFP/eYFP fluorescence intensity ratio (ΔR) corrected for background and bleed-through relative to the baseline ratio (R_0). To account for differences in dynamic range when comparing results obtained using Epac2-camps and Epac2-αKAP, the FRET responses of each probe were normalized to the magnitude of the saturating response elicited in each cell following exposure to maximally stimulating concentrations of the non-selective βAR agonist isoproterenol (Iso, 1 µM) plus the non-selective PDE inhibitor 3-isobutyl-1-methylxanthine (IBMX, 100 µM).

The basal concentration of cAMP detected by Epac2-αKAP *in situ* was estimated using a previously described method[149,178,219]. This involved determining the minimum FRET response following exposure of cells to the adenylyl cyclase (AC) inhibitor MDL 12330A and the maximum FRET response following exposure to Iso plus IBMX.

Electrophysiology

A Multiclamp 700B amplifier, Digidata1440A digitizer, and pClamp software (v11, Molecular Devices, CA) were used to record whole-cell LTCC currents in ARVMs expressing Epac2-αKAP or Epac2-camps or control ARVMs cultured for an equivalent time period. The cells were perfused with a modified extracellular solution in which KCl was replaced with CsCl. Micro-electrodes (1-2 MΩ resistance) were filled with an intracellular solution containing (in mM): 130 CsCl, 20 TEA-Cl, 5 EGTA, 5 MgATP, 0.06 TrisGTP, and 5 HEPES (pH 7.2) at room temperature. The voltage-clamp protocol included a -80 mV holding potential, a 50 ms pre-pulse to -40 mV to inactivate Na$^+$ channels, and a 100 ms test pulse to 0 mV to elicit the L-type Ca^{2+} current (I_{Ca-L}). This protocol was repeated once every 5 s to monitor changes in I_{Ca-L} magnitude.

Materials/Chemicals

Erythro-9-(2-hydroxy-3-nonyl) adenine, cilostamide, rolipram, MDL 12330A, CGP 20712A, and ICI 118,551 were purchased from Tocris Bioscience (Bristol, UK). MEM, penicillin-streptomycin, and insulin-transferrin-selenium were purchased from Life Technologies (Carlsbad, CA). All other chemicals were purchased from Sigma-Aldrich (St. Louis, MO).

Data and Statistical Analysis

Data are presented as the mean ± SEM from the indicated number of cells (*n*) obtained from the indicated number of animals (*N*). Cardiac myocytes from

each rat were randomly allocated to different experimental groups. Power

calculations were used to determine appropriate sample sizes. All experimental

protocols include data from at least one male and one female animal. However,

the numbers of each were not sufficient to allow a valid statistical comparison of

responses based on gender. Because of the easily identifiable nature of the

images, data analysis was not blinded. In addition, because of the limited number

and variability of the results obtained from cells isolated from any given heart, all

values were assumed to be independent measurements[222], and *n* values were

employed for statistical comparisons using SigmaPlot (v13, Systat Software, Inc,

CA). Data normality was tested using the Shapiro-Wilk test. Unpaired two-tailed

Student's t-tests were used for comparison between two unrelated groups and

one-way ANOVAs with multiple comparison (Bonferroni t-test) were performed

for multiple unrelated groups. *Post hoc* tests were only performed if F was

significant and there was no variance inhomogeneity. Statistical significance was

defined as $p < 0.05$. The data and statistical analysis comply with the

recommendations of the *British Journal of Pharmacology* on experimental design

and analysis in pharmacology[223]. The data collected and presented as part of this

study are available upon reasonable request by contacting the corresponding

author.

Nomenclature of Targets and Ligands

Key protein targets and ligands in this article are hyperlinked to

corresponding entries in http://www.guidetopharmacology.org, the common

portal for data from the IUPHAR/BPS Guide to PHARMACOLOGY[224], and are permanently archived in the Concise Guide to PHARMACOLOGY 2019/20[225,226].

3.4   Results

Generation of an SR targeted FRET probe

To study the cAMP signaling dynamics associated with the microdomain surrounding the non-junctional or free SR, we fused the Epac2-camps probe (Nikolaev et al., 2004) to the hydrophobic N-terminal transmembrane domain from the α-kinase anchoring protein (αKAP)[214]. αKAP is a Ca^{2+}/calmodulin-dependent protein kinase II (CaMKII) anchoring protein that targets CaMKII to the SR membrane[228]. αKAP is localized specifically to the free SR[214], where it complexes with SERCA2[229]. More importantly, previous studies have shown that the N-terminal hydrophobic domain is necessary to properly target αKAP to the SR[214,228,229].

Confocal images of ventricular myocytes expressing Epac2-αKAP exhibit a distinct striated pattern, similar to that of immunolabeled SERCA2 (Figure 1A and Supplemental Figure 2). Ground-state depletion with individual molecule return (GSDIM) super-resolution microscopy was performed to demonstrate that the Epac2-αKAP probe is located in close proximity to SERCA2 (Figure 1B). This is in contrast to the Epac2-camps probe, which is expressed in the cytosolic domain of cells[147]. Although cardiac myocytes expressing the Epac2-camps probe also appear to exhibit a striated pattern (Figure 1C), this most likely represents the displacement of the cytosolic free-space by T-tubules and other

intracellular structures (Figure 1D). Previous studies using fluorescence recovery after photobleaching have demonstrated that the rapid diffusion rate of Epac2-camps is consistent with cytosolic expression of Epac2-camps in ARVMs[178].
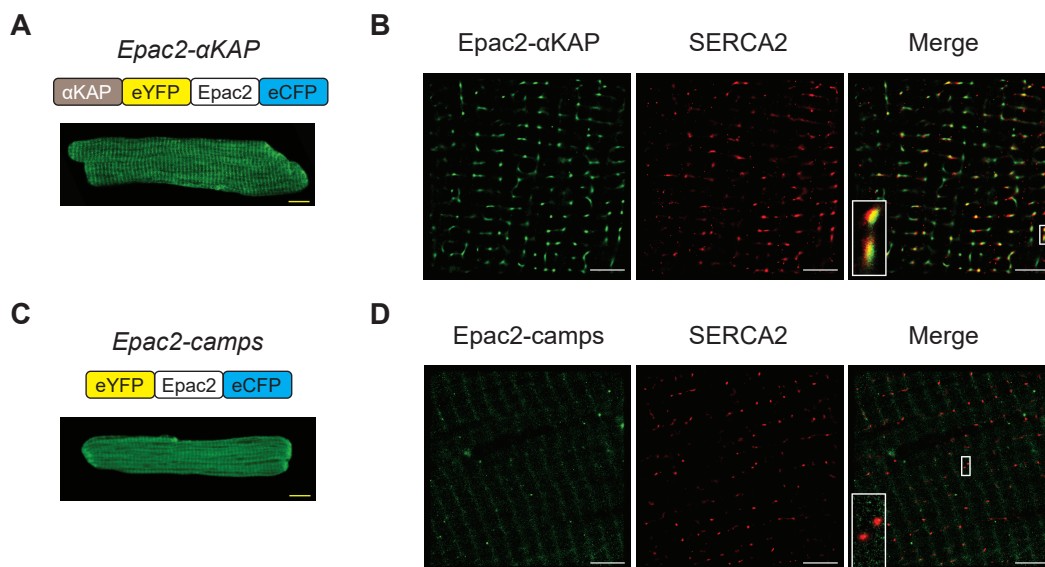
Figure 1: FRET biosensor expression and localization in adult rat ventricular myocytes (ARVMs)

Schematic representation of the Epac2-αKAP **(A)** and Epac2-camps **(C)** biosensors and representative confocal images of myocytes expressing each probe. Representative super-resolution images of fixed ARVMs expressing Epac2-αKAP **(B)** and Epac2-camps **(D)** (n/N = 12/3 for each probe). Left hand panels are of each probe labeled with a GFP antibody. Center panels are the same cells co-labeled with SERCA2 antibody. Right hand panels represent the merged images, with the ROI magnified 4x (insets). White scale bar: 3.0 μm. See Methods for details.

The cAMP sensitivity of Epac2-αKAP was determined by measuring FRET responses of the probe in a cell-free system. The resulting concentration-response curve demonstrates that cAMP activates Epac2-αKAP with an EC_{50} of 0.64 μM and a Hill coefficient of 1.0 (Supplemental Figure 3). This is similar to Epac2-camps, which we previously reported as having an EC_{50} of 0.31 μM and

Hill coefficient: 0.84[149]. Furthermore, the dynamic range of the FRET response of Epac2-αKAP *in vitro* was 25 ± 0.35% (n/N = 6/3).

When expressed in ARVMs, the cAMP response detected by Epac2-αKAP was saturated by exposure to maximally stimulating concentrations of the non-selective βAR agonist isoproterenol (Iso, 1 µM) plus the non-selective phosphodiesterase (PDE) inhibitor 3-isobutyl-1-methylxanthine (IBMX, 100 µM) (Figure 2A). The size of this FRET response was 11 ± 0.40% (n/N = 40/12) (Figure 2C). This is significantly less than the magnitude of the maximal FRET response measured under cell-free conditions (see Supplemental Figure 3). This can be explained if the probe is partially activated under baseline conditions[227]. Consistent with this hypothesis, exposure of cells expressing Epac2-αKAP to the non-selective adenylyl cyclase inhibitor MDL 12330A (MDL, 100 µM) resulted in a decrease in the baseline FRET response by -13 ± 1.8% (n/N = 8/3) (Figure 2B and C). This indicates that the dynamic range of the probe's response *in situ* (24%) is similar to that observed under cell-free conditions.

This information can also be used to estimate the basal cAMP concentration detected by Epac2-αKAP at 816 nM ± 117 nM[178,219]. This means that basal cAMP activity is near the EC_{50} for activation of the probe, making it ideally suited to detect any changes. Furthermore, Epac2-αKAP expressed in ARVMs responded to cAMP produced by exposure to various concentrations of Iso alone with an EC_{50} of 3.8 nM (Figure 2D, E, and F), which is similar to the Iso sensitivity of various functional responses in these cells.
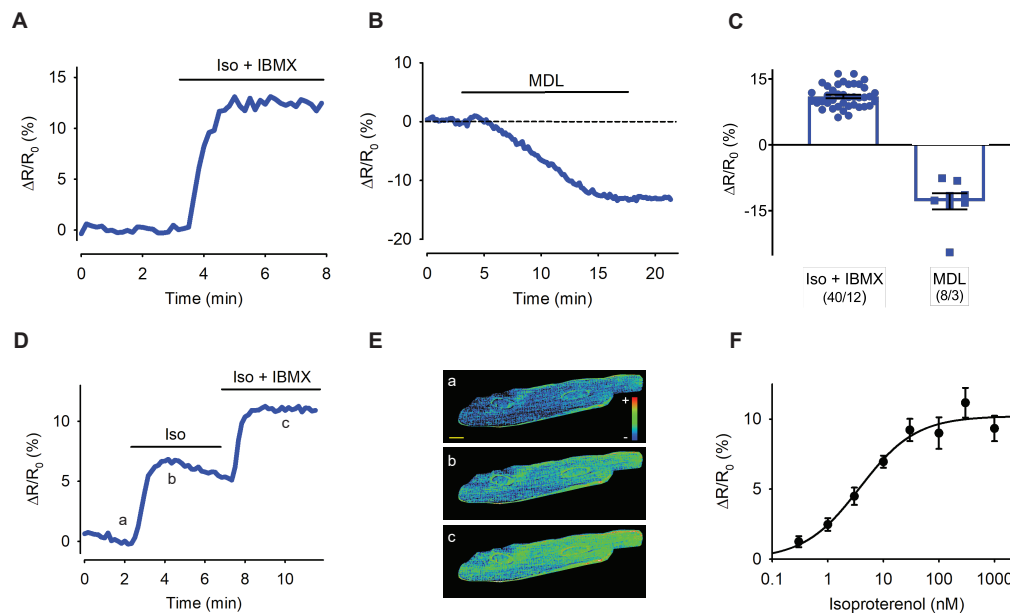
Figure 2: Characterization of Epac2-αKAP cAMP detection *in vivo*

(A) Maximum Epac2-αKAP response in a ventricular myocyte exposed to Iso (1 μM) plus the non-selective phosphodiesterase inhibitor 3-isobutyl-1-methylxanthine (IBMX, 100 μM). **(B)** Minimum Epac2-αKAP response in a ventricular myocyte exposed to the non-selective adenylyl cyclase inhibitor MDL 12330A (MDL, 100 μM). **(C)** Average maximum (positive) and minimum (negative) Epac2-αKAP responses measured in ventricular myocytes. **(D)** Representative time course of Epac2-αKAP response following exposure to Iso (10 nM) and subsequent saturation of the probe with Iso (1 μM) plus IBMX (100 μM) (n/N = 10/3). **(E)** Pseudocolor images of FRET-ratio recorded at time-points indicated in panel D. Yellow scale bar: 10 μm. **(F)** Concentration dependence of Epac2-αKAP response in ventricular myocytes exposed to various concentrations of Iso (EC_{50}, 3.8 nM; Hill Coefficient, 0.9) (n/N = 10-14/3-4).

To determine if expression of these biosensors may have somehow altered the responses they were being used to measure, we evaluated the effect of βAR stimulation on the functional change in I_{Ca-L} produced by exposure to 30 nM Iso using the whole cell patch clamp technique (Supplemental Figure 4). Neither probe affected the magnitude of the I_{Ca-L} current density (control: 3.0 ± 0.6 pA/pF, n/N = 10/6; Epac2-αKAP: 3.4 ± 0.3 pA/pF, n/N = 5/5; and Epac2-

camps: 3.3 ± 0.8 pA/pF, n/N = 6/3). Additionally, there was no significant

difference in the relative change in size of the I_{Ca-L} produced by Iso (control: 102

± 9.2%, n/N = 10/6; Epac2-αKAP: 95 ± 15%, n/N = 5/5; and Epac2-camps: 102 ±

13%, n/N = 6/3). This suggests that expression of the biosensors did not

significantly affect cAMP responses in these cells.

Distinct cAMP responses to selective βAR stimulation

The effects of $β_1$ and $β_2$AR stimulation on cAMP activity were recorded in

ARVMs expressing either Epac2-camps or Epac2-αKAP. The freely diffusible

Epac2-camps probe was used to detect cAMP responses occurring throughout

the entire cytosolic compartment, while the targeted Epac2-αKAP probe was

used to monitor changes in cAMP occurring near SERCA2 in the non-junctional

SR. Epac2-camps and Epac2-αKAP detect similar levels of basal cAMP and the

dynamic range of Epac2-αKAP (24%) is not very different from that of Epac2-

camps (21%)[178]. Therefore, comparisons between the two probes were made by

normalizing the size of the responses to selective $β_1$ or $β_2$AR stimulation to the

magnitude of the saturating response to 1 μM Iso plus 100 μM IBMX in the same

cell.

Selective $β_1$AR stimulation was achieved by exposure to 10 nM Iso in the

presence of the selective $β_2$AR antagonist ICI 118,551 (ICI, 300 nM). Under

these conditions, the Epac2-camps probe detected a FRET response that was

65 ± 2.8% (n/N = 10/4) of the maximal response produced by subsequent

exposure to Iso plus IBMX (Figure 3A and C). The Epac2-αKAP probe detected a

response to β_1AR stimulation that was significantly smaller (46 ± 6.4%, n/N = 10/4) than that detected by Epac2-camps (Figure 3B and C). These results indicate that selective β_1AR stimulation is able to produce a cAMP response that can be observed globally throughout the cytosolic compartment, including the microdomain near SERCA2.

β$_2$AR stimulation was achieved by exposure to the same concentration of Iso (10 nM) in the presence of the selective β_1AR antagonist CGP 20712 (CGP, 100 nM). Under these conditions, Epac2-camps detected a FRET response that was 12 ± 4.5% (n/N = 10/4) of the maximal response to Iso plus IBMX (Figure 3D and F). However, Epac2-αKAP did not appear to respond to β$_2$AR stimulation. The FRET ratio measured in the presence of Iso plus CGP (2.4 ± 2.1%, n/N = 14/4) was significantly smaller than that detected by Epac2-camps (Figure 3E and F). These results indicate that while selective β$_2$AR stimulation is able to stimulate cAMP production in ARVMs, it is not reaching the microdomain near SERCA2 in the non-junctional SR. To verify that the small response detected by Epac2-camps was indeed due to activation of β$_2$ARs and not incomplete block of β_1ARs, we demonstrated that 10 nM Iso produced no change in cAMP activity detected by either probe in the presence of 100 nM CGP plus 300 nM ICI (Supplemental Figure 5).
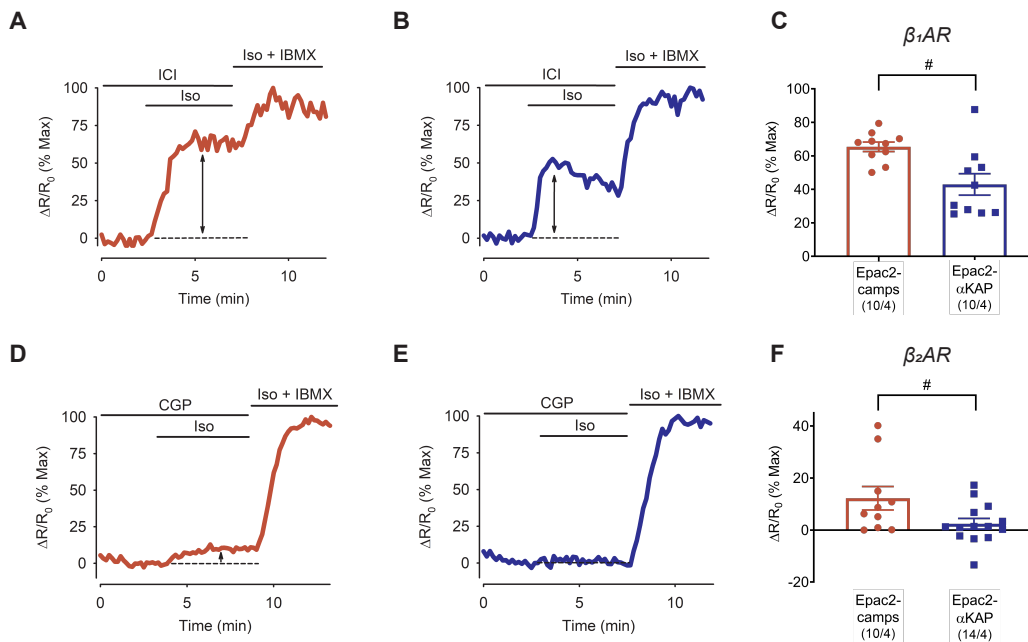
Figure 3: Microdomain specific cAMP responses to selective activation of β₁ or β₂ARs in adult ventricular myocytes

Time course of β_1AR responses elicited by exposure to 10 nM Iso in the presence of the selective β_2AR antagonist ICI 118,551 (ICI, 300 nM) in a myocyte expressing **(A)** Epac2-camps (red) or **(B)** Epac2-αKAP (blue). Time course of β_2AR responses elicited by exposure to 10 nM Iso in the presence of the selective β_2AR antagonist CGP 20712A (CGP, 100 nM) in a myocyte expressing **(D)** Epac2-camps or **(E)** Epac2-αKAP. Responses to β_1 or β_2AR activation were normalized to the magnitude of the maximal FRET response of the probe elicited by subsequent exposure to Iso (1 µM) plus IBMX (100 µM) in the same cell. **(C)** Average β_1AR responses in Epac2-camps or Epac2-αKAP expressing cardiac myocytes. **(F)** Average β_2AR responses in Epac2-camps or Epac2-αKAP expressing cardiac myocytes. Statistical significance between groups (#) was determined by unpaired two-tailed Student's t-tests.

Differential Responses to PDE Inhibition

PDE activity is believed to play an important role in creating segregated cAMP microdomains[230]. The three primary subtypes of cAMP metabolizing PDEs studied in mammalian ventricular myocytes are PDE2, PDE3, and PDE4[231]. To evaluate the relative contribution of each isoform in regulating cAMP activity

within the cytoplasmic domain in general, and the microdomain near SERCA2 in the free SR specifically, we examined the effects of selective PDE inhibition on changes in basal cAMP activity detected by Epac2-camps and Epac2-αKAP.

For Epac2-camps, selective inhibition of PDE3 activity with cilostamide (10 µM) elicited a FRET response ($67 \pm 6.5\%$, n/N = 11/3) that was significantly greater than that produced by inhibition of either PDE2 or PDE4. Furthermore, selective inhibition of PDE2 activity with erythro-9-(2-hydroxy-3-nonyl) adenine (EHNA, 10 µM) elicited a response ($36 \pm 5.4\%$, n/N = 11/4) that was significantly greater than that produced by inhibition of PDE4 activity with rolipram (10 µM) ($12 \pm 4.1\%$, n/N = 10/4) (Figure 4A and B). However, in myocytes expressing Epac2-αKAP, the responses to inhibition of PDE2 ($30 \pm 5.5\%$, n/N = 12/5), PDE3 ($42 \pm 8.4\%$, n/N = 13/6), and PDE4 ($28 \pm 5.8\%$, n/N = 10/4) were not significantly different (Figure 4C and D). These results indicate that while PDE2 and PDE3 play a more important role in regulating cAMP throughout the cytosolic domain, all three isoforms appear to play an important role in regulating cAMP activity in the microdomain near SERCA2.
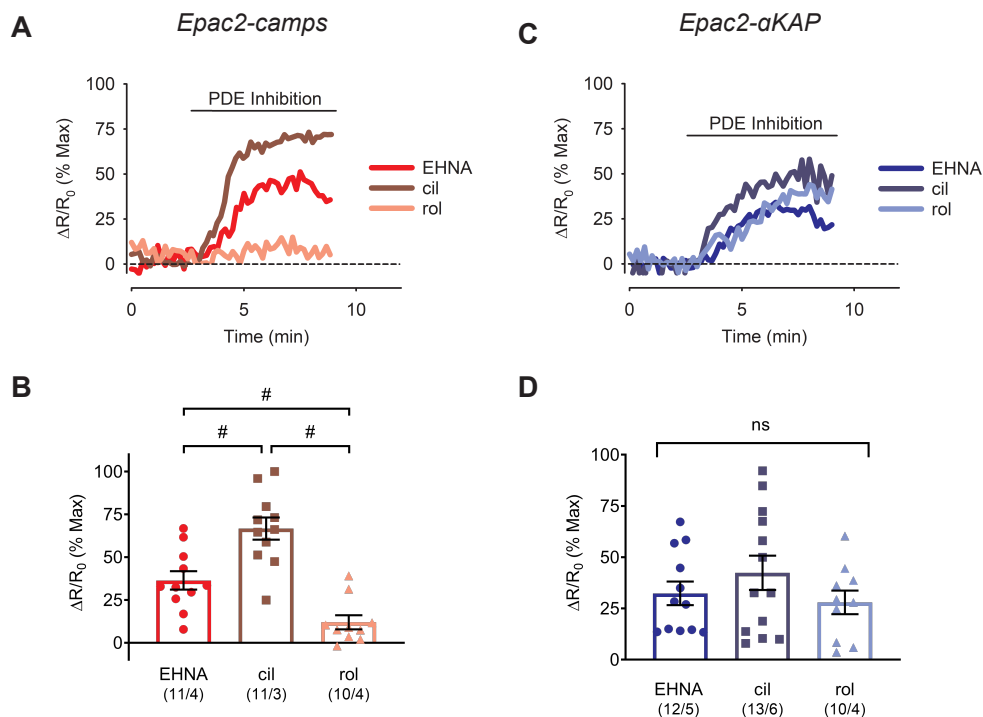
Figure 4: Microdomain specific cAMP responses to selective inhibition of different phosphodiesterase (PDE) isoforms in adult ventricular myocytes

Time course of cAMP responses detected by Epac2-camps **(A)** or Epac2-αKAP **(C)** following selective inhibition of PDE2 with 10 μM EHNA, PDE3 with 10 μM cilostamide (cil), or PDE4 with 10 μM rolipram (rol). Responses to PDE inhibition were normalized to the magnitude of the maximal FRET response of each probe elicited by subsequent exposure to Iso (1 μM) plus IBMX (100 μM), in the same cell (not shown). Average responses to selective PDE inhibitors detected by Epac2-camps **(B)** or Epac2-αKAP **(D)**. Statistically significant responses (#) were identified by one-way ANOVA, with *post hoc* comparison (Bonferroni t-test) between groups where appropriate.

PDE regulation of β_2AR cAMP signaling microdomains

The previous experiments demonstrate the importance of PDE activity in regulating basal cAMP levels within different microdomains. This would suggest that PDEs might also be a factor affecting the ability of cAMP produced by β$_2$AR stimulation from reaching the microdomain where SERCA2 is located. To test

this hypothesis, we examined the effect that selective inhibition of different PDE

isoforms had on the cAMP response detected by Epac2-camps and Epac2-αKAP

following subsequent β_2AR activation.

The responses to β_2AR stimulation detected by Epac2-camps in the

presence of the PDE inhibitors EHNA (15 ± 2.9%, n/N = 11/4), cilostamide (18 ±

3.9%, n/N = 11/3), or rolipram (1.6 ± 2.8%, n/N = 10/4) were not significantly

different from those observed in the absence of PDE inhibition (Figure 5A-D).

However, as opposed to the absence of a response to β_2AR stimulation

observed under control conditions, Epac2-αKAP did detect a significant increase

in cAMP activity in the presence of EHNA (23 ± 5.9%, n/N = 12/5) or cilostamide

(20 ± 5.3%, n/N = 13/6). However, there was still no significant response

detected in the presence of rolipram (3.4 ± 3.9%, n/N = 10/4) (Figure 5E-H).

These results suggest that PDE2 and PDE3, but not PDE4, play an important

role in regulating the ability of cAMP produced by β_2ARs from reaching SERCA2

in the non-junctional SR.

Epac2-camps

A

B

C

β₂AR Response

D

Epac2-αKAP

E

F
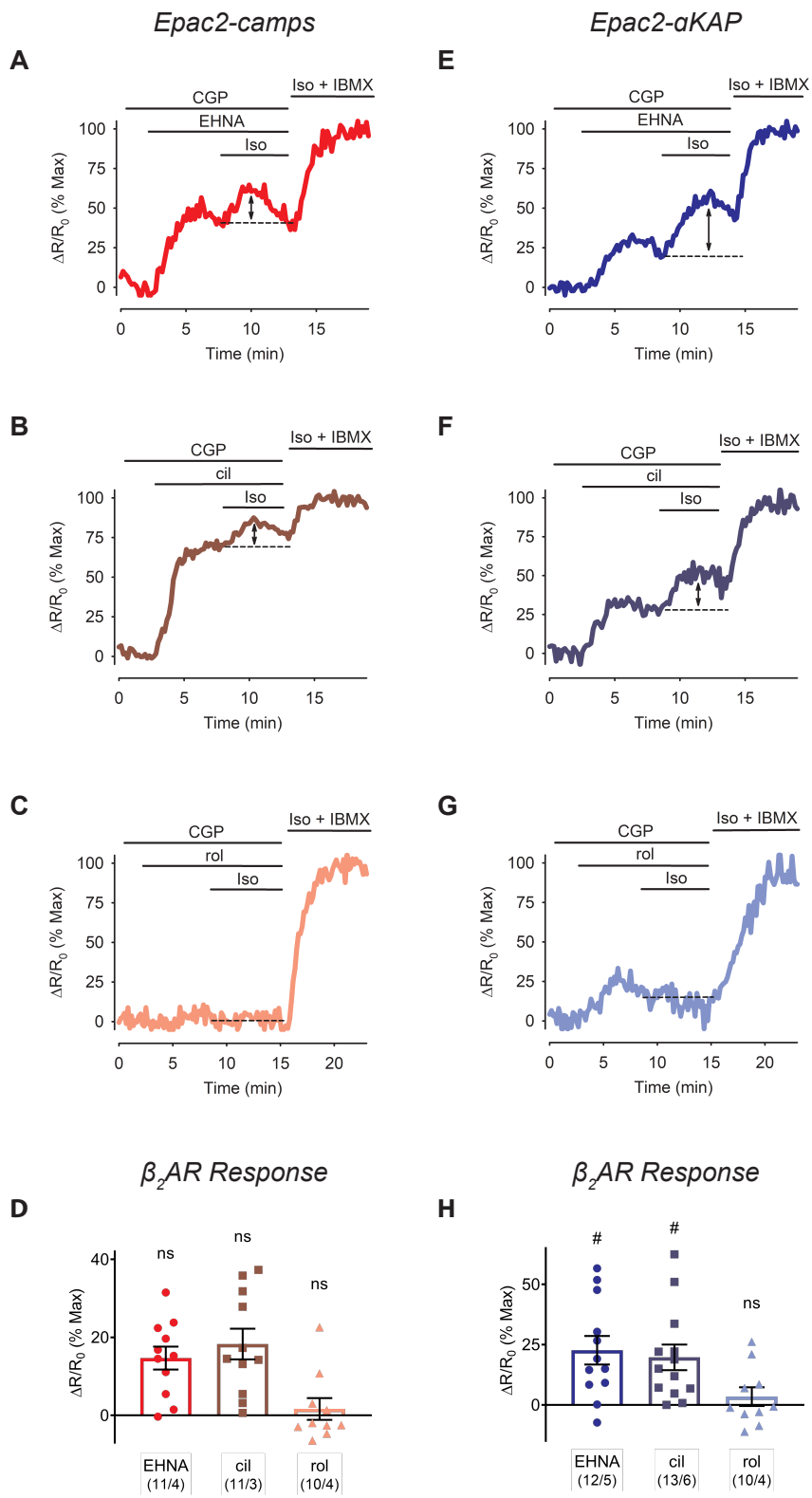

G

β₂AR Response

H

Figure 5: Microdomain specific effects of selective PDE isoform inhibition on the cAMP response produced by β₂AR activation

Time course of cAMP responses to selective activation of β₂ARs with 10 nM Iso in the presence of 100 nM CGP detected by Epac2-camps following inhibition of PDE2 with 10 μM EHNA **(A)**, PDE3 with 10 μM cilostamide **(B)**, or PDE4 with 10 μM rolipram **(C)**. Time courses of cAMP responses to selective activation of β₂ARs with 10 nM Iso in the presence of 100 nM CGP detected by Epac2-αKAP following inhibition of PDE2 with 10 μM EHNA **(E)**, PDE3 with 10 μM cilostamide **(F)**, or PDE4 with 10 μM rolipram **(G)**. Responses to β₂AR activation were normalized to the magnitude of the maximal FRET response of each probe elicited by subsequent exposure to Iso (1 µM) plus IBMX (100 µM), in the same cell. Bar graphs indicate responses to β₂AR stimulation detected by Epac2-camps **(D)** and Epac2-αKAP **(H)** in the presence of EHNA, cilostamide, or rolipram. Statistically significant responses (#) were identified by one-way ANOVA with *post hoc* comparison (Bonferroni t-test) of β₂AR responses measured in the presence of each PDE inhibitor to those measured in the absence of PDE inhibitor (see Figure 3).

3.5   Discussion

In the present study, we used a novel FRET-based biosensor, Epac2-αKAP, to study cAMP responses near SERCA2 in the non-junctional SR of adult ventricular myocytes. Epac2-αKAP has distinct advantages over other FRET-based biosensors that have been used to track cAMP dynamics in the same location. One such probe, Epac1-PLN, which consists of the Epac1-camps biosensor attached to the N-terminus of PLN, has an EC$_{50}$ for cAMP activation of 4.4 µM and a dynamic range of 10%[148]. Another probe, AKAP18δ-CUTie, consists of the cyclic nucleotide binding domain from the type IIβ regulatory subunit of PKA attached to the A kinase anchoring protein 18δ, an AKAP that associates with the PLN/SERCA2 signaling complex. The resulting biosensor has an EC$_{50}$ for cAMP activation of 7.1 µM and a dynamic range of 24%[150]. While the dynamic range of AKAP18δ-CUTie is significantly improved over Epac1-PLN,

both have a relatively low affinity for cAMP. The Epac2-αKAP probe used in the

present study has a dynamic range similar to that of AKAP18δ-CUTie, yet a

significantly higher affinity for cAMP. Exposure to Iso elicited cAMP responses

with an EC_{50} of 3.8 nM. This sensitivity to βAR stimulation is similar to that seen

for regulation of various functional responses in these cells[232,233].

　　　　We then compared the cAMP responses detected by Epac2-camps and

Eapc2-αKAP produced by selective activation of β_1 and β_2AR stimulation. Epac2-

camps, which is expressed uniformly throughout the cytosol of the cell, was able

to detect responses to activation of both types of receptors. However, Epac2-

αKAP was able to detect cAMP responses produced by β_1, but not β_2AR

stimulation (Figure 6A and B). These results are consistent with the idea that

β_1AR stimulation produces a global increase in cAMP in cardiac ventricular

myocytes. This can be attributed to β_1ARs expressed in lipid raft and non-raft

domains of the plasma membrane found in the T-tubules as well as the

peripheral sarcolemma[215,234]. The ability to detect a β_2AR mediated response

with a globally expressed probe like Epac2-camps is also consistent with

previous reports[148,209]. The relatively small magnitude of the response likely

reflects the fact that these receptors are only found in lipid raft domains of the

plasma membrane associated with restricted spaces along T-tubules[105]. As such,

cAMP is only being produced in a small subset of the total cytosolic

compartment.
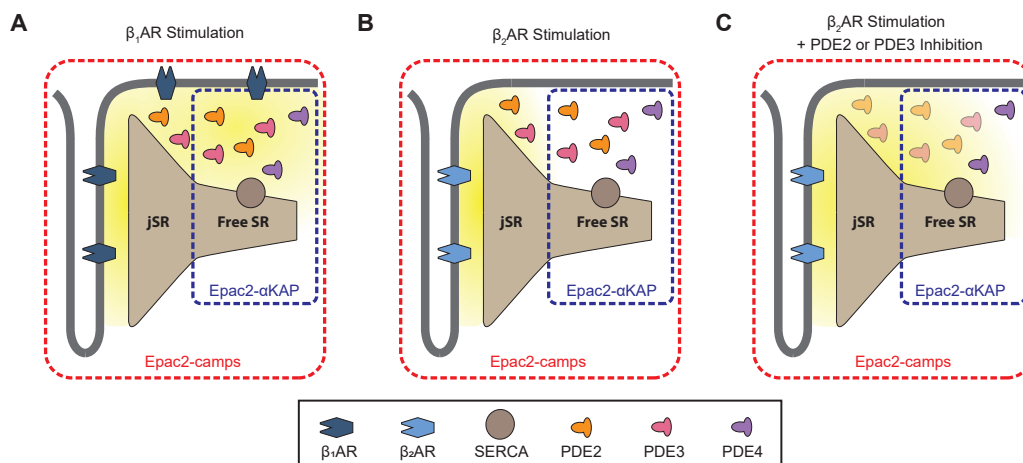
Figure 6: Schematic depiction of βAR compartmentation under varying conditions

(A) β_1ARs are located throughout the sarcolemma of ventricular myocytes. They stimulate production of cAMP that can be detected in dyadic cleft as well as free SR microdomains by Epac2-camps (cytosolic) and Epac2-αKAP (free SR) FRET probes. **(B)** β_2ARs are primarily located in the T-tubules of ventricular myocytes and produce a cAMP signal in dyadic clefts, which can be detected by Epac2-camps. Under normal conditions, cAMP produced by β_2ARs is prevented from reaching the SERCA2 microdomain due to hydrolysis by PDE2 and PDE3. **(C)** Upon selective inhibition of either PDE2 or PDE3, cAMP generated by β_2ARs is able to reach the SERCA2 microdomain, where it can be detected by Epac2-αKAP, indicating a loss of compartmentation.

Sprenger et al. (2015) reported that β_1 and β_2AR stimulation produce responses that can be detected by the globally expressed Epac1-camps biosensor. Yet, only β_1ARs produced a response that could be detected by Epac1-PLN. The inability of Epac1-PLN to detect a β_2AR response might have been explained by its low affinity for cAMP. Our results with Epac2-αKAP support the conclusion the β_2ARs are unable to stimulate a cAMP response that reaches SERCA2 under control conditions. The similarity of these findings also addresses

to maintain our cells in culture while waiting for the biosensors to be expressed, and studies have found that time in culture can affect certain properties of cardiac myocyte[235]. However, βAR responses have been reported to be stable for several days[236], consistent with the present findings. More importantly, the similarity between our findings and those obtained using acutely isolated cardiac myocytes from transgenic animals constitutively expressing FRET biosensors[148,209] suggests that the time in culture did not affect our results.

The ability of β_1 but not β_2ARs to produce a cAMP response that reaches SERCA2 is consistent with the observation that activation of β_1 but not β_2ARs results in PKA-dependent phosphorylation of PLN and a subsequent increase in SERCA2 activity[208]. This may explain why β_2AR stimulation is unable to produce a positive lusitropic response. Several different mechanisms have been suggested to explain this behavior. One involves the fact that β_2ARs couple to an inhibitory G protein (G_i) signaling pathway in addition to stimulatory G protein (G_s)-dependent activation of adenylyl cyclase[237]. Inhibition of G_i signaling with pertussis toxin has been reported to unmask β_2AR phosphorylation of PLN and increase the rate of cardiac myocyte relaxation[140]. The explanation for this observation is not known, but one hypothesis has been that the G_i-dependent effect is due to the activation of a phosphatase[238]. An alternative hypothesis is that G_i signaling somehow prevents cAMP produced by β_2ARs from propagating throughout the cell, where it might result in PKA-dependent phosphorylation of PLN. Previous studies using globally expressed FRET based biosensors have demonstrated that cAMP produced by β_2ARs is not able to move freely

throughout the cell. However, pertussis toxin inhibition of G_i did not affect that behavior[105,209].

It has also been suggested that G_i-independent mechanisms involving PDE activity contribute to the compartmentation of cAMP produced by β_2ARs[239]. We found that inhibition of PDE2, PDE3, or PDE4 alone produced changes in basal cAMP activity detected by Epac2-αKAP. This is consistent with evidence obtained in previous studies demonstrating a close association of PDE3 and PDE4 activity with SERCA2[240,241]. Although these results suggest that all three isoforms play an important role in regulating cAMP activity near SERCA2, they do not necessarily explain what is responsible for preventing cAMP produced by β_2ARs from reaching this location.

Interestingly, we found that inhibition of PDE2, PDE3, or PDE4 did not enhance the response to β_2AR stimulation detected by Epac2-camps. However, inhibition of either PDE2 or PDE3 activity did unmask a cAMP response that could be detected by Epac2-αKAP following β_2AR stimulation (Figure 5H). This is in stark contrast to the absence of a β_2AR mediated cAMP response under control conditions (Figure 3F). Despite evidence that PDE4 is associated with SERCA2, inhibiting its activity did not reveal a response following β_2AR stimulation. This suggests that PDE2 and PDE3 play an important role in preventing cAMP propagation from the β_2AR to SERCA2, but once it reaches that location, all three PDE isoforms play a role in regulating its activity. This is however in contrast to functional studies in rat ventricular tissue demonstrating that inhibition of PDE3 and/or PDE4, but not PDE2, enhances a positive

lusitropic effect attributed to β_2AR stimulation[211,213]. Inhibiting more than one PDE subtype at a time might have revealed a potential role for PDE4 in limiting β_2AR production of cAMP from reaching SERCA2. However, basal adenylyl cyclase activity in these cells is quite high, and inhibition of more than one PDE isoform at a time produces synergistic responses that typically saturate our biosensors, preventing us from testing this possibility.

We also found that inhibition of PDE2 or PDE3 had a much more significant effect on global cAMP activity detected by Epac2-camps under basal conditions, while the effect of inhibiting PDE4 activity was relatively minor. This suggests that PDE2 and PDE3 activity located somewhere between the β_2AR and SERCA2 are important in preventing cAMP from reaching the free SR and enhancing relaxation (Figure 6C). Additional factors affecting the movement of cAMP, such as restricted spaces and PKA-buffering, may be involved as well[129,242]. Interestingly, the cAMP hydrolyzing activity of PDE2 and PDE3 but not PDE4 are differentially regulated by cGMP[243]. cGMP could therefore also be an upstream regulatory factor affecting compartmentation of cAMP produced by β_2ARs.

Contrary to our finding, it has been reported that PDE4 inhibition has a much greater effect on the global cAMP response detected by Epac1-camps under basal conditions in adult mouse ventricular myocytes[148]. The apparent inconsistency may reflect a species-dependent difference. The same study also demonstrated that inhibition of PDE2, PDE3, or PDE4 affects basal cAMP activity detected by Epac1-PLN in the SERCA2 domain of mouse myocytes. This is

similar to our present results using Epac2-αKAP in rat myocytes. Other studies have demonstrated that inhibition of PDE4 activity can influence cAMP production by β_2ARs measured using cytosolic or plasma membrane targeted biosensors[105,209,244]. We are not aware of any study that has examined the effect that inhibiting PDE activity has on β_2AR production of cAMP in the non-junctional SR near SERCA2.

The results from the present study identify potential new targets for pharmaceutical treatment of conditions such as heart failure with preserved ejection fraction, where inadequate relaxation during diastole is a problem[245]. By inhibiting PDE activity, it may be possible to selectively enhance relaxation, while limiting deleterious side effects. For example, PDE3 inhibitors such as milrinone are currently used to provide short term benefits in treating some forms of heart failure. However, long term use is limited by their propensity to cause life threatening arrhythmias[246]. Selective inhibition of PDE2 or PDE4 activity may represent novel approaches to enhancing relaxation during diastole by facilitating cAMP-dependent regulation of SERCA2. Future studies are needed to identify specific PDE isoform subfamilies that may be involved in humans.

3.6   Supplemental Information

647 nm Laser	523 nm Laser	Merge
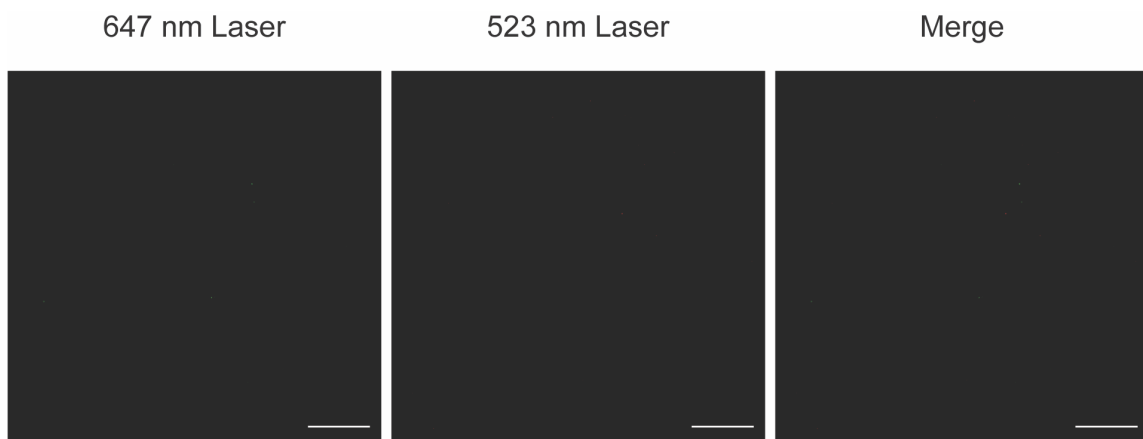
Supplemental Figure 1

Epac2-αKAP (647 nm) and SERCA2 (523 nm) super-resolution negative controls. Representative images from each super-resolution laser channel of non-transduced ARVMs prepared for super-resolution microscopy without SERCA2 primary antibody as described in the Methods section (n/N = 12/3). White scale bar: 3 μm.
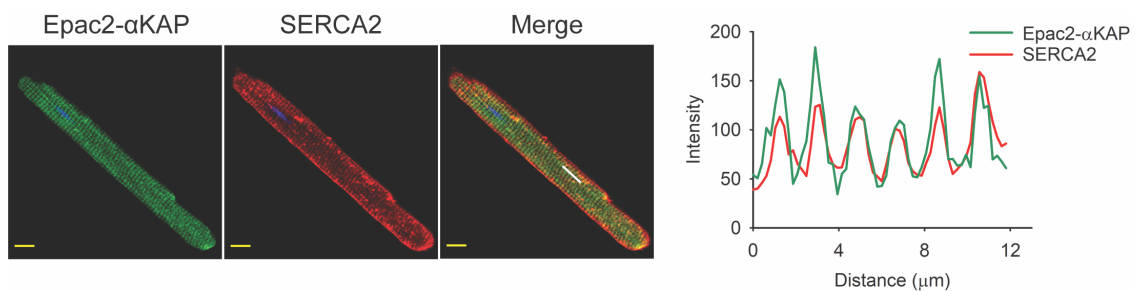
Supplemental Figure 2

Epac2-αKAP and SERCA2 immunocytochemistry confocal images and line scan. **(A)** Representative confocal images of a fixed myocyte expressing Epac2-αKAP (left) that has been immunolabeled with a SERCA2 antibody (center) (n/N = 14/4). Correct targeting of Epac2-αKAP was confirmed by overlap of fluorescence in merged image (right). Fluorescence intensity profile of Epac2-αKAP (green) and labeled SERCA2 (red) measured along the white line in the merged image (far right). Yellow scale bar: 10 μm.
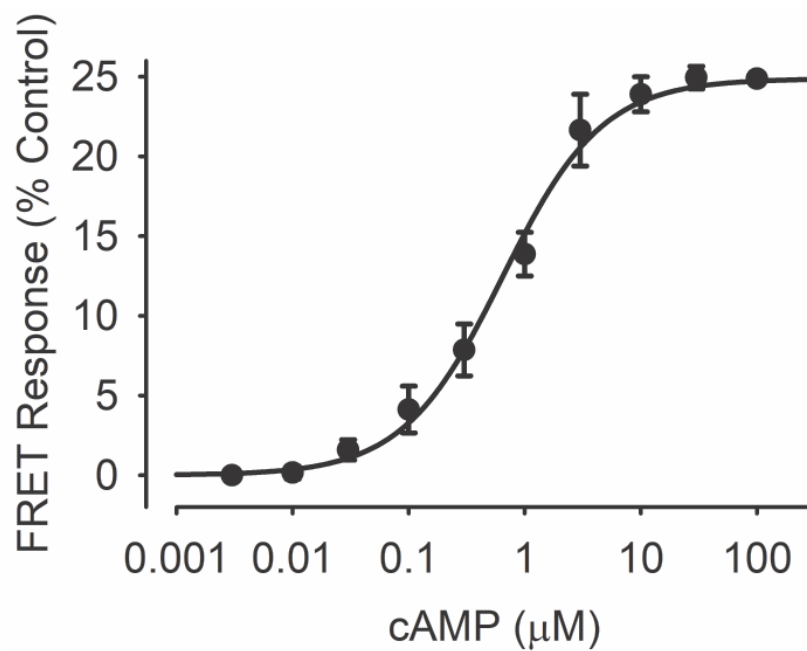
Supplemental Figure 3

Concentration dependent response of Epac2-αKAP to cAMP in a cell free system. See methods for details. EC_{50} = 0.64 μM and Hill coefficient = 1.0 (n/N = 6/3). The dynamic range was 25 ± 0.35%.
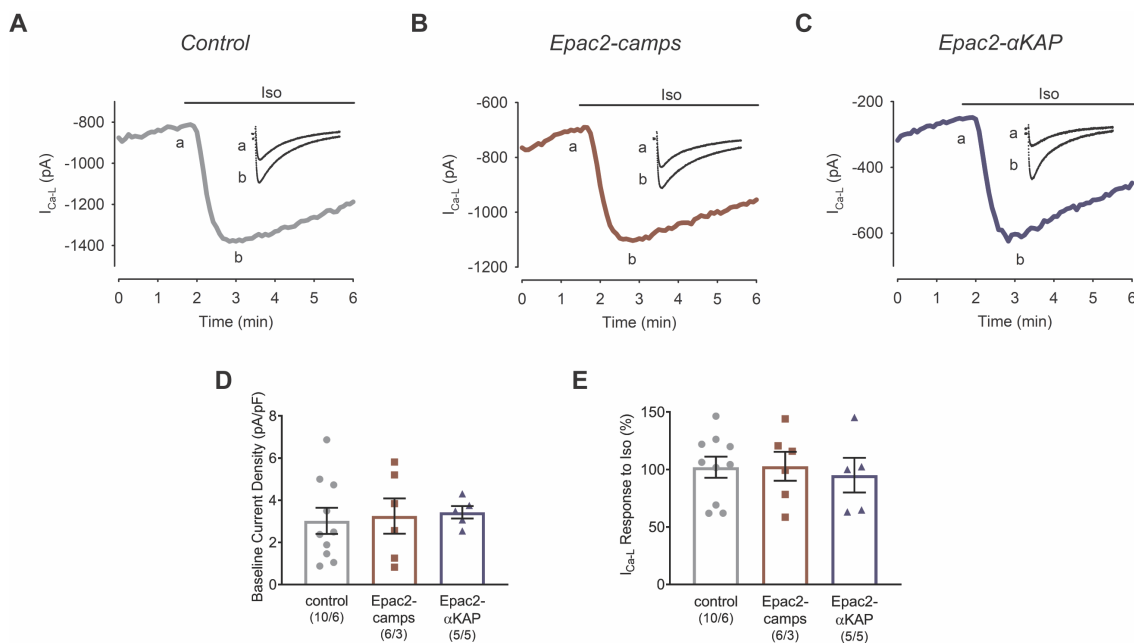
Supplemental Figure 4

β-Adrenergic receptor (βAR) modulation of L-type Ca^{2+} current (I_{Ca-L}) in control cultured (72 hrs.) adult rat ventricular myocytes (ARVM) and cultured ARVMs (72 hrs.) expressing Epac2-αKAP or Epac2-camps. Representative tracings of peak amplitude I_{Ca-L} (pA) with corresponding inset I_{Ca-L} channel currents for **(A)** control, **(B)** Epac2-camps, and **(C)** Epac2-αKAP ARVMs. βAR responses elicited through 30 nM isoproterenol (Iso). **(D)** Quantification of baseline I_{Ca-L} current densities between control, Epac2-camps, and Epac2-αKAP reveal no significant differences. **(E)** No significant difference in I_{Ca-L} peak amplitude responses to 30 nM Iso between control, Epac2-camps, and Epac2-αKAP.
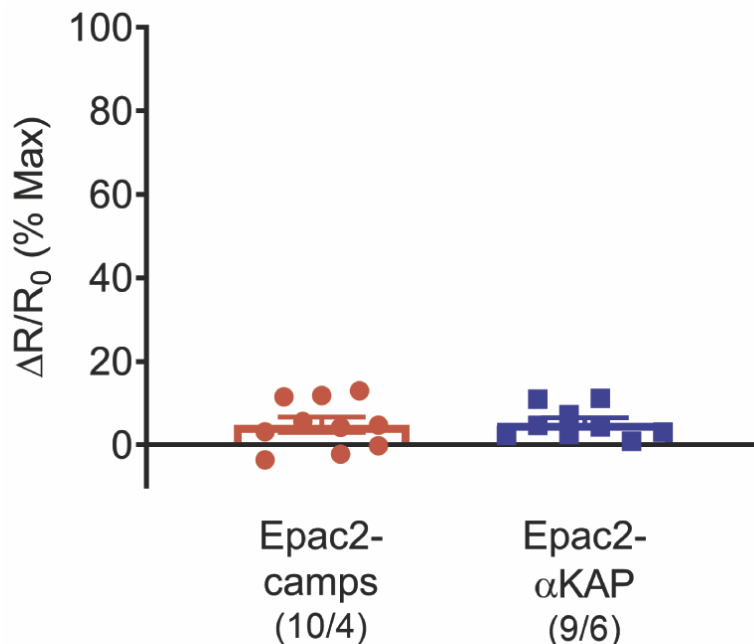
Supplemental Figure 5

Complete inhibition of the response to 10 nM Iso in the presence of the selective $\beta_1 AR$ antagonist CGP 20712A (CGP, 100 nM) and the selective $\beta_2 AR$ antagonist ICI 118,551 (ICI, 300 nM). Average responses detected by Epac2-camps and Epac2-αKAP in adult ventricular myocytes. Measurements were normalized to the magnitude of the maximal FRET response of each probe elicited by subsequent exposure to Iso (1 μM) plus IBMX (100 μM), in the same cell.

Chapter 4

Conclusion: Future Directions and Clinical Significance

4.1   Conclusion

In testament to the vast and complex nature of cAMP signaling in the heart, much is yet to be discovered even after more than six decades of intense investigatory focus. The research contained in this dissertation explores two critical aspects of this area of study: cardiac myocyte receptor regulation of cAMP and cAMP compartmentation.

Chapter 2 directly addresses the effects of α_1-adrenergic receptor (α_1AR) activity on cardiac myocyte cAMP. Previous studies have demonstrated that α_1AR activation was able to inhibit β-adrenergic receptor (βAR) induced functional effects. However, the canonical α_1AR G-protein signaling pathway does not directly rely on cAMP like the βAR signaling pathway. The research presented in this dissertation provides evidence that α_1AR activation triggers a tyrosine kinase mediated signaling pathway that acts at the level of the βAR to regulate cAMP. Furthermore, it was shown that this pathway did not involve upregulation of phosphodiesterase (PDE) activity and occurred in response to endogenous catecholamine (norepinephrine) stimulation.

While this research has provided important advances in the comprehension of α_1AR signaling in the heart, there are many questions remaining. Of primary interest, is to further define and clarify the signaling pathway starting from α_1AR stimulation and ending with inhibition of βAR-triggered cAMP production. One of the first tasks is to confirm which α_1AR isoforms are involved in the signaling pathway. In cardiac myocytes, the α_{1A}AR

and α_{1B}AR isoforms are expressed[169]. Studies involving transgenic mice and pharmacologically specifically stimulated receptor subtypes have shown that the α_1AR subtypes have differential effects, especially in regards to contractile properties[197,247]. It has been suggested that α_{1A}ARs are the isoform responsible for the α_1AR inhibition of βAR functional effects. Therefore, repeating several key experiments from the study described in Chapter 2 using isoform specific pharmacological agents could help confirm if the α_{1A}AR isoform is also responsible for the α_1AR regulation of cAMP.

Once the subtype of α_1AR at play is identified, the specific type of G-protein coupling to these receptors can be determined as well. As previously described, the G_q G-proteins are commonly accepted as the main G-proteins coupled to α_1AR receptors. However, evidence has been found that α_1ARs may also couple to $G_{i/o}$ G-proteins[40,248]. These observations would suggest several possible avenues of G-protein signaling. However, a prior study demonstrated that the α_1AR inhibition of βAR induced functional effects is insensitive to pertussis toxin (PTX), which inhibits $G_{i/o}$ signaling[175]. Additionally, another functional study demonstrated that the α_1AR effect persisted in the presence of PKC inhibition[173]. These two observations would indicate that the method of G-protein signaling is a non-PKC G_q pathway. Confirmation of these results in cAMP studies and further investigation to determine the responsible pathway are still needed.

The results in Chapter 2 demonstrated that the α_1AR regulation of cAMP involves tyrosine kinase (TK) signaling, but the specific TKs involved still need to be ascertained. A useful first step would be to identify whether the TK is receptor or non-receptor in form[249]. The inhibitors used in the experiments of Chapter 2 (lavendustin A and genistein) are non-selective for receptor and non-receptor TKs[250]. Therefore, future experiments should employ more specific inhibitors to help differentiate among the types and families of TKs.

Trying to predict the TK signaling pathway(s) involved with the currently available evidence is a daunting task. A multitude of TKs exist in the heart, each forming elaborate signaling networks with intricate regulatory mechanisms[251]. Making matters more complicated, receptor coupled G-protein regulation of many different TK signaling pathways is well documented[252]. As previously discussed, determining the G-protein coupled to the α_1AR in this case would be very useful. G_q has been shown to activate the ERK1/2, JNK, p38MAPK, p38MAPKγ/ERK6, ERK5 tyrosine kinase pathways. G_i, on the other hand, has been shown to stimulate ERK1/2 (through α or $\beta\gamma$ subunits) and JNK. Without further clarification on the type of coupled G-protein, focusing on the four best characterized mitogenic activated protein kinase (MAPK) pathways (ERK1/2, JNK, p38, ERK5) would be a solid starting point. Another approach to determining which TKs are involved would be to investigate receptor tyrosine kinases (RTKs) directly. RTKs, such as the insulin and insulin-like growth factor-I receptor, have been shown to directly phosphorylate β_2ARs leading to inhibition of β_2AR function[194]. Narrowing down which TK pathways and/or receptors are involved could be performed

through pharmacological or genetic manipulation of individual TKs in each pathway.

Beyond expanding the basic science understanding of cardiac signaling, discovering the modality behind α_1AR regulation of βAR induced cAMP could have important consequences for the treatment of heart failure. α_1ARs are largely believed to mediate cardioprotective physiological responses in cases of heart failure including adaptive hypertrophy, increased inotropy, ischemic preconditioning, and cardiac myocyte survival[34]. This is in contrast to chronic βAR stimulation in heart failure, which leads to deleterious cardiac results[8]. As seen in the results from Chapter 2 of this dissertation, the α_1AR inhibitory effect of βAR cAMP activity occurs in response to the endogenous catecholamine norepinephrine (NE). Therefore, it is possible that the cardioprotective effects of α_1AR signaling could be tied to its inhibition of βAR signaling. Validation of this concept could be initially tested through NE and NE + Prazosin FRET experiments, similar to the ones performed in Chapter 2, utilizing cardiac myocytes from animals with induced heart failure. These experiments could reveal whether the α_1AR inhibition of βAR cAMP still occurs or even possibly increases in the setting of heart failure. If this signaling pathway still occurs, it could be possibly leveraged through the application of α_1AR agonists as a therapeutic treatment.

While studies focusing on direct receptor mediated regulation of cAMP have provided for a strong basis in sympathetic signaling research, recent

investigation in the field has been heavily focused on understanding cAMP compartmentation and its role in creating receptor-dependent functional responses. The relatively recent advent and optimization of cAMP-sensitive FRET biosensors has allowed for a never before opportunity to investigate intracellular cardiac cAMP dynamics at unprecedented levels of spatiotemporal sensitivity. The application of these biosensors has revealed striking heterogeneity of cAMP control within cells, further illuminating and complicating the picture of cAMP regulation and signaling in the heart.

In Chapter 3 of this dissertation, a novel targeted-FRET probe, Epac2-αKAP, was characterized and validated for measuring cAMP activity near non-junctional sarcoplasmic reticulum (jSR) in cardiac myocytes. Moreover, specific stimulation of β_1ARs or β_2ARs resulted in unique cAMP response that were measured in the general cytosol with Epac2-camps and in the non-jSR with Epac2-αKAP. The pattern of the results indicated that the β_2AR response was most likely compartmentalized, which could explain differences between the functional effects elicited by specific β_1AR or β_2AR stimulation. Further experiments revealed differential levels of cAMP regulation through various PDE isoforms. Interestingly, PDE2 and PDE3 appeared to play a role in compartmentalizing the β_2AR cAMP response detected by Epac2-αKAP.

The research in Chapter 3 shed important light on the cAMP signaling domain surrounding SERCA2 (non-jSR region). As a result, subsequent questions emerged. Of foremost importance is how the cAMP signaling translates to cardiac functional changes. The lack of a lusitropic effect due to

β_2AR specific stimulation in cardiac tissue under normal conditions was a key observation that led to the premise of this investigation[140]. Therefore, some of the experiments performed in Chapter 3, involving specific βAR subtype stimulation and PDE inhibition, should be repeated using techniques that measure the changes in cardiac myocyte functional properties, such as contraction and Ca^{2+} transient recording. A key experiment would be to determine if there is an increase in the rate of relaxation and Ca^{2+} transient decay in the presence of β_2AR specific stimulation with additional PDE2 or PDE3 inhibition contrasted with no change in relaxation or decay rates to solely β_2AR specific stimulation. These experiments are especially important as there is possibly conflicting data that has been previously published by other groups suggesting that PDE3 and/or PDE4 but not PDE2 regulates functional cardiac lusitropic change due to β_2AR specific stimulation[211,213].

PDEs are an important part of cAMP regulation, but they cannot be the sole compartmentation mechanism in cardiac myocytes[129]. Other factors such as cAMP buffering, export, localized production, and physical intracellular barriers have been proposed to also be involved in compartmentation[101]. A further interesting application of the Epac2-αKAP biosensor would be to investigate if/how physical intracellular barriers affect cAMP compartmentation in cardiac myocytes. Specifically, studies involving whether the dyadic cleft, the 10-12 nm intracellular space between the t-tubular sarcolemma and the jSR, leads to a compartmentalized β_1AR or β_2AR cAMP signal could be tested with the Epac2-

αKAP biosensor. Appendix 1 documents initial attempts at disrupting the dyadic cleft to allow for these investigations.

The results from the research in Chapter 3 not only validated a new FRET biosensor but also provided evidence for possible pharmacological therapeutics. The treatment of heart failure, specifically a subtype known as heart failure with preserved ejection fraction (HFpEF), has been incredibly difficult due to a lack of viable treatment options[253]. In HFpEF, which accounts for 40-50% of heart failure cases, there is a decrease in the relaxation of the left ventricle, which results in inadequate blood pumping activity due to inadequate prior filling[254,255]. In Chapter 3, it was demonstrated that β_2AR selective stimulation was able to produce a cAMP signal in the SERCA region with the simultaneous application of PDE2 or PDE3 inhibitors. This would theoretically lead to an increase in lusitropy (rate of relaxation), which could relieve the decrease in relaxation seen in HFpEF.

The application of PDE inhibitors as a treatment for heart failure is not a novel approach as milrinone, a PDE3 inhibitor, is approved for acute treatment of heart failure, but contraindicated for chronic use due to high risk of cardiac complications[246]. Many other PDE inhibitors have been tested and had promising results but were sidelined due to safety and efficacy concerns[256]. The combinatorial approach of β_2AR selective stimulation plus PDE2 or PDE3 inhibitors may provide a new approach to treat HFpEF. However, specific pre-clinical investigations need to be conducted into whether the reported arrhythmic effects of selective β_2AR stimulation still occur in the presence of PDE2 or PDE3 inhibition[257]. With 1 in 5 men and women developing heart failure during their

lifetime[258], the health burden and cost to society will only keep increasing as the

general population ages. Therefore, any insight into the treatment of heart failure

cannot be ignored. The research included in this dissertation provides several

advancements and discoveries in the field of cAMP signaling, which are in

themselves important from a basic science understanding of cardiac autonomic

signaling. However, the application of the included research also has greater

ramifications in the overall picture of the treatment of heart failure.

Appendix 1

Cardiac Dyadic Cleft Disruption

A.1.1 Abstract

Computer modeling studies have suggested that cAMP compartmentation in adult cardiac myocytes requires not only phosphodiesterase catabolic activity and distinct signaling protein localization, but a further factor that reduces the cAMP diffusion rate. We hypothesize that physical intracellular barriers due to anatomical structures inside cardiac myocytes could be part of this mechanism of reducing cAMP diffusion. We suspect that cardiac dyadic clefts, 10-12 nm junctional membrane complexes created by the close placement of the junctional sarcoplasmic reticulum and t-tubule plasma membrane, are sites of cAMP compartmentation partially due to being a tightly physically restricted intracellular location. Previous studies where the structural protein junctophilin 2 (JPH2) had been knocked down led to dysregulated dyadic clefts. Therefore, three different approaches were employed to knockdown or disrupt JPH2, so that the importance of restricted physical spaces as a means of cAMP compartmentation could be tested. The first approach utilized JPH2-targeting morpholinos, synthetic oligonucleotides which bind to complementary mRNA and prevent translation. Morpholino exposure led to unhealthy cardiac myocytes and could not be conclusively shown to be knocking down JPH2 expression. The second approach used a commercial JPH2-targeting shRNA adenovirus. Although cell quality and transduction rate was greatly improved compared to morpholinos, it was again inconclusive on whether JPH2 was being knocked down. The final method took a different approach and utilized a peptide to inhibit JPH2 binding to the plasma membrane. Ca^{2+} transient and shortening studies found some

changes to cardiac myocyte functional properties, but the benchmark decrease in Ca^{2+} transient magnitude consistently seen in previous dyadic cleft disruption studies was not present. While each method utilized resulted in varying levels of success, a definitive approach to disrupt dyadic clefts was not found. Continued experiments with an adapted adenoviral shRNA are in progress.

A.1.2 Introduction

Until recently, the distinct distribution of the β-adrenergic receptor (βAR) subtypes (β_1AR: all throughout; β_2AR: t-tubules/lipid rafts) in cardiomyocytes was believed to be one of the primary reasons for unique functional responses to selective adrenergic stimulation[259]. However, recent data in rat HF cardiomyocytes has shown that β_2AR cAMP compartmentation was decreased before the redistribution of β_2ARs from their traditional locations in the t-tubules to the sarcolemma crests[260]. This would indicate that other factors play a crucial role in creating a compartmentalized β_2AR signal ultimately responsible for unique functional responses. In Chapter 3, I showed that this was the case through phosphodiesterases (PDEs), specifically PDE2 and PDE3, playing an important role in creating a compartmentalized β_2AR cAMP response. Yet, modelling studies have predicted that PDEs do not fully explain the segregation of the cAMP signaling domains. These modeling studies demonstrated that to have unique cAMP responses, cAMP must be produced in distinctly different locations and travel at a significantly slower rate than free diffusion[149,227,261]. To

explain this criteria for compartmentation, we hypothesized that physical restriction of cAMP through intracellular anatomical barriers in combination with receptor location and PDE activity is necessary for cAMP compartmentation.

We decided to test this hypothesis by investigating cAMP compartmentation in dyadic clefts, which are 10-12 nm intracellular gaps created by the close placement of t-tubules and junctional sarcoplasmic reticulum (jSR) in cardiac myocytes[262]. Junctophilin 2 (JPH2), a structural protein and the most common junctophilin isoform in cardiomyocytes, tethers the jSR and t-tubule sarcolemma at a set distance to maintain the tight spacing of the dyadic cleft[263]. This allows for normal cardiac excitation-contraction (EC) coupling[264]. The downregulation of JPH2 leads to the disruption of dyadic clefts[265]. The disruption of dyadic clefts in cardiomyocytes causes many pathophysiological issues including T-tubule disorganization[266,267], destabilization of ryanodine receptors[268], and decreases in excitation-contraction (EC) coupling through the suppression of Ca^{2+}-induced Ca^{2+} release (CICR)[269,270]. We therefore hypothesized that the disruption of dyadic clefts would also disrupt cAMP compartmentation, especially β_2AR cAMP compartmentation, in the region.

The experiments in Chapter 3 had shown that β_2AR cAMP was compartmentalized and that it could not be detected by the Epac2-αKAP FRET probe. Prior research confirmed that β_2ARs are located in caveolin-enriched lipid raft plasma membrane fractions in t-tubules indicating that β_2AR cAMP compartmentation could be occurring in the dyadic clefts[105]. We theorized that

disrupting dyadic clefts would allow for the detection of a β_2AR cAMP signal with the Epac2-αKAP biosensor indicating a loss of compartmentation similar to the PDE inhibition experiments in Chapter 3 (Figure 1).
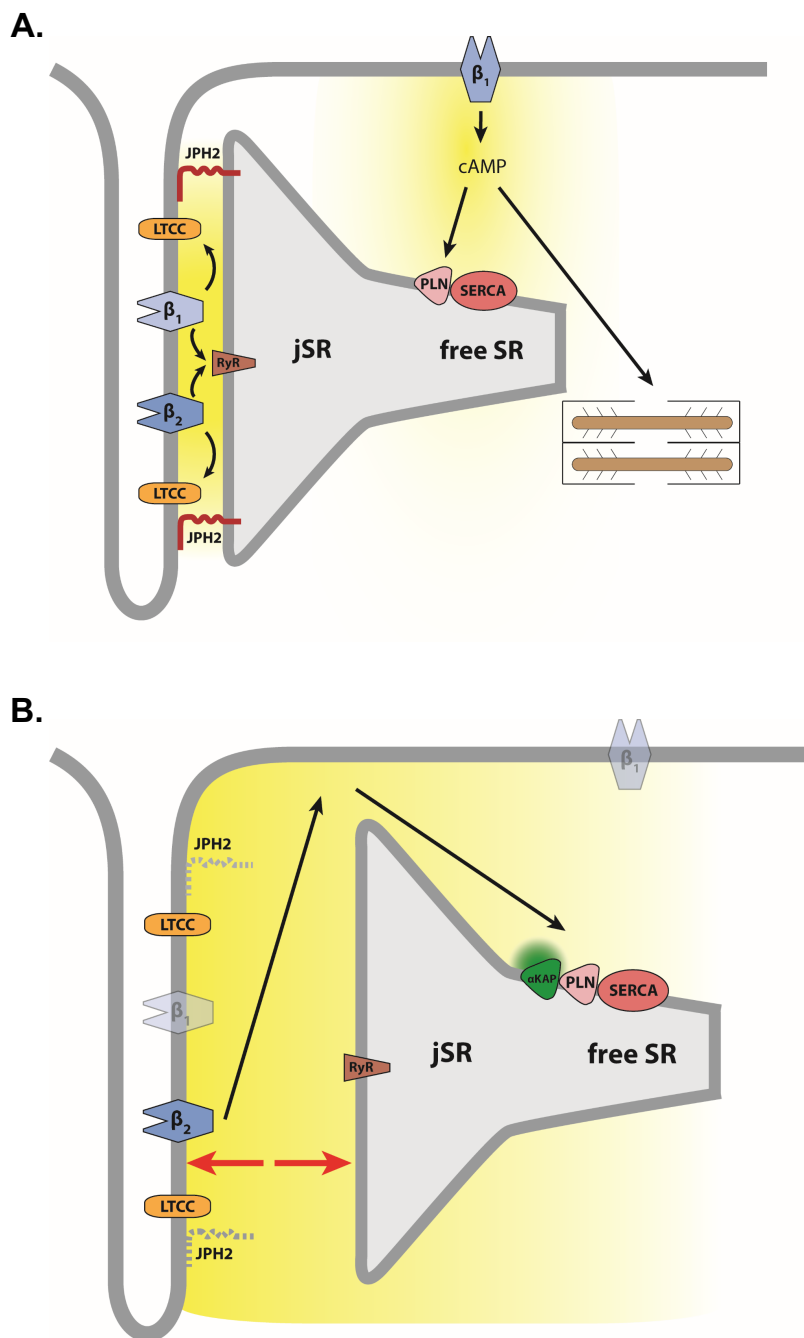
A.

B.

Figure 1: Schematic diagram of select β-AR signaling complexes in a cardiac myocyte

(A) Before and **(B)** after β_2-AR cAMP compartmentation loss due to dyadic cleft disruption. (αKAP = Epac2-αKAP FRET biosensor; $\beta1$ = β_1AR; $\beta2$ = β_2AR; free SR = free sarcoplasmic reticulum; JPH2 = junctophilin 2; jSR = junctional sarcoplasmic reticulum; LTCC = L-type Ca^{2+} channels; PLN = phospholamban; RyR = ryanodine receptor; SERCA = sarco/endoplasmic reticulum Ca2+-ATPase)

The first step to test these hypotheses was to develop a method to disrupt dyadic clefts. Due to the prior research showing that JPH2 knockdown disrupted dyadic clefts, we first focused on methods to knockdown JPH2 protein in our isolated ventricular myocyte model.

A.1.3 Morpholinos

Our first approach to knockdown JPH2 in guinea pig ventricular myocytes (GPVMs) was through morphpolinos due to my previous experience with the technique[271]. Morpholinos are stable, nuclease-resistant, highly specific, and low toxicity antisense oligonucleotides specifically designed to sterically bind to a target mRNA sequence and prevent protein translation (https://www.gene-tools.com/). A vivo-morpholino is a morpholino bound to an octaguanidine dendrimer delivery moiety to allow for *in vivo* delivery of morpholinos. Vivo-morpholinos also work in cell culture and have the advantage of not needing a delivery reagent to transport morpholinos to the cellular cytosol.

To determine if vivo-morpholinos would be a viable technique to knockdown protein expression in isolated cardiac myocytes, a carboxyfluorescein-labelled control vivo-morpholino (no mRNA target) was cultured with isolated GPVMs for 24 to 72 hours. Concentrations of vivo-

morpholino ranging from 100 nM to 5 µM were tested. Verification of cardiac myocyte uptake of the vivo-morpholino was performed with a laser scanning confocal microscope (60x 1.4 numerical aperture oil immersion objective lens). Images of live cardiac myocytes cultured with vivo-morpholinos were taken at 24 hr, 48 hr, and 72 hr time points. As can be seen in Figure 2, the cardiac myocytes that did appear to take up the vivo-morpholino appeared morphologically unhealthy. They looked boxy and granular with blebby fluorescent patterns. Increasing culture time and vivo-morpholino concentration helped increase the fluorescence intensity and the likelihood of vivo-morpholino uptake in the cultured cell populations but at the cost of cell quality and viability.

A regular control morpholino conjugated with a lissamine rhodamine fluorophore was therefore tested to determine if better quality cells and fluorescence could be achieved with a non-vivo morpholino. Endo-porter, a peptide delivery system (https://www.gene-tools.com/endo_porter) and Lipofectamine 3000 transfection reagent were used to transfect the morpholinos into the cells. While cell quality was greatly improved, the level of fluorescence was quite low with a puncta-like pattern, which increased in intensity with longer culture times (Figure 2).
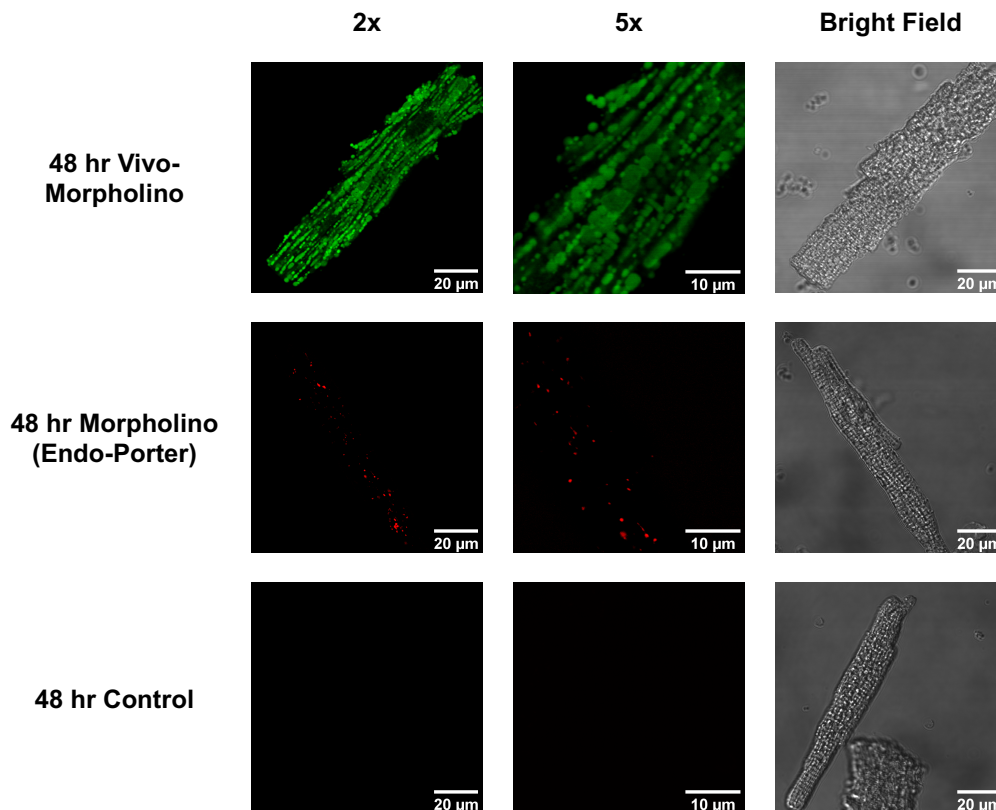
Figure 2: Fluorescently-labeled morpholino uptake in cardiac myocytes

Guinea pig ventricular myocytes were cultured with 1 μM control carboxyfluorescein-labeled vivo-morpholino (top row), 10 μM control lissamine rhodamine-labeled morpholino with Endo-Porter delivery reagent (middle row), or no morpholino (bottom row) for 48 hours. Confocal images were then taken of the live GPVMs in PBS at 2x (left column) and 5x (middle column) zoom using 488/510 nm excitation/emission for carboxyfluorescein and 543/598 nm for lissamine rhodamine and control GPVMs. Bright field images (right column) taken at 2x with the 488nm channel for vivo-morpholino and 543 nm channel for morpholino and control.

Based on the better transfection efficiency, albeit less healthy cells, of the

vivo-morpholinos, vivo-morpholinos targeted to the mRNA sequence of JPH2

were applied to isolated GPVMs in culture to knockdown JPH2 protein

expression. Traditional Western blots and Wes Simple Westerns were performed

to ascertain if JPH2 knockdown was occurring. Between the two protein quantifications methods, no conclusive proof could be found that the vivo-morpholinos were consistently knocking down protein expression.

Figure 3 is an example of a traditional Western blot that was performed on protein isolated from guinea pig cardiomyocytes that were incubated with JPH2 targeted vivo-morpholinos for various time lengths. As can be seen in Figure 3A, the JPH2 bands appear to decrease due to vivo-morpholino knockdown at 48 hr and 72 hr. However, when the JPH2 bands are normalized to GAPDH (Figure 3B), there actually is an increase in JPH2 protein with vivo-morpholinos. This is in contrast to the 24 hr vivo-morpholino sample, which appears to have a drastic JPH2 knockdown effect when normalized to GAPDH. When Western blots and Simple Westerns were repeated, the results varied each time, preventing a conclusion from being drawn on the JPH2 knockdown effect of vivo-morpholinos.

A.

JPH2   100 kDA —

GAPDH   37 kDA —

B.
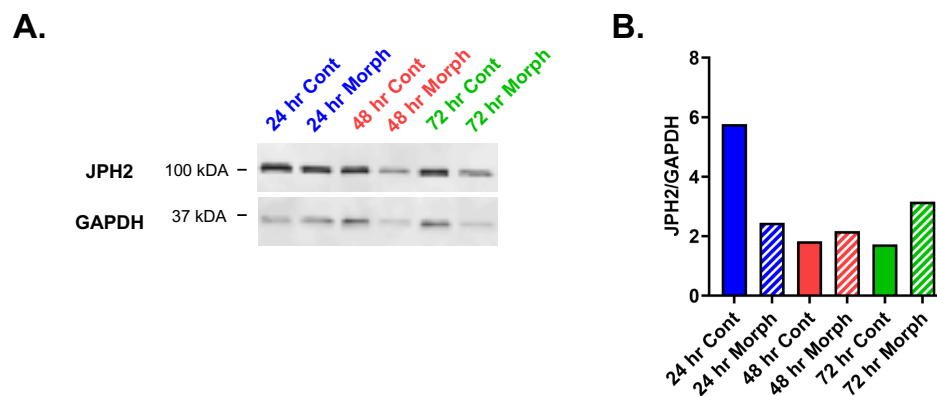
Figure 3: Quantifying JPH2 protein expression in cardiac myocytes treated with vivo-morpholinos

(A) Example Western blot probed for JPH2 and GAPDH. Protein lysate samples from guinea pig ventricular myocytes (GPVMs) cultured with JPH2-targeted vivo-morpholinos (Morph) for 24 hr (blue), 48 hr (red), or 72 hr (green) paired with time matched controls (Cont). **(B)** Quantification of JPH2 protein levels in (A) with GAPDH as a loading control for GPVM without (solid color) or with morpholino (diagonal color) treatment.

Even studies where immunocytochemistry and confocal imaging were performed to visualize JPH2 in vivo-morpholino transfected GPVM, no solid evidence that JPH2 knockdown occurred could be gathered. Unfortunately, RT-qPCR could not be performed as an alternative to determine JPH2 mRNA inhibition due to the method of action of morpholinos.

A.1.3 Ad-JPH2-shRNA Virus

The lack of clear JPH2 knockdown due to vivo-morpholino application along with the resulting poor cell quality prompted us to attempt another JPH2 knockdown approach. After researching various other means of knockdown, an adenoviral short hairpin RNA (Ad-shRNA) approach was decided upon. Ad-

shRNA is an RNA interference technology where an adenovirus vector delivers a shRNA coding sequence into the nucleus[272]. The sequence is then transcribed into shRNA, which is processed into an siRNA. The siRNA then inhibits or degrades the target mRNA sequence leading to downregulation of the target protein. This knockdown approach is widely used and generally successful when appropriately applied[273]. Furthermore, the adenoviral delivery system was amenable to our lab expertise and facilities.

As we had changed animal model systems in the lab from guinea pig to rat, we were going to develop an Ad-shRNA targeted to rat JPH2. Instead, we found a premade Ad-shRNA designed to knockdown mouse JPH2 for a lower cost and faster delivery time. The shRNA targeting region was 100% conserved in rat JPH2, so we decided to purchase Ad-RFP-U6-rm-JPH2-shRNA (Ad-JPH2) from Vector Biolabs. In addition to producing JPH2 targeted shRNA under the U6 promoter, the adenovirus also produced the dsRed RFP monomer under the CMV promoter so we could track cellular viral transduction. Although the virus was uncited in published scientific literature, in-house Vector Biolabs testing had shown that the Ad-shRNA was capable of ~50% knockdown of JPH2 at the protein level in a cardiac cell line (HL-1 cells).

Upon receiving the virus, I expanded it in HEK293 cells and tested what quantities of virus were needed to achieve RFP expression in ARVMs. Consistent ~6% of all cells (~42% live cell) RFP expression was achieved in the ARVMs after 72 hr of culture. While these transduction rates were fine for single cell microscopy experiments, such as FRET or confocal imaging, we were

worried we would run into issues where it would be impossible to determine JPH2 knockdown due to all the other non-transduced cells muddling the protein/RNA quantification results. Therefore, we decided to perform Fluorescence Activated Cell Sorting (FACS) to isolate a live and Ad-JPH2 transduced population of myocytes. FACS is a form of flow cytometry where cells can be sorted based on their fluorescent properties[274]. In this case, we attempted to sort our transduced cardiac myocytes based on the presence of RFP fluorescence and Hoechst 33258 staining. The RFP fluorescence detected Ad-JPH2 transduction and the Hoechst stain detected cell viability so that our isolated population of cells would ideally be live transduced (RFP expressing) cardiac myocytes.

Unfortunately, the FACS was unsuccessful even after three attempts spread over multiple days and cell preparations. When observed under a brightfield and epifluorescent microscope, the supposed RFP/live sorted cell populations only contained a few cells and cell fragments that in almost all cases were not RFP expressing. The other collected cell populations (no RFP and middle ground) contained similar cell conditions. RNA isolation from the sorted RFP/live cell population was unsuccessful, most likely due to the low cell count and poor cell quality. Epac2-camps transduced cardiac myocytes were used for the final FACS run and even with a different fluorescent indicator, the sort resulted in the same issues as with the Ad-JPH2 ARVMs. Based on the unsuccessful sorting regardless of the fluorescence indicator and resulting cell fragments, we suspected that the cardiac myocytes were shearing in the FACS

sorting nozzle. This would not only reduce the number of viable myocytes, but also disrupt proper sorting of the myocytes that did make it through the nozzle intact. The largest FACS nozzle available at the UNR FACS Core is 130 μm, which could be problematic as it is recommended to have a nozzle that is 5x the cell size. As ARVM cell length is ~120 μm, the utilized nozzle size clearly falls well outside of the recommendation[275]. The UC Davis FACS Core used a 200 μm nozzle at a minimum for their cardiac myocyte sorting indicating that the smaller nozzle size here at UNR is most likely an issue.

In tandem with the FACS experiments, I isolated mRNA from unsorted control and Ad-JPH2 expressing populations of ARVMs. RT-qPCR analyzing JPH2 mRNA levels was then performed on these samples, but returned mixed results. Some of the mRNA samples indicated Ad-JPH2 transduction led to an increase in JPH2 mRNA while others indicated a decrease. Therefore, alternative cell sorting methods were explored to help achieve consistent JPH2 quantification results.

First, laser microdissection (LMD) was attempted to sort the fluorescent cells. By placing populations of transduced ARVM on a special dissection slide, the individual fluorescent cells could be theoretically identified and then collected with a LMD system. However, LMD is primarily designed for fixed tissues, which meant the collection of live cardiac myocytes was very difficult, tedious, and generally unsuccessful. Therefore, another sorting method was attempted with patch pipettes. Transduced ARVM were diluted and placed on a epifluorescent microscope. Fluorescently expressing ARVM were then manually aspirated with

a large bore patch pipette pulled from capillary glass. This method was by far the most successful resulting in the collection of populations of RFP expressing ARVM. RNA was then collected from these sorted populations of cells, but the quality/quantity of RNA collected from these sorted populations was not sufficient to perform standard cDNA synthesis and RT-qPCR. A microplate dilution sorting method was also attempted to increase the number of fluorescent cells collected by each sort, but this method proved to be less effective compared to the manual patch pipette collection technique. To address the low quantity of RNA being retrieved from the sorted Ad-JPH2 cells, a specialized low cell qPCR kit (TaKaRa CellAmp™ Whole Transcriptome Amplification Kit (Real Time), Ver. 2) was acquired. Even with the specialized kit, JPH2 transcript levels could not be determined in the sorted cell populations.

Two Hail Marys were attempted at this point through confocal imaging and FRET experiments. First, the fluorescence of immunolabeled JPH2 in Ad-JPH2 expressing ARVMs was compared to control JPH2-labeled ARVMs. This approach is highly subjective and therefore a striking difference in JPH2 fluorescence between the two groups must be seen to suggest JPH2 knockdown. Unfortunately, the striking difference needed to indicate knockdown was not present overall. Second, FRET experiments were performed on ARVMs transduced with Ad-JPH2 and Epac2-αKAP. The Epac2-αKAP detected cAMP levels due to β_2AR stimulation were slightly higher in Ad-JPH2 transduced ARVM compared to control ARVM, which could indicate dyadic cleft disruption. However, the results were not significantly different.

At this point, my attempts at knocking down JPH2 with Ad-JPH2 was put on hold and a research scientist in our lab took over this endeavor. He reamplified Ad-JPH2 and was able to get even greater levels of Ad-JPH2 transduction in ARVMs (Figure 4A). He then performed protein extractions from these ARVM populations followed by Western blots examining JPH2 protein levels. Similar to previous successful RT-qPCR experiments, these Western blots showed inconclusive results with occasional slight JPH2 knockdown to no knockdown in Ad-JPH2 treated ARVMs (Figure 4B and C). I performed β_2AR stimulation FRET experiments again with Ad-JPH2 + Epac2-αKAP expressing ARVM with the newly amplified Ad-JPH2 and a scrambled shRNA + Epac2-αKAP as the control comparison. Unfortunately, there again was no significant difference between the Ad-JPH2 and Ad-Scrambled (control) cells.
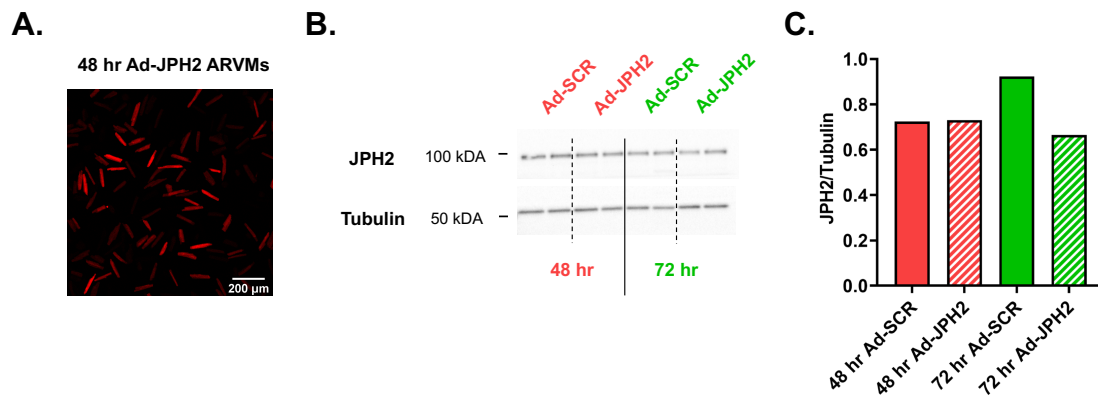
Figure 4: Adenoviral JPH2 shRNA expression and JPH2 protein knockdown quantification

(A) Representative live cell confocal image of dsRed RFP expression in isolated adult rat ventricular myocytes (ARVMs) transduced with 20 MOI Ad-JPH2 after 48 hr. **(B)** Example Western blot of ARVMs transduced with a control scrambled shRNA adenovirus (Ad-SCR) or Ad-JPH2 for 48 hr (red) or 72 hr (green). **(C)** Quantification of JPH2 in (B) with a tubulin loading control in Ad-SCR (solid color) and Ad-JPH2 treated (diagonal color) ARVMs. Bars represent the JPH2/Tubulin densitometry average of the two replicate bands for each test condition. *Data provided by Karni Moshal, PhD.*

A.1.4 TAT-MORN Peptide

As the chances of success with the Ad-JPH2 approach dwindled, a peptide approach at disrupting ARVM dyadic clefts was attempted. JPH2 contains eight N-terminal Membrane Occupation and Recognition Nexus (MORN) motifs, which cause JPH2 to bind to the sarcolemma[276]. Previous research by the Earley lab, demonstrated that that an inhibitory peptide homologous to the MORN domain of JPH2 caused a decrease in spontaneous transient outward current (STOC) frequency in murine vascular smooth muscle cells (SMCs)[277]. This decrease in STOC frequency was attributed to the disruption of peripheral coupling sites located between the SR and plasma

membrane of SMCs normally held together by JPH2. Therefore, we hypothesized that this MORN peptide could also dysregulate dyadic clefts by disrupting JPH2 in cardiac myocytes.

In the previously mentioned SMC experiments, the MORN peptide was delivered directly into the cell through a patch pipette during electrophysiological recordings. Our FRET experiments do not utilize a patch pipette, so we wanted to develop a cell permeable version of the MORN peptide. We decided to utilize the transactivator of transcription (TAT) sequence from HIV-1, a common cell penetrating peptide[278]. We designed a TAT-MORN peptide, which utilized the TAT sequence attached to the same MORN sequence used by the Earley lab (GRKKRRQRRRC[s-s]CYEGTWNNGLQDGYGTETYAD). The two sequences were connected by a disulfide bond so that the bond would be reduced by intracellular glutathione upon cellular entry. The free MORN peptide would then be able to inhibit JPH2/plasma membrane binding with less risk of steric hindrance and inappropriate localization due to the TAT sequence[279].

A commercial FITC-labeled TAT peptide (Anaspec, 47-57) was purchased to determine TAT peptide loading conditions for freshly isolated ARVMs. Many different TAT loading protocols for ARVMs and other cell types were tested and none showed much success at loading the fluorescent TAT peptide into healthy live ARVMs or HEK293 cells. Using an epifluorescent microscope, I observed that dead cells appeared to be taking up the peptide and, under certain conditions, some unhealthy but alive ARVMs appeared to take up the peptide slightly. Although less than ideal, the most successful peptide loading technique,

which was adapted from MacDougall et al.[238], was then employed so that a comparative ARVM Ca^{2+} transient and shortening study could be performed. While a control scrambled-TAT peptide would have been the ideal control group for these experiments, the cost of acquiring one was quite high and we wanted to collect some preliminary results before investing more resources.

Previous studies had shown that Ca^{2+} transient amplitude was decreased when dyadic clefts were disrupted due to JPH2 knockdown[269]. As can be seen in Figure 5, the peptide treatment caused a significant decrease in ARVM shortening magnitude, but no significant change to the time to 50% relaxation. More importantly, the Ca^{2+} transient amplitude of TAT-MORN peptide treated ARVMs was less than control ARVMs on average but not significantly decreased, in contrast to previous dyadic cleft disruption studies where there had been a clear and significant decrease in Ca^{2+} transient amplitude. Interestingly, the time to 50% decay of the Ca^{2+} transient was significantly decreased in our experiments. This decrease in time to 50% decay mirrors the findings found in another study where JPH2 was knocked down in HL-1 cells (cardiac cell line)[265]. However, this HL-1 study also found a prominent decrease in Ca^{2+} transient amplitude not seen in our current study.
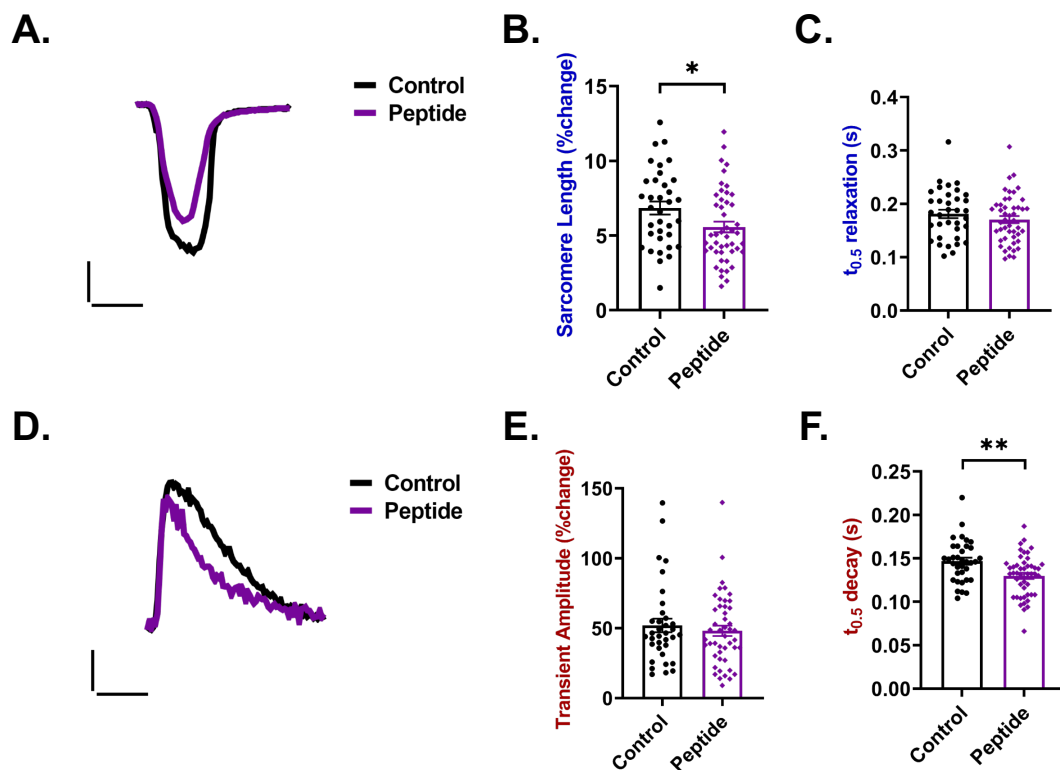
Figure 5: Effects of the TAT-MORN peptide on adult rat ventricular myocyte (ARVM) Ca^{2+} transients and shortening

Representative 2 Hz electric field stimulated sarcomere shortening **(A)** or Ca^{2+} transient **(D)** tracings in freshly isolated ARVM either treated with 10 μM TAT-MORN peptide (purple) or no peptide (black) for 30 min at 37°C. Vertical scale bars: 0.05 μM (shortening) or 0.1 Fura-2 fluorescence ratio (Ca^{2+} transient). Horizontal scale bars: 0.1 sec (both). Average cell shortening **(B)** and time to 50% shortening relaxation **(C)** for control (black, n/N: 35/4) and peptide treated (purple, n/N: 47/6) ARVMs. Average Ca^{2+} transient magnitude responses **(E)** and time to 50% decay **(F)** for control (black, n/N: 35/4) and peptide treated (purple, n/N: 47/6) ARVMs. Statistical significances determined through two-tailed Student's t-tests with * = $p < 0.05$ and ** = $p < 0.005$.

The TAT-MORN experiments were therefore put on hold as the main Ca^{2+} transient benchmark consistently seen in previous JPH2 knockdown and dyadic cleft disruption studies (significantly/dramatically decreased Ca^{2+} transient amplitude) was not seen in our dyadic disruption approach. While we found some

potentially promising results, such as the decrease in Ca^{2+} transient decay time, there was not enough positive evidence to continue with this line of experimentation.

A.1.5 Conclusion

Examining the published scientific literature reveals that investigation into cAMP compartmentation through intracellular physical barriers is far less common than studies investigating the contribution of phosphodiesterase and intracellular signaling protein location to cAMP compartmentation. One reason for this trend, that is now apparent, is the difficulty in directly perturbing some of these cardiac intracellular structures, such as dyadic clefts.

The morpholino technique used in this study was probably the least successful of the methods tried. The unhealthy myocytes that resulted from vivo-morpholino exposure most likely led to some of the difficulties in attaining consistent results when assaying levels of JPH2 knockdown. As can be seen in the GAPDH bands at 48 and 72 hr in Figure 3, the vivo-morpholino treated loading control bands are much lighter than the time matched loading control bands. This could indicate a lower quality protein cell lysate from vivo-morpholino treated cells due to an increased level of cell death. While investing more time into this technique is not recommended due to other more promising techniques, varying the cell culture protocol could possibly improve vivo-morpholino loading and the resulting cell quality. Alternatively, using normal morpholinos or a

different JPH2 targeting sequence could possibly improve the level of JPH2 knockdown.

The adenoviral shRNA method attempted in this study displayed the most promise. High levels and frequency of Ad-JPH2 uptake visualized by RFP expression was achieved in populations of ARVMs. Unfortunately, inconsistent JPH2 knockdown was confirmed by two researchers working independently. Due to the high transduction rate and high quality cell populations used in collecting protein, the most likely culprit for inconsistent JPH2 knockdown is the JPH2 inhibiting shRNA sequence. Therefore, the current approach to knockdown JPH2 and disrupt dyadic clefts being employed in our lab is a refinement of the Ad-shRNA technique. The lab has identified multiple new shRNA coding sequences targeting JPH2, which are now being loaded into adenoviral vectors. Exposing ARVMs to several different JPH2 targeting shRNAs simultaneously will hopefully give a greater chance of knocking down JPH2.

An additional consideration that may be leading to the difficulty in knocking down JPH2 through mRNA disruption (morpholinos and shRNA) may be a low turnover in JPH2 protein in ARVMs. Increasing culture time may help alleviate this concern, but the increased culture time will eventually lead to phenotypical changes in ARVM properties[235]. Therefore, a precarious balancing act between JPH2 knockdown and culture time would have to be employed using this refinement.

Utilizing a peptide to block JPH2 plasma membrane interaction approaches dyadic clefts disruption from a different angle compared to the

mRNA interference techniques previously attempted. The success of the MORN peptide in the Earley lab indicates that this is still possibly a viable approach. The key differences between our study and the previous successful research was the difference in cell type, functional measurement technique used, and peptide design. Changing the cell type we use would change the research question, so focusing on changing the measurement of dyadic cleft disruption and peptide design would be preferred. Performing electrophysiological patch clamping experiments is an option to measure changes in functional effects, but the ideal current to measure in this situation, L-type Ca^{2+} channel current ($I_{Ca,L}$), would not be advisable as it has been shown to remain constant after dyadic cleft disruption[269]. Trying to directly visualize dyadic cleft disruption through electron microscopy or super resolution fluorescence studies is another option, but both of these techniques require fixing the cells, which could lead to unrepresentative results due to the method of action of the peptide. Lastly, changing the peptide structure could be an option for improvement, as one of the key issues from these experiments was achieving good levels of peptide loading. Using a different linker between the TAT sequence and MORN peptide or attaching another cell penetrating peptide to the MORN peptide could prove successful. The downside to these modifications are that new peptides would have to be synthesized, which could prove to be very costly.

If the proposed changes to the previously attempted techniques prove unsuccessful, more drastic measures could be taken such as changing the research model animal or intracellular anatomical region. Changing our animal

model to mouse would allow us to use a characterized transgenic mouse with conditional knockdown of JPH2[269]. Even though this model has been previously characterized, it has been only utilized in several studies indicating a possible difficulty of use. Furthermore, mouse cardiac myocytes compared to rat cardiomyocytes are even less similar to human cardiac myocytes in terms of physiological properties[280]. A possible compromise would be the development of a transgenic rat that has a conditional JPH2 knockdown. However, this would be extremely costly to develop and labor intensive to manage and utilize.

Finally, other locations of tight intracellular anatomical spacing and possible cAMP compartmentation in cardiac myocytes could be a better model for disruption. The spacing between cardiac sarcoplasmic reticulum (SR) and mitochondria has been estimated to be 10-50 nm indicating that this may be a location worth investigating[281]. Additionally, these SR-mitochondrial spaces are held together by tethering structures, which could be targeted for disruption[282]. While these more radical approaches of changing model organisms or intracellular locations may work, adjusting one of the previously attempted approaches taken in this appendix would most likely be the best chance at success while remaining economically prudent.

Appendix 2

Reprint Permission for Previously Published Work

JOHN WILEY AND SONS LICENSE
TERMS AND CONDITIONS

Mar 09, 2021

This Agreement between Michael Rudokas ("You") and John Wiley and Sons ("John Wiley and Sons") consists of your license details and the terms and conditions provided by John Wiley and Sons and Copyright Clearance Center.

License Number	5024930491738
License date	Mar 09, 2021
Licensed Content Publisher	John Wiley and Sons
Licensed Content Publication	British Journal of Pharmacology
Licensed Content Title	Compartmentation of β2-adrenoceptor stimulated cAMP responses by phosphodiesterase types 2 and 3 in cardiac ventricular myocytes
Licensed Content Author	Michael W. Rudokas, John P. Post, Alejandra Sataray-Rodriguez, et al
Licensed Content Date	Feb 20, 2021
Licensed Content Volume	178
Licensed Content Issue	7

Licensed Content Pages	14
Type of use	Dissertation/Thesis
Requestor type	Author of this Wiley article
Format	Print and electronic
Portion	Full article
Will you be translating?	No
Title	The Complexities of cAMP Signaling in the Heart
Institution name	University of Nevada, Reno
Expected presentation date	Mar 2021
Requestor Location	Michael Rudokas 1664 N Virginia St MS#573 RENO, NV 89557 United States Attn: Michael Rudokas
Publisher Tax ID	EU826007151
Total	0.00 USD

Terms and Conditions

TERMS AND CONDITIONS

This copyrighted material is owned by or exclusively licensed to John Wiley & Sons, Inc. or one of its group companies (each a"Wiley Company") or handled on behalf of a society with which a Wiley Company has exclusive publishing rights in relation to a particular work (collectively "WILEY"). By clicking "accept" in connection with completing this licensing transaction, you agree that the following terms and conditions apply to this transaction (along with the billing and payment terms and conditions established by the Copyright Clearance Center Inc., ("CCC's Billing and Payment terms and conditions"), at the time that you opened your RightsLink account (these are available at any time at http://myaccount.copyright.com).

Terms and Conditions

- The materials you have requested permission to reproduce or reuse (the "Wiley Materials") are protected by copyright.

- You are hereby granted a personal, non-exclusive, non-sub licensable (on a stand-alone basis), non-transferable, worldwide, limited license to reproduce the Wiley Materials for the purpose specified in the licensing process. This license, **and any CONTENT (PDF or image file) purchased as part of your order,** is for a one-time use only and limited to any maximum distribution number specified in the license. The first instance of republication or reuse granted by this license must be completed within two years of the date of the grant of this license (although copies prepared before the end date may be distributed thereafter). The Wiley Materials shall not be used in any other manner or for any other purpose, beyond what is granted in the license. Permission is granted subject to an appropriate acknowledgement given to the author, title of the material/book/journal and the publisher. You shall also duplicate the copyright notice that appears in the Wiley publication in your use of the Wiley Material. Permission is also granted on the understanding that nowhere in the text is a previously published source acknowledged for all or part of this Wiley Material. Any third party content is expressly excluded from this permission.

- With respect to the Wiley Materials, all rights are reserved. Except as expressly granted by the terms of the license, no part of the Wiley Materials may be copied, modified, adapted (except for minor reformatting required by the new Publication), translated, reproduced, transferred or distributed, in any form or by any means, and no derivative works may be made based on the Wiley Materials without the prior permission of the respective copyright owner.**For STM Signatory Publishers clearing permission under the terms of the STM Permissions Guidelines only, the terms of the license are extended to include subsequent editions and for editions in other languages, provided such editions are for the work as a whole in situ and does not involve the separate exploitation of the permitted figures or extracts,** You may not alter, remove or suppress in any manner any copyright, trademark or other notices displayed by the Wiley Materials. You may not license, rent, sell, loan, lease, pledge, offer as security, transfer or assign the Wiley Materials on a stand-alone basis, or any of the rights granted to you hereunder to any other person.

- The Wiley Materials and all of the intellectual property rights therein shall at all times remain the exclusive property of John Wiley & Sons Inc, the Wiley Companies, or

their respective licensors, and your interest therein is only that of having possession of and the right to reproduce the Wiley Materials pursuant to Section 2 herein during the continuance of this Agreement. You agree that you own no right, title or interest in or to the Wiley Materials or any of the intellectual property rights therein. You shall have no rights hereunder other than the license as provided for above in Section 2. No right, license or interest to any trademark, trade name, service mark or other branding ("Marks") of WILEY or its licensors is granted hereunder, and you agree that you shall not assert any such right, license or interest with respect thereto

- NEITHER WILEY NOR ITS LICENSORS MAKES ANY WARRANTY OR REPRESENTATION OF ANY KIND TO YOU OR ANY THIRD PARTY, EXPRESS, IMPLIED OR STATUTORY, WITH RESPECT TO THE MATERIALS OR THE ACCURACY OF ANY INFORMATION CONTAINED IN THE MATERIALS, INCLUDING, WITHOUT LIMITATION, ANY IMPLIED WARRANTY OF MERCHANTABILITY, ACCURACY, SATISFACTORY QUALITY, FITNESS FOR A PARTICULAR PURPOSE, USABILITY, INTEGRATION OR NON-INFRINGEMENT AND ALL SUCH WARRANTIES ARE HEREBY EXCLUDED BY WILEY AND ITS LICENSORS AND WAIVED BY YOU.

- WILEY shall have the right to terminate this Agreement immediately upon breach of this Agreement by you.

- You shall indemnify, defend and hold harmless WILEY, its Licensors and their respective directors, officers, agents and employees, from and against any actual or threatened claims, demands, causes of action or proceedings arising from any breach of this Agreement by you.

- IN NO EVENT SHALL WILEY OR ITS LICENSORS BE LIABLE TO YOU OR ANY OTHER PARTY OR ANY OTHER PERSON OR ENTITY FOR ANY SPECIAL, CONSEQUENTIAL, INCIDENTAL, INDIRECT, EXEMPLARY OR PUNITIVE DAMAGES, HOWEVER CAUSED, ARISING OUT OF OR IN CONNECTION WITH THE DOWNLOADING, PROVISIONING, VIEWING OR USE OF THE MATERIALS REGARDLESS OF THE FORM OF ACTION, WHETHER FOR BREACH OF CONTRACT, BREACH OF WARRANTY, TORT, NEGLIGENCE, INFRINGEMENT OR OTHERWISE (INCLUDING, WITHOUT LIMITATION, DAMAGES BASED ON LOSS OF PROFITS, DATA, FILES, USE, BUSINESS OPPORTUNITY OR CLAIMS OF THIRD PARTIES), AND WHETHER OR NOT THE PARTY HAS BEEN ADVISED OF THE POSSIBILITY OF SUCH DAMAGES. THIS LIMITATION SHALL APPLY NOTWITHSTANDING ANY FAILURE OF ESSENTIAL PURPOSE OF ANY LIMITED REMEDY PROVIDED HEREIN.

- Should any provision of this Agreement be held by a court of competent jurisdiction to be illegal, invalid, or unenforceable, that provision shall be deemed amended to achieve as nearly as possible the same economic effect as the original provision, and the legality, validity and enforceability of the remaining provisions of this Agreement shall not be affected or impaired thereby.

- The failure of either party to enforce any term or condition of this Agreement shall not

constitute a waiver of either party's right to enforce each and every term and condition of this Agreement. No breach under this agreement shall be deemed waived or excused by either party unless such waiver or consent is in writing signed by the party granting such waiver or consent. The waiver by or consent of a party to a breach of any provision of this Agreement shall not operate or be construed as a waiver of or consent to any other or subsequent breach by such other party.

- This Agreement may not be assigned (including by operation of law or otherwise) by you without WILEY's prior written consent.

- Any fee required for this permission shall be non-refundable after thirty (30) days from receipt by the CCC.

- These terms and conditions together with CCC's Billing and Payment terms and conditions (which are incorporated herein) form the entire agreement between you and WILEY concerning this licensing transaction and (in the absence of fraud) supersedes all prior agreements and representations of the parties, oral or written. This Agreement may not be amended except in writing signed by both parties. This Agreement shall be binding upon and inure to the benefit of the parties' successors, legal representatives, and authorized assigns.

- In the event of any conflict between your obligations established by these terms and conditions and those established by CCC's Billing and Payment terms and conditions, these terms and conditions shall prevail.

- WILEY expressly reserves all rights not specifically granted in the combination of (i) the license details provided by you and accepted in the course of this licensing transaction, (ii) these terms and conditions and (iii) CCC's Billing and Payment terms and conditions.

- This Agreement will be void if the Type of Use, Format, Circulation, or Requestor Type was misrepresented during the licensing process.

- This Agreement shall be governed by and construed in accordance with the laws of the State of New York, USA, without regards to such state's conflict of law rules. Any legal action, suit or proceeding arising out of or relating to these Terms and Conditions or the breach thereof shall be instituted in a court of competent jurisdiction in New York County in the State of New York in the United States of America and each party hereby consents and submits to the personal jurisdiction of such court, waives any objection to venue in such court and consents to service of process by registered or certified mail, return receipt requested, at the last known address of such party.

WILEY OPEN ACCESS TERMS AND CONDITIONS

Wiley Publishes Open Access Articles in fully Open Access Journals and in Subscription journals offering Online Open. Although most of the fully Open Access journals publish open access articles under the terms of the Creative Commons Attribution (CC BY) License only, the subscription journals and a few of the Open Access Journals offer a choice of Creative Commons Licenses. The license type is clearly identified on the article.

The Creative Commons Attribution License

The Creative Commons Attribution License (CC-BY) allows users to copy, distribute and transmit an article, adapt the article and make commercial use of the article. The CC-BY license permits commercial and non-

Creative Commons Attribution Non-Commercial License

The Creative Commons Attribution Non-Commercial (CC-BY-NC)License permits use, distribution and reproduction in any medium, provided the original work is properly cited and is not used for commercial purposes.(see below)

Creative Commons Attribution-Non-Commercial-NoDerivs License

The Creative Commons Attribution Non-Commercial-NoDerivs License (CC-BY-NC-ND) permits use, distribution and reproduction in any medium, provided the original work is properly cited, is not used for commercial purposes and no modifications or adaptations are made. (see below)

Use by commercial "for-profit" organizations

Use of Wiley Open Access articles for commercial, promotional, or marketing purposes requires further explicit permission from Wiley and will be subject to a fee.

Further details can be found on Wiley Online Library http://olabout.wiley.com/WileyCDA /Section/id-410895.html

Other Terms and Conditions:

v1.10 Last updated September 2015

Questions? customercare@copyright.com or +1-855-239-3415 (toll free in the US) or +1-978-646-2777.

References

1. Hall, J. E. *Guyton and Hall Textbook of Medical Physiology*. (Elsevier, 2016).

2. Bers, D. M. Cardiac excitation–contraction coupling. *Nature* **415**, 198–205 (2002).

3. Cannon, W. B. *Bodily changes in pain, hunger, fear, and rage: An account of recent researches into the function of emotional excitement*. (D. Appleton and Company, 1916).

4. Eaton, M. J. & Duplan, H. Useful cell lines derived from the adrenal medulla. *Mol. Cell. Endocrinol.* **228**, 39–52 (2004).

5. Rockman, H. A., Koch, W. J. & Lefkowitz, R. J. Seven-transmembrane-spanning receptors and heart function. *Nature* **415**, 206–212 (2002).

6. Molinoff, P. B. Alpha- and Beta-Adrenergic Receptor Subtypes Properties, Distribution and Regulation. *Drugs* **28**, 1–15 (1984).

7. Gauthier, C., Tavernier, G., Charpentier, F., Langin, D. & Le Marec, H. Functional beta3-adrenoceptor in the human heart. *J. Clin. Invest.* **98**, 556–62 (1996).

8. de Lucia, C., Eguchi, A. & Koch, W. J. New Insights in Cardiac β-Adrenergic Signaling During Heart Failure and Aging. *Front. Pharmacol.* **9**, 904 (2018).

9. Bristow, M. R. *et al.* Beta 1- and beta 2-adrenergic-receptor subpopulations in nonfailing and failing human ventricular myocardium: coupling of both

receptor subtypes to muscle contraction and selective beta 1-receptor down- regulation in heart failure. *Circ. Res.* **59**, 297–309 (1986).

10. Kamato, D. *et al.* Structure, Function, Pharmacology, and Therapeutic Potential of the G Protein, Gq/11. *Front. Cardiovasc. Med.* **2**, (2015).

11. Wang, J., Gareri, C. & Rockman, H. A. G-Protein–Coupled Receptors in Heart Disease. *Circ. Res.* **123**, 716–735 (2018).

12. MacLennan, D. H. & Kranias, E. G. Calcium: Phospholamban: a crucial regulator of cardiac contractility. *Nat. Rev. Mol. Cell Biol.* **4**, 566–577 (2003).

13. Li, L., Desantiago, J., Chu, G., Kranias, E. G. & Bers, D. M. Phosphorylation of phospholamban and troponin I in beta-adrenergic-induced acceleration of cardiac relaxation. *Am. J. Physiol. Heart Circ. Physiol.* **278**, H769-79 (2000).

14. Liu, G. *et al.* Mechanism of adrenergic CaV1.2 stimulation revealed by proximity proteomics. *Nature* **577**, 695–700 (2020).

15. Marx, S. O. *et al.* PKA Phosphorylation Dissociates FKBP12.6 from the Calcium Release Channel (Ryanodine Receptor). *Cell* **101**, 365–376 (2000).

16. Valdivia, H., Kaplan, J., Ellis-Davies, G. & Lederer, W. Rapid adaptation of cardiac ryanodine receptors: modulation by Mg2+ and phosphorylation. *Science (80-.).* **267**, 1997–2000 (1995).

17. Li, Y., Kranias, E. G., Mignery, G. A. & Bers, D. M. Protein kinase A phosphorylation of the ryanodine receptor does not affect calcium sparks in

mouse ventricular myocytes. *Circ. Res.* **90**, 309–16 (2002).

18. Hoffman, B. B. & Lefkowitz, R. J. *Goodman and Gilman's The Pharmacological Basis of Therapeutics*. (McGraw-Hill, 1996).

19. Fedida, D., Braun, A. P. & Giles, W. R. Alpha 1-adrenoceptors in myocardium: functional aspects and transmembrane signaling mechanisms. *Physiol. Rev.* **73**, 469–487 (1993).

20. Stewart, A. F. *et al.* Cloning of the rat alpha 1C-adrenergic receptor from cardiac myocytes. alpha 1C, alpha 1B, and alpha 1D mRNAs are present in cardiac myocytes but not in cardiac fibroblasts. *Circ. Res.* **75**, 796–802 (1994).

21. Rokosh, D. G. & Simpson, P. C. Knockout of the 1A/C-adrenergic receptor subtype: The 1A/C is expressed in resistance arteries and is required to maintain arterial blood pressure. *Proc. Natl. Acad. Sci.* **99**, 9474–9479 (2002).

22. O'Connell, T. D. *et al.* The α1A/C- and α1B-adrenergic receptors are required for physiological cardiac hypertrophy in the double-knockout mouse. *J. Clin. Invest.* **111**, 1783–1791 (2003).

23. Graham, R. M., Perez, D. M., Hwa, J. & Piascik, M. T. α 1 -Adrenergic Receptor Subtypes. *Circ. Res.* **78**, 737–749 (1996).

24. Akhter, S. A. *et al.* Transgenic mice with cardiac overexpression of alpha1B-adrenergic receptors. In vivo alpha1-adrenergic receptor-mediated regulation of beta-adrenergic signaling. *J. Biol. Chem.* **272**, 21253–9 (1997).

25. Mizuno, N. & Itoh, H. Functions and Regulatory Mechanisms of Gq-Signaling Pathways. *Neurosignals* **17**, 42–54 (2009).

26. Jensen, B. C., O'Connell, T. D. & Simpson, P. C. Alpha-1-adrenergic receptors: Targets for agonist drugs to treat heart failure. *J. Mol. Cell. Cardiol.* **51**, 518–528 (2011).

27. Endoh, M. Cardiac α 1 -Adrenoceptors and Inotropy. *Circ. Res.* **119**, 587–590 (2016).

28. Chu, C. *et al.* Intraventricular and interventricular cellular heterogeneity of inotropic responses to α 1 -adrenergic stimulation. *Am. J. Physiol. Circ. Physiol.* **304**, H946–H953 (2013).

29. Apkon, M. & Nerbonne, J. M. Alpha 1-adrenergic agonists selectively suppress voltage-dependent K+ current in rat ventricular myocytes. *Proc. Natl. Acad. Sci.* **85**, 8756–8760 (1988).

30. Zhang, S., Hiraoka, M. & Hirano, Y. Effects ofα1-adrenergic Stimulation on L-type Ca2+Current in Rat Ventricular Myocytes. *J. Mol. Cell. Cardiol.* **30**, 1955–1965 (1998).

31. Belevych, A. E., Nulton-Persson, A., Sims, C. & Harvey, R. D. Role of tyrosine kinase activity in alpha-adrenergic inhibition of the beta-adrenergically regulated L-type Ca2+ current in guinea-pig ventricular myocytes. *J. Physiol.* **537**, 779–792 (2001).

32. Terzic, A., Pucéat, M., Clément, O., Scamps, F. & Vassort, G. Alpha 1-adrenergic effects on intracellular pH and calcium and on myofilaments in single rat cardiac cells. *J. Physiol.* **447**, 275–292 (1992).

33. Hartmann, M., Stumpe, T. & Schrader, J. α1-Adrenoceptor stimulation inhibits the isoproterenol-induced effects on myocardial contractility and protein phosphorylation. *Eur. J. Pharmacol.* **287**, 57–64 (1995).

34. O'Connell, T. D., Jensen, B. C., Baker, A. J. & Simpson, P. C. Cardiac Alpha 1 -Adrenergic Receptors: Novel Aspects of Expression, Signaling Mechanisms, Physiologic Function, and Clinical Importance. *Pharmacol. Rev.* **66**, 308–333 (2014).

35. Huang, Y. *et al.* An α1A-Adrenergic–Extracellular Signal-Regulated Kinase Survival Signaling Pathway in Cardiac Myocytes. *Circulation* **115**, 763–772 (2007).

36. Aries, A., Paradis, P., Lefebvre, C., Schwartz, R. J. & Nemer, M. Essential role of GATA-4 in cell survival and drug-induced cardiotoxicity. *Proc. Natl. Acad. Sci.* **101**, 6975–6980 (2004).

37. Pu, W. T., Ma, Q. & Izumo, S. NFAT Transcription Factors Are Critical Survival Factors That Inhibit Cardiomyocyte Apoptosis During Phenylephrine Stimulation In Vitro. *Circ. Res.* **92**, 725–731 (2003).

38. Banerjee, A. *et al.* Preconditioning against myocardial dysfunction after ischemia and reperfusion by an alpha 1-adrenergic mechanism. *Circ. Res.* **73**, 656–670 (1993).

39. Filipeanu, C. M., Zhou, F., Fugetta, E. K. & Wu, G. Differential Regulation of the Cell-Surface Targeting and Function of β- and α 1 -Adrenergic Receptors by Rab1 GTPase in Cardiac Myocytes. *Mol. Pharmacol.* **69**, 1571–1578 (2006).

40. O-Uchi, J. *et al.* Interaction of α 1 -Adrenoceptor Subtypes With Different G Proteins Induces Opposite Effects on Cardiac L-type Ca 2+ Channel. *Circ. Res.* **102**, 1378–1388 (2008).

41. Fujita, T. Accumulation of molecules involved in α1-adrenergic signal within caveolae: caveolin expression and the development of cardiac hypertrophy. *Cardiovasc. Res.* **51**, 709–716 (2001).

42. Wright, C. D. *et al.* Nuclear α1-Adrenergic Receptors Signal Activated ERK Localization to Caveolae in Adult Cardiac Myocytes. *Circ. Res.* **103**, 992–1000 (2008).

43. Wright, C. D., Wu, S. C., Dahl, E. F., Sazama, A. J. & O'Connell, T. D. Nuclear localization drives α1-adrenergic receptor oligomerization and signaling in cardiac myocytes. *Cell. Signal.* **24**, 794–802 (2012).

44. Olshansky, B., Sabbah, H. N., Hauptman, P. J. & Colucci, W. S. Parasympathetic Nervous System and Heart Failure. *Circulation* **118**, 863–871 (2008).

45. Saternos, H. C. *et al.* Distribution and function of the muscarinic receptor subtypes in the cardiovascular system. *Physiol. Genomics* **50**, 1–9 (2018).

46. Peralta, E. G. *et al.* Distinct primary structures, ligand-binding properties and tissue-specific expression of four human muscarinic acetylcholine receptors. *EMBO J.* **6**, 3923–9 (1987).

47. Bonner, T. I., Young, A. C., Brann, M. R. & Buckley, N. J. Cloning and expression of the human and rat m5 muscarinic acetylcholine receptor genes. *Neuron* **1**, 403–10 (1988).

48. Caulfield, M. P. & Birdsall, N. J. International Union of Pharmacology. XVII. Classification of muscarinic acetylcholine receptors. *Pharmacol. Rev.* **50**, 279–90 (1998).

49. Offermanns, S. *et al.* Transfected muscarinic acetylcholine receptors selectively couple to Gi-type G proteins and Gq/11. *Mol. Pharmacol.* **45**, 890–8 (1994).

50. Reuveny, E. *et al.* Activation of the cloned muscarinic potassium channel by G protein beta gamma subunits. *Nature* **370**, 143–6 (1994).

51. Löffelholz, K. & Pappano, A. J. The parasympathetic neuroeffector junction of the heart. *Pharmacol. Rev.* **37**, 1–24 (1985).

52. Sharma, V. K., Colecraft, H. M., Rubin, L. E. & Sheu, S. S. Does mammalian heart contain only the M2 muscarinic receptor subtype? *Life Sci.* **60**, 1023–9 (1997).

53. Wang, H., Shi, H., Lu, Y., Yang, B. & Wang, Z. Pilocarpine modulates the cellular electrical properties of mammalian hearts by activating a cardiac M3 receptor and a K+ current. *Br. J. Pharmacol.* **126**, 1725–34 (1999).

54. Shi, H., Wang, H. & Wang, Z. Identification and characterization of multiple subtypes of muscarinic acetylcholine receptors and their physiological functions in canine hearts. *Mol. Pharmacol.* **55**, 497–507 (1999).

55. Dhein, S., van Koppen, C. J. & Brodde, O. E. Muscarinic receptors in the mammalian heart. *Pharmacol. Res.* **44**, 161–82 (2001).

56. Brodde, O. E. & Michel, M. C. Adrenergic and muscarinic receptors in the human heart. *Pharmacol. Rev.* **51**, 651–90 (1999).

57. McMorn, S. O., Harrison, S. M., Zang, W. J., Yu, X. J. & Boyett, M. R. A direct negative inotropic effect of acetylcholine on rat ventricular myocytes. *Am. J. Physiol.* **265**, H1393-400 (1993).

58. Endoh, M., Maruyama, M. & Iijima, T. Attenuation of muscarinic cholinergic inhibition by islet-activating protein in the heart. *Am. J. Physiol.* **249**, H309-20 (1985).

59. Hescheler, J., Kameyama, M. & Trautwein, W. On the mechanism of muscarinic inhibition of the cardiac Ca current. *Pflugers Arch.* **407**, 182–9 (1986).

60. Sunahara, R. K., Dessauer, C. W. & Gilman, A. G. Complexity and diversity of mammalian adenylyl cyclases. *Annu. Rev. Pharmacol. Toxicol.* **36**, 461–80 (1996).

61. Gao, B. N. & Gilman, A. G. Cloning and expression of a widely distributed (type IV) adenylyl cyclase. *Proc. Natl. Acad. Sci. U. S. A.* **88**, 10178–82 (1991).

62. Federman, A. D., Conklin, B. R., Schrader, K. A., Reed, R. R. & Bourne, H. R. Hormonal stimulation of adenylyl cyclase through Gi-protein beta gamma subunits. *Nature* **356**, 159–61 (1992).

63. Harvey, R. D. & Belevych, A. E. Muscarinic regulation of cardiac ion channels. *Br. J. Pharmacol.* **139**, 1074–84 (2003).

64. Han, X., Kobzik, L., Severson, D. & Shimoni, Y. Characteristics of nitric oxide-mediated cholinergic modulation of calcium current in rabbit sino-atrial node. *J. Physiol.* **509 (Pt 3**, 741–54 (1998).

65. Vandecasteele, G., Verde, I., Rücker-Martin, C., Donzeau-Gouge, P. & Fischmeister, R. Cyclic GMP regulation of the L-type Ca 2+ channel current in human atrial myocytes. *J. Physiol.* **533**, 329–340 (2001).

66. Shirayama, T. & Pappano, A. J. Biphasic effects of intrapipette cyclic guanosine monophosphate on L-type calcium current and contraction of guinea pig ventricular myocytes. *J. Pharmacol. Exp. Ther.* **279**, 1274–81 (1996).

67. Wang, Y. G. & Lipsius, S. L. Acetylcholine Elicits a Rebound Stimulation of Ca 2+ Current Mediated by Pertussis Toxin–Sensitive G Protein and cAMP-Dependent Protein Kinase A in Atrial Myocytes. *Circ. Res.* **76**, 634–644 (1995).

68. Zakharov, S. I., Pieramici, S., Kumar, G. K., Prabhakar, N. R. & Harvey, R. D. Nitric Oxide Synthase Activity in Guinea Pig Ventricular Myocytes Is Not Involved in Muscarinic Inhibition of cAMP-Regulated Ion Channels. *Circ. Res.* **78**, 925–935 (1996).

69. Méry, P. F., Hove-Madsen, L., Chesnais, J. M., Hartzell, H. C. & Fischmeister, R. Nitric oxide synthase does not participate in negative inotropic effect of acetylcholine in frog heart. *Am. J. Physiol.* **270**, H1178-88 (1996).

70. Zakharov, S. I. & Harvey, R. D. Rebound stimulation of the cAMP-regulated Cl- current by acetylcholine in guinea-pig ventricular myocytes. *J. Physiol.* **499 (Pt 1**, 105–20 (1997).

71. Simons, F. E. R. Advances in H 1 -Antihistamines. *N. Engl. J. Med.* **351**,

2203–2217 (2004).

72. McNeill, J. H. Histamine and the heart. *Can. J. Physiol. Pharmacol.* **62**, 720–726 (1984).

73. Matsuda, N. *et al.* Histamine H 1 and H 2 Receptor Gene and Protein Levels Are Differentially Expressed in the Hearts of Rodents and Humans. *J. Pharmacol. Exp. Ther.* **309**, 786–795 (2004).

74. Takahama, H. *et al.* A histamine H2 receptor blocker ameliorates development of heart failure in dogs independently of β-adrenergic receptor blockade. *Basic Res. Cardiol.* **105**, 787–794 (2010).

75. Hescheler, J., Tang, M., Jastorff, B. & Trautwein, W. On the mechanism of histamine induced enhancement of the cardiac Ca2+ current. *Pfl gers Arch. Eur. J. Physiol.* **410**, 23–29 (1987).

76. Eckel, L., Gristwood, R. W., Nawrath, H., Owen, D. A. & Satter, P. Inotropic and electrophysiological effects of histamine on human ventricular heart muscle. *J. Physiol.* **330**, 111–123 (1982).

77. Fredholm, B. B. *et al.* Structure and function of adenosine receptors and their genes. *Naunyn. Schmiedebergs. Arch. Pharmacol.* **362**, 364–374 (2000).

78. Mustafa, S. J., Morrison, R. R., Teng, B. & Pelleg, A. Adenosine Receptors and the Heart: Role in Regulation of Coronary Blood Flow and Cardiac Electrophysiology. in 161–188 (2009). doi:10.1007/978-3-540-89615-9_6

79. Belardinelli, L. & Isenberg, G. Actions of adenosine and isoproterenol on isolated mammalian ventricular myocytes. *Circ. Res.* **53**, 287–297 (1983).

80. Song, Y., Thedford, S., Lerman, B. B. & Belardinelli, L. Adenosine-sensitive afterdepolarizations and triggered activity in guinea pig ventricular myocytes. *Circ. Res.* **70**, 743–753 (1992).

81. Lucchesi, B. R. Cardiac actions of glucagon. *Circ. Res.* (1968). doi:10.1161/01.RES.22.6.777

82. Ali, S. *et al.* Cardiomyocyte glucagon receptor signaling modulates outcomes in mice with experimental myocardial infarction. *Mol. Metab.* **4**, 132–143 (2015).

83. Aromataris, E. C., Roberts, M. L., Barritt, G. J. & Rychkov, G. Y. Glucagon activates Ca 2+ and Cl − channels in rat hepatocytes. *J. Physiol.* **573**, 611–625 (2006).

84. Rodgers, R. L. Glucagon and cyclic AMP: time to turn the page? *Curr. Diabetes Rev.* **8**, 362–81 (2012).

85. Qiao, A. *et al.* Structural basis of Gs and Gi recognition by the human glucagon receptor. *Science* **367**, 1346–1352 (2020).

86. Méry, P. F., Brechler, V., Pavoine, C., Pecker, F. & Fischmeister, R. Glucagon stimulates the cardiac Ca2+ current by activation of adenylyl cyclase and inhibition of phosphodiesterase. *Nature* (1990). doi:10.1038/345158a0

87. Farah, A. E. Glucagon and the circulation. *Pharmacol. Rev.* **35**, 181–217 (1983).

88. Kaumann, A. J., Sanders, L., Brown, A. M., Murray, K. J. & Brown, M. J. A 5-hydroxytryptamine receptor in human atrium. *Br. J. Pharmacol.* (1990).

doi:10.1111/j.1476-5381.1990.tb14108.x

89. Ayme-Dietrich, E., Aubertin-Kirch, G., Maroteaux, L. & Monassier, L. Cardiovascular remodeling and the peripheral serotonergic system. *Arch. Cardiovasc. Dis.* **110**, 51–59 (2017).

90. Jahnel, U., Rupp, J., Ertl, R. & Nawrath, H. Positive inotropic response to 5-HT in human atrial but not in ventricular heart muscle. *Naunyn. Schmiedebergs. Arch. Pharmacol.* **346**, 482–5 (1992).

91. Brattelid, T. *et al.* Functional serotonin 5-HT4 receptors in porcine and human ventricular myocardium with increased 5-HT4 mRNA in heart failure. *Naunyn. Schmiedebergs. Arch. Pharmacol.* (2004). doi:10.1007/s00210-004-0963-0

92. Suzuki, J. *et al.* Roles of Prostaglandin E2 in Cardiovascular Diseases. *Int. Heart J.* (2011). doi:10.1536/ihj.52.266

93. Xiao, C. Y. *et al.* Prostaglandin E2 protects the heart from ischemia-reperfusion injury via its receptor subtype EP4. *Circulation* (2004). doi:10.1161/01.CIR.0000128046.54681.97

94. Agarwal, S., Ostrom, R. & Harvey, R. Membrane Microdomains and cAMP Compartmentation in Cardiac Myocytes. in *Microdomains in the Cardiovascular System* (eds. Nikolaev, V. & Zaccolo, M.) (Springer International, 2017). doi:10.1007/978-3-319-54579-0_2

95. Narumiya, S., Sugimoto, Y. & Ushikubi, F. Prostanoid receptors: Structures, properties, and functions. *Physiological Reviews* (1999). doi:10.1152/physrev.1999.79.4.1193

96. Hayes, J. S., Brunton, L. L., Brown, J. H., Reese, J. B. & Mayer, S. E. Hormonally specific expression of cardiac protein kinase activity. *Proc. Natl. Acad. Sci. U. S. A.* **76**, 1570–4 (1979).

97. Brunton, L. L., Hayes, J. S. & Mayer, S. E. Hormonally specific phosphorylation of cardiac troponin I and activation of glycogen phosphorylase. *Nature* **280**, 78–80 (1979).

98. Xiao, R. P. & Lakatta, E. G. Beta 1-adrenoceptor stimulation and beta 2-adrenoceptor stimulation differ in their effects on contraction, cytosolic Ca2+, and Ca2+ current in single rat ventricular cells. *Circ. Res.* **73**, 286–300 (1993).

99. Kuznetsov, V., Pak, E., Robinson, R. B. & Steinberg, S. F. Beta 2-adrenergic receptor actions in neonatal and adult rat ventricular myocytes. *Circ. Res.* **76**, 40–52 (1995).

100. Brunton, L. L., Hayes, J. S. & Mayer, S. E. Functional compartmentation of cyclic AMP and protein kinase in heart. *Adv Cycl. Nucleotide Res* **391**–**7**, (1981).

101. Saucerman, J. J., Greenwald, E. C. & Polanowska-Grabowska, R. Mechanisms of cyclic AMP compartmentation revealed by computational models. *J. Gen. Physiol.* **143**, 39–48 (2014).

102. Hooper, N. M. Detergent-insoluble glycosphingolipid/cholesterol-rich membrane domains, lipid rafts and caveolae (Review). *Mol. Membr. Biol.* **16**, 145–156 (1999).

103. Ostrom, R. S. & Insel, P. A. The evolving role of lipid rafts and caveolae in

G protein-coupled receptor signaling: implications for molecular pharmacology. *Br. J. Pharmacol.* **143**, 235–245 (2004).

104. Johnstone, T. B., Agarwal, S. R., Harvey, R. D. & Ostrom, R. S. cAMP Signaling Compartmentation: Adenylyl Cyclases as Anchors of Dynamic Signaling Complexes. *Mol. Pharmacol.* **93**, 270–276 (2018).

105. Nikolaev, V. O. *et al.* Beta2-adrenergic receptor redistribution in heart failure changes cAMP compartmentation. *Science* **327**, 1653–7 (2010).

106. Timofeyev, V. *et al.* Adenylyl cyclase subtype-specific compartmentalization: differential regulation of L-type Ca2+ current in ventricular myocytes. *Circ. Res.* **112**, 1567–76 (2013).

107. Søberg, K., Moen, L. V., Skålhegg, B. S. & Laerdahl, J. K. Evolution of the cAMP-dependent protein kinase (PKA) catalytic subunit isoforms. *PLoS One* **12**, e0181091 (2017).

108. Skalhegg, Bjorn, S. Specificity in the cAMP/PKA signaling pathway. differential expression, regulation, and subcellular localization of subunits of PKA. *Front. Biosci.* **5**, d678 (2000).

109. Taylor, S. S., Knighton, D. R., Zheng, J., Ten Eyck, L. F. & Sowadski, J. M. Structural framework for the protein kinase family. *Annual Review of Cell Biology* (1992). doi:10.1146/annurev.cb.08.110192.002241

110. Cummings, D. E. *et al.* Genetically lean mice result from targeted disruption of the RII beta subunit of protein kinase A. *Nature* **382**, 622–6 (1996).

111. Dostmann, W. R. G. *et al.* Probing the cyclic nucleotide binding sites of

cAMP-dependent protein kinases I and II with analogs of adenosine 3',5'-cyclic phosphorothioates. *J. Biol. Chem.* (1990).

112. Colledge, M. & Scott, J. D. AKAPs: from structure to function. *Trends Cell Biol.* **9**, 216–221 (1999).

113. Stanley McKnight, G. Cyclic AMP second messenger systems. *Curr. Opin. Cell Biol.* **3**, 213–217 (1991).

114. Beene, D. L. & Scott, J. D. A-kinase anchoring proteins take shape. *Curr. Opin. Cell Biol.* **19**, 192–198 (2007).

115. Lygren, B. *et al.* AKAP complex regulates Ca 2+ re-uptake into heart sarcoplasmic reticulum. *EMBO Rep.* **8**, 1061–1067 (2007).

116. Conti, M. & Jin, S.-L. C. The Molecular Biology of Cyclic Nucleotide Phosphodiesterases. in 1–38 (1999). doi:10.1016/S0079-6603(08)60718-7

117. Jurevicius, J. & Fischmeister, R. cAMP compartmentation is responsible for a local activation of cardiac Ca2+ channels by beta-adrenergic agonists. *Proc. Natl. Acad. Sci.* **93**, 295–299 (1996).

118. Baillie, G. S., Scott, J. D. & Houslay, M. D. Compartmentalisation of phosphodiesterases and protein kinase A: opposites attract. *FEBS Lett.* **579**, 3264–3270 (2005).

119. Conti, M. & Beavo, J. Biochemistry and Physiology of Cyclic Nucleotide Phosphodiesterases: Essential Components in Cyclic Nucleotide Signaling. *Annu. Rev. Biochem.* **76**, 481–511 (2007).

120. Lugnier, C. Cyclic nucleotide phosphodiesterase (PDE) superfamily: A new target for the development of specific therapeutic agents. *Pharmacol. Ther.*

109, 366–398 (2006).

121. Mongillo, M. *et al.* Compartmentalized Phosphodiesterase-2 Activity Blunts β-Adrenergic Cardiac Inotropy via an NO/cGMP-Dependent Pathway. *Circ. Res.* **98**, 226–234 (2006).

122. Wang, H., Robinson, H. & Ke, H. The Molecular Basis for Different Recognition of Substrates by Phosphodiesterase Families 4 and 10. *J. Mol. Biol.* **371**, 302–307 (2007).

123. Omori, K. & Kotera, J. Overview of PDEs and Their Regulation. *Circ. Res.* **100**, 309–327 (2007).

124. Kim, G. E. & Kass, D. A. Cardiac Phosphodiesterases and Their Modulation for Treating Heart Disease. in 249–269 (2016). doi:10.1007/164_2016_82

125. Mongillo, M. *et al.* Fluorescence Resonance Energy Transfer–Based Analysis of cAMP Dynamics in Live Neonatal Rat Cardiac Myocytes Reveals Distinct Functions of Compartmentalized Phosphodiesterases. *Circ. Res.* **95**, 67–75 (2004).

126. Lynch, M. J., Hill, E. V. & Houslay, M. D. Intracellular Targeting of Phosphodiesterase-4 Underpins Compartmentalized cAMP Signaling. in 225–259 (2006). doi:10.1016/S0070-2153(06)75007-4

127. Dodge, K. L. mAKAP assembles a protein kinase A/PDE4 phosphodiesterase cAMP signaling module. *EMBO J.* **20**, 1921–1930 (2001).

128. Chen, W., Levine, H. & Rappel, W.-J. A mathematical analysis of second

messenger compartmentalization. *Phys. Biol.* **5**, 046006 (2008).

129. Yang, P.-C. *et al.* A Computational Modeling and Simulation Approach to Investigate Mechanisms of Subcellular cAMP Compartmentation. *PLOS Comput. Biol.* **12**, e1005005 (2016).

130. Bacskai, B. *et al.* Spatially resolved dynamics of cAMP and protein kinase A subunits in Aplysia sensory neurons. *Science (80-.).* **260**, 222–226 (1993).

131. Rich, T. C. *et al.* Cyclic Nucleotide–Gated Channels Colocalize with Adenylyl Cyclase in Regions of Restricted Camp Diffusion. *J. Gen. Physiol.* **116**, 147–162 (2000).

132. Parfenov, A. S., Salnikov, V., Lederer, W. J. & Lukyánenko, V. Aqueous Diffusion Pathways as a Part of the Ventricular Cell Ultrastructure. *Biophys. J.* **90**, 1107–1119 (2006).

133. Poppe, H. *et al.* Cyclic nucleotide analogs as probes of signaling pathways. *Nat. Methods* **5**, 277–278 (2008).

134. Khac, L., Harbon, S. & Clauser, H. J. Intracellular Titration of Cyclic AMP Bound to Receptor Proteins and Correlation with Cyclic-AMP Levels in the Surviving Rat Diaphragm. *Eur. J. Biochem.* **40**, 177–185 (1973).

135. Corbin, J. D., Sugden, P. H., Lincoln, T. M. & Keely, S. L. Compartmentalization of adenosine 3':5'-monophosphate and adenosine 3':5'-monophosphate-dependent protein kinase in heart tissue. *J. Biol. Chem.* **252**, 3854–61 (1977).

136. Xiao, R. P., Ji, X. & Lakatta, E. G. Functional coupling of the β2-

adrenoceptor to a pertussis toxin- sensitive G protein in cardiac myocytes. *Mol. Pharmacol.* (1995).

137. Xiao, R. P. *et al.* Coupling of β2-adrenoceptor to G(i) proteins and its physiological relevance in murine cardiac myocytes. *Circ. Res.* (1999). doi:10.1161/01.RES.84.1.43

138. Kilts, J. D. *et al.* β 2 -Adrenergic and Several Other G Protein–Coupled Receptors in Human Atrial Membranes Activate Both G s and G i. *Circ. Res.* **87**, 705–709 (2000).

139. Taussig, R. & Gilman, A. G. Mammalian Membrane-bound Adenylyl Cyclases. *J. Biol. Chem.* **270**, 1–4 (1995).

140. Kuschel, M. *et al.* G(i) protein-mediated functional compartmentalization of cardiac beta(2)-adrenergic signaling. *J. Biol. Chem.* **274**, 22048–52 (1999).

141. Brady, J. D. *et al.* Interplay between PIP3 and calmodulin regulation of olfactory cyclic nucleotide-gated channels. *Proc. Natl. Acad. Sci. U. S. A.* **103**, 15635–40 (2006).

142. Sekar, R. B. & Periasamy, A. Fluorescence resonance energy transfer (FRET) microscopy imaging of live cell protein localizations. *J. Cell Biol.* **160**, 629–633 (2003).

143. Clegg, R. M. Fluorescence resonance energy transfer. *Curr. Opin. Biotechnol.* **6**, 103–110 (1995).

144. Bajar, B., Wang, E., Zhang, S., Lin, M. & Chu, J. A Guide to Fluorescent Protein FRET Pairs. *Sensors* **16**, 1488 (2016).

145. Adams, S. R., Harootunian, A. T., Buechler, Y. J., Taylor, S. S. & Tsien, R.

Y. Fluorescence ratio imaging of cyclic AMP in single cells. *Nature* **349**, 694–697 (1991).

146. de Rooij, J. *et al.* Epac is a Rap1 guanine-nucleotide-exchange factor directly activated by cyclic AMP. *Nature* **396**, 474–477 (1998).

147. Nikolaev, V. O., Bünemann, M., Hein, L., Hannawacker, A. & Lohse, M. J. Novel single chain cAMP sensors for receptor-induced signal propagation. *J. Biol. Chem.* **279**, 37215–37218 (2004).

148. Sprenger, J. U. *et al.* In vivo model with targeted cAMP biosensor reveals changes in receptor–microdomain communication in cardiac disease. *Nat. Commun.* **6**, 6965 (2015).

149. Agarwal, S. R. *et al.* Role of Membrane Microdomains in Compartmentation of cAMP Signaling. *PLoS One* **9**, e95835 (2014).

150. Surdo, N. C. *et al.* FRET biosensor uncovers cAMP nano-domains at β-adrenergic targets that dictate precise tuning of cardiac contractility. *Nat. Commun.* **8**, 15031 (2017).

151. Virani, S. S. *et al.* Heart Disease and Stroke Statistics—2020 Update: A Report From the American Heart Association. *Circulation* **141**, (2020).

152. McMurray, J. J. & Pfeffer, M. A. Heart failure. *Lancet* **365**, 1877–1889 (2005).

153. RONA, G. Catecholamine cardiotoxicity. *J. Mol. Cell. Cardiol.* **17**, 291–306 (1985).

154. Mann, D. L., Kent, R. L., Parsons, B. & Cooper, G. Adrenergic effects on the biology of the adult mammalian cardiocyte. *Circulation* **85**, 790–804

(1992).

155. Colucci, W. S. The effects of norepinephrine on myocardial biology: Implications for the therapy of heart failure. *Clin. Cardiol.* **21**, 20–24 (1998).

156. Bristow, M. R., Minobe, W., Rasmussen, R., Hershberger, R. E. & Hoffman, B. B. Alpha-1 adrenergic receptors in the nonfailing and failing human heart. *J. Pharmacol. Exp. Ther.* **247**, 1039–45 (1988).

157. Effect of metoprolol CR/XL in chronic heart failure: Metoprolol CR/XL Randomised Intervention Trial in-Congestive Heart Failure (MERIT-HF). *Lancet* **353**, 2001–2007 (1999).

158. The Cardiac Insufficiency Bisoprolol Study II (CIBIS-II): a randomised trial. *Lancet* **353**, 9–13 (1999).

159. Packer, M. *et al.* Effect of Carvedilol on Survival in Severe Chronic Heart Failure. *N. Engl. J. Med.* **344**, 1651–1658 (2001).

160. Yancy, C. W. *et al.* 2017 ACC/AHA/HFSA Focused Update of the 2013 ACCF/AHA Guideline for the Management of Heart Failure: A Report of the American College of Cardiology/American Heart Association Task Force on Clinical Practice Guidelines and the Heart Failure Society of Amer. *Circulation* **136**, (2017).

161. Owan, T. E. *et al.* Trends in Prevalence and Outcome of Heart Failure with Preserved Ejection Fraction. *N. Engl. J. Med.* **355**, 251–259 (2006).

162. Wachter, R. *et al.* Blunted frequency-dependent upregulation of cardiac output is related to impaired relaxation in diastolic heart failure. *Eur. Heart J.* **30**, 3027–3036 (2009).

163. Florea, V. G. & Cohn, J. N. The Autonomic Nervous System and Heart Failure. *Circ. Res.* **114**, 1815–1826 (2014).

164. Davis, B. R. Major cardiovascular events in hypertensive patients randomized to doxazosin vs chlorthalidone: The antihypertensive and lipid-lowering treatment to prevent heart attack trial (ALLHAT). *J. Am. Med. Assoc.* (2000). doi:10.1001/jama.283.15.1967

165. Diuretic Versus α-Blocker as First-Step Antihypertensive Therapy. *Hypertension* **42**, 239–246 (2003).

166. Zhang, D. Y. & Anderson, A. S. The sympathetic nervous system and heart failure. *Cardiol. Clin.* **32**, 33–45, vii (2014).

167. Post, S. R., Hammond, H. K. & Insel, P. A. β-adrenergic Receptors and Receptor Signaling in Heart Failure. *Annu. Rev. Pharmacol. Toxicol.* **39**, 343–360 (1999).

168. Triposkiadis, F. *et al.* The Sympathetic Nervous System in Heart Failure. *J. Am. Coll. Cardiol.* **54**, 1747–1762 (2009).

169. Jensen, B. C., O'Connell, T. D. & Simpson, P. C. Alpha-1–Adrenergic Receptors in Heart Failure. *J. Cardiovasc. Pharmacol.* **63**, 291–301 (2014).

170. Buxton, I. L. O. & Brunton, L. L. Action of the cardiac α1-adrenergic receptor. Activation of cyclic AMP degradation. *J. Biol. Chem.* **26**, 6733–6737 (1985).

171. Boutjdir, M., Restivo, M., Wei, Y. & El-Sherif, N. a 1- and b-adrenergic interactions on L-type calcium current in cardiac myocytes. *Pflugers Arch. Eur. J. Physiol.* **421**, 397–399 (1992).

172. Iyadomi, I., Hirahara, K. & Ehara, T. alpha-Adrenergic inhibition of the beta-adrenoceptor-dependent chloride current in guinea-pig ventricular myocytes. *J. Physiol.* **489**, 95–104 (1995).

173. Oleksa, L. M., Hool, L. C. & Harvey, R. D. α1-adrenergic inhibition of the β-adrenergically activated Cl- current in guinea pig ventricular myocytes. *Circ. Res.* (1996). doi:10.1161/01.RES.78.6.1090

174. Chen, L., El-Sherif, N. & Boutjdir, M. α1-Adrenergic activation inhibits β-adrenergic-stimulated unitary Ca2+ currents in cardiac ventricular myocytes. *Circ. Res.* (1996). doi:10.1161/01.RES.79.2.184

175. Hool, L. C., Oleksa, L. M. & Harvey, R. D. Role of G proteins in α1-adrenergic inhibition of the β- adrenergically activated chloride current in cardiac myocytes. *Mol. Pharmacol.* (1997). doi:10.1124/mol.51.5.853

176. Belevych, A. E., Nulton-Persson, A., Sims, C. & Harvey, R. D. Role of tyrosine kinase activity in α-adrenergic inhibition of the β-adrenergically regulated L-type Ca2+ current in guinea-pig ventricular myocytes. *J. Physiol.* **537**, 779–792 (2001).

177. Rudokas, M. W. *et al.* Compartmentation of β 2 -adrenoceptor stimulated cAMP responses by phosphodiesterase types 2 and 3 in cardiac ventricular myocytes. *Br. J. Pharmacol.* bph.15382 (2021). doi:10.1111/bph.15382

178. Agarwal, S. R. *et al.* Compartmentalized cAMP Signaling Associated With Lipid Raft and Non-raft Membrane Domains in Adult Ventricular Myocytes. *Front. Pharmacol.* **9**, (2018).

179. McGraw, D. W. & Liggett, S. B. Molecular mechanisms of beta2-adrenergic receptor function and regulation. *Proc. Am. Thorac. Soc.* **2**, 292–6; discussion 311-2 (2005).

180. Velmurugan, B. K., Baskaran, R. & Huang, C.-Y. Detailed insight on β-adrenoceptors as therapeutic targets. *Biomed. Pharmacother.* **117**, 109039 (2019).

181. Shahid, M. & Nicholson, C. D. Comparison of cyclic nucleotide phosphodiesterase isoenzymes in rat and rabbit ventricular myocardium: positive inotropic and phosphodiesterase inhibitory effects of Org 30029, milrinone and rolipram. *Naunyn. Schmiedebergs. Arch. Pharmacol.* (1990). doi:10.1007/BF00175715

182. O-Uchi, J. *et al.* Alpha1-adrenenoceptor stimulation inhibits cardiac excitation-contraction coupling through tyrosine phosphorylation of beta1-adrenoceptor. *Biochem. Biophys. Res. Commun.* (2013). doi:10.1016/j.bbrc.2013.02.072

183. Stiles, G. L. & Lefkowitz, R. J. Cardiac adrenergic receptors. *Annu. Rev. Med.* **35**, 149–164 (1984).

184. Maletic, V., Eramo, A., Gwin, K., Offord, S. J. & Duffy, R. A. The Role of Norepinephrine and Its α-Adrenergic Receptors in the Pathophysiology and Treatment of Major Depressive Disorder and Schizophrenia: A Systematic Review. *Front. Psychiatry* **8**, (2017).

185. Watanabe, A. M., Hathaway, D. R., Besch, H. R., Farmer, B. B. & Harris, R. A. alpha-Adrenergic reduction of cyclic adenosine monophosphate

concentrations in rat myocardium. *Circ. Res.* **40**, 596–602 (1977).

186. Barrett, S., Honbo, N. & Karliner, J. S. Alpha1-adrenoceptor-mediated inhibition of cellular cAMP accumulation in neonatal rat ventricular myocytes. *Naunyn. Schmiedebergs. Arch. Pharmacol.* (1993). doi:10.1007/BF00165388

187. Gallego, M. *et al.* α 1 -Adrenoceptors stimulate a G αs protein and reduce the transient outward K + current via a cAMP/PKA-mediated pathway in the rat heart. *Am. J. Physiol. Physiol.* **288**, C577–C585 (2005).

188. Schümann, H. J., Endoh, M. & Brodde, O. E. The time course of the effects of beta-and alpha-adrenoceptor stimulation by isoprenaline and methoxamine on the contractile force and cAMP level of the isolated rabbit papillary muscle. *Naunyn. Schmiedebergs. Arch. Pharmacol.* **289**, 291–302 (1975).

189. Karoor, V., Baltensperger, K., Paul, H., Czech, M. P. & Malbon, C. C. Phosphorylation of Tyrosyl Residues 350/354 of the β-Adrenergic Receptor Is Obligatory for Counterregulatory Effects of Insulin. *J. Biol. Chem.* **270**, 25305–25308 (1995).

190. Warne, T. *et al.* Structure of a β1-adrenergic G-protein-coupled receptor. *Nature* **454**, 486–491 (2008).

191. Malbon, C. C. & Karoor, V. G-Protein-Linked Receptors as Tyrosine Kinase Substrates. *Cell. Signal.* **10**, 523–527 (1998).

192. Hadcock, J. R., Port, J. D., Gelman, M. S. & Malbon, C. C. Cross-talk between tyrosine kinase and G-protein-linked receptors. Phosphorylation

of β2-adrenergic receptors in response to insulin. *J. Biol. Chem.* (1992). doi:10.1016/s0021-9258(18)35710-7

193. Karoor, V. & Malbon, C. C. Insulin-like growth factor receptor-1 stimulates phosphorylation of the β2-adrenergic receptor in vivo on sites distinct from those phosphorylated in response to insulin. *J. Biol. Chem.* (1996). doi:10.1074/jbc.271.46.29347

194. Baltensperger, K. *et al.* The β-adrenergic receptor is a substrate for the insulin receptor tyrosine kinase. *J. Biol. Chem.* (1996). doi:10.1074/jbc.271.2.1061

195. Paxton, W. G. *et al.* The angiotensin II AT1 receptor is tyrosine and serine phosphorylated and can serve as a substrate for the src family of tyrosine kinases. *Biochem. Biophys. Res. Commun.* (1994). doi:10.1006/bbrc.1994.1443

196. Wang, G.-Y. *et al.* Heart failure switches the RV alpha1-adrenergic inotropic response from negative to positive. *Am. J. Physiol. Heart Circ. Physiol.* **298**, H913-20 (2010).

197. Gambassi, G., Spurgeon, H. A., Ziman, B. D., Lakatta, E. G. & Capogrossi, M. C. Opposing effects of α 1 -adrenergic receptor subtypes on Ca 2+ and pH homeostasis in rat cardiac myocytes. *Am. J. Physiol. Circ. Physiol.* **274**, H1152–H1162 (1998).

198. Ross, S. A. *et al.* The alpha(1B)-adrenergic receptor decreases the inotropic response in the mouse Langendorff heart model. *Cardiovasc. Res.* **60**, 598–607 (2003).

199. O-Uchi, J. *et al.* alpha1-adrenoceptor stimulation potentiates L-type Ca2+ current through Ca2+/calmodulin-dependent PK II (CaMKII) activation in rat ventricular myocytes. *Proc. Natl. Acad. Sci. U. S. A.* **102**, 9400–5 (2005).

200. Lemire, I., Allen, B. G., Rindt, H. & Hebert, T. E. Cardiac-specific Overexpression of α1BAR Regulates βAR Activity Via Molecular Crosstalk. *J. Mol. Cell. Cardiol.* **30**, 1827–1839 (1998).

201. Lohse, M. J., Engelhardt, S., Danner, S. & Böhm, M. Mechanisms of beta-adrenergic receptor desensitization: from molecular biology to heart failure. *Basic Res. Cardiol.* **91**, 29–34 (1996).

202. Jensen, B. C., Swigart, P. M., De Marco, T., Hoopes, C. & Simpson, P. C. α1-Adrenergic Receptor Subtypes in Nonfailing and Failing Human Myocardium. *Circ. Hear. Fail.* **2**, 654–663 (2009).

203. Lymperopoulos, A., Rengo, G. & Koch, W. J. Adrenergic Nervous System in Heart Failure. *Circ. Res.* **113**, 739–753 (2013).

204. Zaccolo, M. cAMP signal transduction in the heart: understanding spatial control for the development of novel therapeutic strategies. *Br. J. Pharmacol.* **158**, 50–60 (2009).

205. Perera, R. K. & Nikolaev, V. O. Compartmentation of cAMP signalling in cardiomyocytes in health and disease. *Acta Physiol. (Oxf).* **207**, 650–62 (2013).

206. Lompré, A.-M. *et al.* Ca2+ cycling and new therapeutic approaches for heart failure. *Circulation* **121**, 822–30 (2010).

207. Li, L., Desantiago, J., Chu, G., Kranias, E. G. & Bers, D. M.

Phosphorylation of phospholamban and troponin I in β-adrenergic-induced acceleration of cardiac relaxation. *Am. J. Physiol. Circ. Physiol.* **278**, H769–H779 (2000).

208. Kuschel, M. *et al.* Beta2-adrenergic cAMP signaling is uncoupled from phosphorylation of cytoplasmic proteins in canine heart. *Circulation* **99**, 2458–65 (1999).

209. Nikolaev, V. O., Bünemann, M., Schmitteckert, E., Lohse, M. J. & Engelhardt, S. Cyclic AMP imaging in adult cardiac myocytes reveals far-reaching beta1-adrenergic but locally confined beta2-adrenergic receptor-mediated signaling. *Circ. Res.* **99**, 1084–91 (2006).

210. Balijepalli, R. C., Foell, J. D., Hall, D. D., Hell, J. W. & Kamp, T. J. Localization of cardiac L-type Ca2+ channels to a caveolar macromolecular signaling complex is required for beta2-adrenergic regulation. *Proc. Natl. Acad. Sci.* **103**, 7500–7505 (2006).

211. Christ, T., Galindo-Tovar, A., Thoms, M., Ravens, U. & Kaumann, A. J. Inotropy and L-type Ca 2+ current, activated by β 1 - and β 2 - adrenoceptors, are differently controlled by phosphodiesterases 3 and 4 in rat heart. *Br. J. Pharmacol.* **156**, 62–83 (2009).

212. Molenaar, P. *et al.* PDE3, but not PDE4, reduces $β_1$ - and $β_2$-adrenoceptor-mediated inotropic and lusitropic effects in failing ventricle from metoprolol-treated patients. *Br. J. Pharmacol.* **169**, 528–38 (2013).

213. Afzal, F. *et al.* Differential regulation of β2 -adrenoceptor-mediated inotropic and lusitropic response by PDE3 and PDE4 in failing and non-

failing rat cardiac ventricle. *Br. J. Pharmacol.* **162**, 54–71 (2011).

214. Nori, A. *et al.* Targeting of alpha-kinase-anchoring protein (alpha KAP) to sarcoplasmic reticulum and nuclei of skeletal muscle. *Biochem J* **370**, 873–880 (2003).

215. Agarwal, S. R. *et al.* Effects of cholesterol depletion on compartmentalized cAMP responses in adult cardiac myocytes. *J. Mol. Cell. Cardiol.* **50**, 500–509 (2011).

216. Kilkenny, C., Browne, W. J., Cuthill, I. C., Emerson, M. & Altman, D. G. Improving bioscience research reporting: the ARRIVE guidelines for reporting animal research. *PLoS Biol.* **8**, e1000412 (2010).

217. Dixon, R. E., Vivas, O., Hannigan, K. I. & Dickson, E. J. Ground State Depletion Super-resolution Imaging in Mammalian Cells. *J. Vis. Exp.* (2017). doi:10.3791/56239

218. Theer, P., Mongis, C. & Knop, M. PSFj: know your fluorescence microscope. *Nat. Methods* **11**, 981–982 (2014).

219. Börner, S. *et al.* FRET measurements of intracellular cAMP concentrations and cAMP analog permeability in intact cells. *Nat. Protoc.* **6**, 427–438 (2011).

220. Warrier, S. *et al.* cAMP microdomains and L-type Ca2+ channel regulation in guinea-pig ventricular myocytes. *J. Physiol.* **580**, 765–76 (2007).

221. Warrier, S. *et al.* Beta-adrenergic- and muscarinic receptor-induced changes in cAMP activity in adult cardiac myocytes detected with FRET-based biosensor. *Am. J. Physiol. Cell Physiol.* **289**, C455-61 (2005).

222. Sikkel, M. B. *et al.* Hierarchical statistical techniques are necessary to draw reliable conclusions from analysis of isolated cardiomyocyte studies. *Cardiovasc. Res.* **113**, 1743–1752 (2017).

223. Curtis, M. J. *et al.* Experimental design and analysis and their reporting II: updated and simplified guidance for authors and peer reviewers. *Br. J. Pharmacol.* **175**, 987–993 (2018).

224. Harding, S. D. *et al.* The IUPHAR/BPS Guide to PHARMACOLOGY in 2018: updates and expansion to encompass the new guide to IMMUNOPHARMACOLOGY. *Nucleic Acids Res.* **46**, D1091–D1106 (2018).

225. Alexander, S. P. H. *et al.* THE CONCISE GUIDE TO PHARMACOLOGY 2019/20: G protein-coupled receptors. *Br. J. Pharmacol.* **176**, (2019).

226. Alexander, S. P. H. *et al.* THE CONCISE GUIDE TO PHARMACOLOGY 2019/20: Ion channels. *Br. J. Pharmacol.* **176**, (2019).

227. Iancu, R. V. *et al.* Cytoplasmic cAMP concentrations in intact cardiac myocytes. *AJP Cell Physiol.* **295**, C414–C422 (2008).

228. Bayer, K. U., Harbers, K. & Schulman, H. alphaKAP is an anchoring protein for a novel CaM kinase II isoform in skeletal muscle. *EMBO J.* **17**, 5598–605 (1998).

229. Singh, P., Salih, M. & Tuana, B. S. α-Kinase Anchoring Protein αKAP Interacts with SERCA2A to Spatially Position Ca 2+ /Calmodulin-dependent Protein Kinase II and Modulate Phospholamban Phosphorylation. *J. Biol. Chem.* **284**, 28212–28221 (2009).

230. Conti, M., Mika, D. & Richter, W. Cyclic AMP compartments and signaling specificity: Role of cyclic nucleotide phosphodiesterases. *J. Gen. Physiol.* **143**, 29–38 (2014).

231. Mika, D., Leroy, J., Vandecasteele, G. & Fischmeister, R. PDEs create local domains of cAMP signaling. *J. Mol. Cell. Cardiol.* **52**, 323–329 (2012).

232. Vescovo, G., Jones, S. M., Harding, S. E. & Poole-Wilson, P. A. Isoproterenol sensitivity of isolated cardiac myocytes from rats with monocrotaline-induced right-sided hypertrophy and heart failure. *J. Mol. Cell. Cardiol.* **21**, 1047–61 (1989).

233. Wang, X. & Fitts, R. H. Ventricular action potential adaptation to regular exercise: role of β-adrenergic and K ATP channel function. *J. Appl. Physiol.* **123**, 285–296 (2017).

234. Head, B. P. *et al.* G-protein-coupled Receptor Signaling Components Localize in Both Sarcolemmal and Intracellular Caveolin-3-associated Microdomains in Adult Cardiac Myocytes. *J. Biol. Chem.* **280**, 31036–31044 (2005).

235. Mitcheson, J., Hancox, J. & Levi, A. Cultured adult cardiac myocytes: Future applications, culture methods, morphological and electrophysiological properties. *Cardiovasc. Res.* **39**, 280–300 (1998).

236. Lundgren, E., Terracio, L., Allen, D. O. & Borg, T. K. Modulation of β-receptors as adult and neonatal cardiac myocytes progress into culture. *Vitr. Cell. Dev. Biol.* **24**, 28–34 (1988).

237. Daaka, Y., Luttrell, L. M. & Lefkowitz, R. J. Switching of the coupling of the

beta2-adrenergic receptor to different G proteins by protein kinase A. *Nature* **390**, 88–91 (1997).

238. MacDougall, D. A. *et al.* Caveolae compartmentalise β2-adrenoceptor signals by curtailing cAMP production and maintaining phosphatase activity in the sarcoplasmic reticulum of the adult ventricular myocyte. *J. Mol. Cell. Cardiol.* **52**, 388–400 (2012).

239. Xiang, Y. *et al.* Phosphodiesterase 4D is required for beta2 adrenoceptor subtype-specific signaling in cardiac myocytes. *Proc. Natl. Acad. Sci. U. S. A.* **102**, 909–14 (2005).

240. Ahmad, F. *et al.* Regulation of sarcoplasmic reticulum Ca2+ ATPase 2 (SERCA2) activity by phosphodiesterase 3A (PDE3A) in human myocardium: phosphorylation-dependent interaction of PDE3A1 with SERCA2. *J. Biol. Chem.* **290**, 6763–76 (2015).

241. Beca, S. *et al.* Phosphodiesterase type 3A regulates basal myocardial contractility through interacting with sarcoplasmic reticulum calcium ATPase type 2a signaling complexes in mouse heart. *Circ. Res.* **112**, 289–97 (2013).

242. Agarwal, S. R., Clancy, C. E. & Harvey, R. D. Mechanisms Restricting Diffusion of Intracellular cAMP. *Sci. Rep.* **6**, 19577 (2016).

243. Zaccolo, M. & Movsesian, M. A. cAMP and cGMP signaling cross-talk: role of phosphodiesterases and implications for cardiac pathophysiology. *Circ. Res.* **100**, 1569–78 (2007).

244. Wright, P. T. *et al.* Cardiomyocyte Membrane Structure and cAMP

Compartmentation Produce Anatomical Variation in β2AR-cAMP Responsiveness in Murine Hearts. *Cell Rep.* **23**, 459–469 (2018).

245. Zile, M. R., Baicu, C. F. & Gaasch, W. H. Diastolic Heart Failure — Abnormalities in Active Relaxation and Passive Stiffness of the Left Ventricle. *N. Engl. J. Med.* **350**, 1953–1959 (2004).

246. Packer, M. *et al.* Effect of oral milrinone on mortality in severe chronic heart failure. The PROMISE Study Research Group. *N. Engl. J. Med.* **325**, 1468–75 (1991).

247. Woodcock, E. A. ROLES OF alpha1A - AND alpha1B - ADRENOCEPTORS IN HEART: INSIGHTS FROM STUDIES OF GENETICALLY MODIFIED MICE. *Clin. Exp. Pharmacol. Physiol.* **34**, 884–888 (2007).

248. Steinberg, S. F., Drugge, E. D., Bilezikian, J. P. & Robinson, R. B. Acquisition by innervated cardiac myocytes of a pertussis toxin-specific regulatory protein linked to the alpha 1-receptor. *Science* **230**, 186–8 (1985).

249. Garcia-Alvarez, A., Garcia-Albeniz, X., Esteve, J., Rovira, M. & Bosch, X. Cardiotoxicity of Tyrosine-Kinase-Targeting Drugs. *Cardiovasc. Hematol. Agents Med. Chem.* (2010). doi:10.2174/187152510790796192

250. Baier, A. & Szyszka, R. Compounds from Natural Sources as Protein Kinase Inhibitors. *Biomolecules* **10**, 1546 (2020).

251. Rose, B. A., Force, T. & Wang, Y. Mitogen-Activated Protein Kinase Signaling in the Heart: Angels Versus Demons in a Heart-Breaking Tale.

Physiol. Rev. **90**, 1507–1546 (2010).

252. Goldsmith, Z. G. & Dhanasekaran, D. N. G Protein regulation of MAPK networks. *Oncogene* **26**, 3122–3142 (2007).

253. Mazurek, J. A. & Jessup, M. Understanding Heart Failure. *Heart Fail. Clin.* **13**, 1–19 (2017).

254. Pfeffer, M. A., Shah, A. M. & Borlaug, B. A. Heart Failure With Preserved Ejection Fraction In Perspective. *Circ. Res.* **124**, 1598–1617 (2019).

255. Ho, J. E. *et al.* Predicting Heart Failure With Preserved and Reduced Ejection Fraction. *Circ. Hear. Fail.* **9**, (2016).

256. Sala, V. *et al.* Therapeutic Targeting of PDEs and PI3K in Heart Failure with Preserved Ejection Fraction (HFpEF). *Curr. Heart Fail. Rep.* **14**, 187–196 (2017).

257. Lowe, M. D. beta2 Adrenergic receptors mediate important electrophysiological effects in human ventricular myocardium. *Heart* **86**, 45–51 (2001).

258. Lloyd-Jones, D. M. *et al.* Lifetime risk for developing congestive heart failure: the Framingham Heart Study. *Circulation* **106**, 3068–72 (2002).

259. Dodge-Kafka, K. L. Compartmentation of Cyclic Nucleotide Signaling in the Heart: The Role of A-Kinase Anchoring Proteins. *Circ. Res.* **98**, 993–1001 (2006).

260. Schobesberger, S. *et al.* T-tubule remodelling disturbs localized β2-adrenergic signalling in rat ventricular myocytes during the progression of heart failure. *Cardiovasc. Res.* **113**, 770–782 (2017).

261. Iancu, R. V., Jones, S. W. & Harvey, R. D. Compartmentation of cAMP Signaling in Cardiac Myocytes: A Computational Study. *Biophys. J.* **92**, 3317–3331 (2007).

262. Koh, X., Srinivasan, B., Ching, H. S. & Levchenko, A. A 3D Monte Carlo Analysis of the Role of Dyadic Space Geometry in Spark Generation. *Biophys. J.* **90**, 1999–2014 (2006).

263. Beavers, D. L., Landstrom, A. P., Chiang, D. Y. & Wehrens, X. H. T. Emerging roles of junctophilin-2 in the heart and implications for cardiac diseases. *Cardiovascular Research* **103**, 198–205 (2014).

264. Takeshima, H., Hoshijima, M. & Song, L.-S. Ca2+ microdomains organized by junctophilins. *Cell Calcium* **58**, 349–356 (2015).

265. Landstrom, A. P. *et al.* Junctophilin-2 Expression Silencing Causes Cardiocyte Hypertrophy and Abnormal Intracellular Calcium-Handling. *Circ. Hear. Fail.* **4**, 214–223 (2011).

266. Han, J., Wu, H. D., Wang, Q. W. & Wang, S. Q. Morphogenesis of T-tubules in heart cells: The role of junctophilin-2. *Sci. China Life Sci.* **56**, 647–652 (2013).

267. Munro, M. L. *et al.* Junctophilin-2 in the nanoscale organisation and functional signalling of ryanodine receptor clusters in cardiomyocytes. *J. Cell Sci.* (2016). doi:10.1242/jcs.196873

268. Beavers, D. L. *et al.* Mutation E169K in Junctophilin-2 Causes Atrial Fibrillation Due to Impaired RyR2 Stabilization. *J. Am. Coll. Cardiol.* **62**, 2010–2019 (2013).

269. Van Oort, R. J. *et al.* Disrupted junctional membrane complexes and hyperactive ryanodine receptors after acute junctophilin knockdown in mice. *Circulation* **123**, 979–988 (2011).

270. Wu, H. Di *et al.* Ultrastructural remodelling of Ca2+ signalling apparatus in failing heart cells. *Cardiovasc. Res.* **95**, 430–438 (2012).

271. Pires, P. W. *et al.* The angiotensin II receptor type 1b is the primary sensor of intraluminal pressure in cerebral artery smooth muscle cells. *J. Physiol.* **595**, 4735–4753 (2017).

272. Motegi, Y. *et al.* An effective gene-knockdown using multiple shRNA-expressing adenovirus vectors. *J. Control. Release* **153**, 149–153 (2011).

273. Taxman, D. J., Moore, C. B., Guthrie, E. H. & Huang, M. T.-H. Short Hairpin RNA (shRNA): Design, Delivery, and Assessment of Gene Knockdown. in 139–156 (2010). doi:10.1007/978-1-60761-657-3_10

274. Liao, X., Makris, M. & Luo, X. M. Fluorescence-activated Cell Sorting for Purification of Plasmacytoid Dendritic Cells from the Mouse Bone Marrow. *J. Vis. Exp.* (2016). doi:10.3791/54641

275. Campbell, S. E., Gerdes, A. M. & Smith, T. D. Comparison of regional differences in cardiac myocyte dimensions in rats, hamsters, and guinea pigs. *Anat. Rec.* (1987). doi:10.1002/ar.1092190110

276. Landstrom, A. P., Beavers, D. L. & Wehrens, X. H. T. The junctophilin family of proteins: From bench to bedside. *Trends in Molecular Medicine* **20**, 353–362 (2014).

277. Yamasaki, E., Pritchard, H. A. T., Pires, P. W. & Earley, S. Junctophilin-2

Supports Functional Coupling Between Type 2 Ryanodine Receptors and BK Channels in Vascular Smooth Muscle Cells. *Exp. Biol. 2018 Meet. Abstr.* **32**, 843.6-843.6 (2018).

278. Green, M. & Loewenstein, P. M. Autonomous functional domains of chemically synthesized human immunodeficiency virus tat trans-activator protein. *Cell* **55**, 1179–1188 (1988).

279. Faruque, O. M. *et al.* Cell-permeable peptide-based disruption of endogenous PKA-AKAP complexes: A tool for studying the molecular roles of AKAP-mediated PKA subcellular anchoring. *Am. J. Physiol. - Cell Physiol.* (2009). doi:10.1152/ajpcell.00216.2008

280. Milani-Nejad, N. & Janssen, P. M. L. Small and large animal models in cardiac contraction research: advantages and disadvantages. *Pharmacol. Ther.* **141**, 235–49 (2014).

281. Ruiz-Meana, M., Fernandez-Sanz, C. & Garcia-Dorado, D. The SR-mitochondria interaction: a new player in cardiac pathophysiology. *Cardiovasc. Res.* **88**, 30–39 (2010).

282. Boncompagni, S. *et al.* Mitochondria Are Linked to Calcium Stores in Striated Muscle by Developmentally Regulated Tethering Structures. *Mol. Biol. Cell* **20**, 1058–1067 (2009).